NG KOK SENG (MIKE)

Bachelor's in Engineering (Environmental)

Comparison of conventional and advanced physical cleaning methods for BASF inge® Multibore® ultrafiltration membranes in seawater applications focusing on membrane fouling

Dissertation for obtaining the Master degree in Membrane Engineering

Erasmus Mundus Master in Membrane Engineering

Advisor:	Mr. Christian Staaks, M.Sc, inge GmbH
Co-advisors:	Mr. Michael Hoffman, B.Eng, inge GmbH
	Dr. Svetlozar Velizarov, FCT-UNL

Jury:

Chair:	Dr. Isabel Coelhoso - *Universidade Nova de Lisboa*
Examiners:	Dr. Damien Quemrner - *Université de Montpellier*
	Dr. Vlastimil Fíla - *University of Chemistry and Technology Prague*
	Dr. João Crespo - *Universidade Nova de Lisboa*
Member:	Mr. Christian Staaks - *inge GmbH*

FACULDADE DE CIÊNCIAS E TECNOLOGIA
UNIVERSIDADE NOVA DE LISBOA

July 2017

NG KOK SENG (MIKE)

Bachelor's in Engineering (Environmental)

Comparison of conventional and advanced physical cleaning methods for BASF inge® Multibore® ultrafiltration membranes in seawater applications focusing on membrane fouling

Dissertation presented to Faculdade de Ciências e Tecnologia, Universidade Nova de Lisboa for obtaining the master degree in Membrane Engineering

July 2017

Comparison of conventional and advanced physical cleaning methods for BASF inge® Multibore® ultrafiltration membranes in seawater applications focusing on membrane fouling

The EM3E Master is an Education Programme supported by the European Commission, the European Membrane Society (EMS), the European Membrane House (EMH), and a large international network of industrial companies, research centres and universities (http://em3e-4sw.eu/em3e/).

Projecto financiado com o apoio da Comissão Europeia. A informação contida nesta publicação vincula exclusivamente o autor, não sendo a Comissão responsável pela utilização que dela possa ser feita.

Confidential Clause

This final thesis with the title “Comparison of conventional and advanced physical cleaning methods for BASF inge® Multibore® ultrafiltration membranes in seawater applications focusing on membrane fouling” is based on internal, confidential data and information of the following enterprise:

inge GmbH

Flurstraße 27

86926 Greifenberg

Germany

ACKNOWLEDGMENTS

The author, Ng Kok Seng (Mike), would like to thank the following whom have made this semester of his Master's thesis, a memorable learning experience. The author would also like to put forward his appreciation to these individuals for sharing their invaluable experience, knowledge and providing support, encouragement and assistance for his Master's thesis work.

- To my family, thank you for your unconditional love and support.
- The company, inge GmbH, for giving the author the chance to do a combined summer internship and to write the Master's thesis.
- Mr. Christian Staaks and Mr. Michael Hoffman, who were the author's advisor and co-advisor, respectively. They taught the author on technical knowledge and shared their experiences. The author is appreciative of their patient coaching.
- Mrs. Michaela Krug, Mrs. Cornelia Werzinger and Ms. Sointu Parviainen, who guided the author during the two months internship during the summer of 2016. Special thanks to Ms. Sointu Parviainen for helping the author in accommodation matters.
- The process development team in inge GmbH, for providing assistance to and answering the author's inquiries.
- Dr. Svetlozar Velizarov, the author's co-advisor from FCT-UNL. Thank you for your advice, guidance and encouragement.
- Professors, lecturers and staff from Université de Montpellier, Université Paul Sabatier, University of Chemistry and Technology Prague, Universidade Nova De Lisboa, for your patience (with my questions), teachings and the effort in helping EM3E students with administration matters.
- Current and ex-internship/Master's thesis students in inge GmbH who shared their experiences, knowledge and approach to problem solving. The author enjoyed the free-flowing communication.
- Lastly, EM3E students from the 5th batch. Thank you for making this journey a memorable experience filled with joy and laughter. The author wishes everyone the best of luck in future, be it in the academics or in the industry.

Abstract

Membrane fouling is a major hurdle for ultrafiltration membrane applications. It may increase the operational costs and shorten the lifespan of membrane. Effective and efficient methods are required for its control and minimisation. In this work, the effect of Capillary Drain was investigated with a pilot plant in the Middle East using inge® Dizzer® XL modules with non-treated seawater. Capillary Drain is a novel method proposed by process development team from inge GmbH to improve the cleaning and foulant removal efficiency.

The process was operated at different flux and filtration times to keep the recovery and feed loading constant. Fouling indices developed by A.H. Nguyen [48] (Total Fouling and Hydraulic Irreversible Fouling Index) and the change in permeability were used for comparison of the efficiency of Capillary Drain.

Membrane process performance with and without Capillary Drain were compared. The former resulted in a lower fouling index, indicating that Capillary Drain slowed down the rate of increase in resistance due to fouling. Effect of Capillary Drain was also investigated when it was introduced one filtration cycle after a chemical enhanced backwash (CEB) and in between CEBs. Better results were seen in the latter. At higher operating flux, Capillary Drain also proved to be effective.

The pilot plant experienced a tremendous increase of Trans-Membrane-Pressure when chlorophyll-a concentration reached levels of 4 µg/l. When this happened, Capillary Drain seemed to be able to remove fouling better than CEB alone. Possible explanations for Capillary Drain's positive effect are also proposed.

Correlation between feed water parameters were investigated using a statistical program, Minitab® 2017. Most of the parameters compared seem to have no statistically significant relationships between them at confidence interval of 95%. Feasibility of Capillary Drain application in large scale ultrafiltration-plants was analysed.

Finally, recommendations were made to further understand Capillary Drain.

Keywords: ultrafiltration, capillary drain, algae, membrane fouling

Table of Contents

Index of Figures

Index of Tables

List of abbreviations and symbols

Abbreviations

MF	microfiltration	SDI	Silt Density Index
UF	ultrafiltration	TFI	Total Fouling Index
NF	nanofiltration	HIFI	Hydraulic Irreversible Fouling Index
RO	reverse osmosis	CIFI	Chemical Irreversible Fouling Index
rcBW	reverse combined backwash	TMP	trans membrane pressure
CEB	chemical enhanced backwash	TEP	Transparent Exopolymer Particles
CD	Capillary Drain	AOM	Algal Organic Matter

Symbols		**Units**
J_v	flux	$l/(m^2 \cdot h)$
Q	volumetric flowrate	l/h
A_m	active membrane surface area	m^2
P_f	feed pressure	bar
P_p	Permeate (or filtrate) pressure	bar
g	gravitational acceleration	m/s^2
ρ	density of filtrated medium	kg/m^3
Perm	permeability	$l/(m^2 \cdot h \cdot bar)$
Perm’	normalized permeability	-
ΔPerm	Change in permeability	$l/(m^2 \cdot h \cdot bar)$
η	water viscosity	Pa·s
T	temperature	°C
S_{vol}	specific volume	m^3/m^2
$S_{vol,bw}$	backwash specific volume	m^3/m^2
t_{filt}	total filtration time	h
t_{bw}	total backwash time	h
t_{CEB}	total time for CEB	h
θ	recovery	%
$V_{p,available}$	final permeate volume available as product	m^3
V_{feed}	feed volume	m^3
$V_{p,BW}$	permeate volume used during backwash	m^3
$V_{p,CEB}$	permeate volume used during CEB	m^3
V_{FF}	feed volume used during forward flush	m^3

V_{pipe}	feed volume used during pipe rinsing	m^3
α	availability	%
α_{CD}	availability with Capillary Drain	%
R^2	*coefficient of determination*	-
Am^3/h	Actual meters cubed per hour	Am^3/h
Im^3/h	Inlet meters cubed per hour	Im^3/h
Nm^3/h	Normal meters cubed per hour	Nm^3/h
τ_{LLiq}	shear stresses on the wall by air slug	Pa
τ_{Lair}	shear stresses on the wall by liquid slug	Pa
P_{ref}	reference pressure in bar absolute	bar
P_s	compressor suction pressure in bar absolute	bar
P_{std}	standard barometric pressure, equals to 1 bar absolute	bar
T_{ref}	reference temperature	K
T_s	compressor suction temperature	K
T_{std}	standard temperature	K
t_{ccc}	total time of one chemical cleaning cycle	h
t_{CD}	total time for conducting Capillary Drain	h
INT	interval of conducting the Capillary Drain	-
n	number of filtration cycles between two CEBs	-
TFI	Total Fouling Index	m^2/m^3
HIFI	Hydraulic Irreversible Fouling Index	m^2/m^3
CIFI	Chemical Irreversible Fouling Index	m^2/m^3

1. Introduction

This section aims to provide the background and motivation behind the work of the Master's thesis at inge GmbH.

Rapid increase in global population and urbanization has resulted in water scarcity. 70% of the world's population are expected to live in urban areas by 2050 [1]. By 2025, half of the world's population will be living in water-stressed areas [2].

A higher reliance on membrane technologies in applications such as desalination, wastewater recovery and other treatment processes is expected to satisfy the world's water and wastewater treatment needs.

It is common knowledge that membrane fouling is a major hurdle for pressure driven membrane applications. Fouling may result in an increase in operational costs (due to an increased energy demand), additional labour for maintenance, cleaning chemical costs, and shorter membrane life [3]. Therefore, advanced pressure driven membrane applications need requires effective and efficient methods for its control and minimisation.

The company, inge GmbH, is interested to apply and understand novel methods for cleaning the membrane and removal of various kinds of fouling. The **Capillary Drain** process, a novel method proposed by process development team of inge GmbH, was investigated to unveil its potential in better fouling removal in additional to hydraulic backwash and chemical enhanced backwash. For the work of the Master's thesis, a pilot plant in seawater applications was available.

The scope of work and objectives include:

1) Fouling control: Effect of Capillary Drain in comparison to conventional cleaning regime,
2) Biological background of different algae classes,
3) Correlation between algae occurrence and process stability,
4) Correlation between algae and other water parameters (e.g. turbidity),
5) Feasibility of Capillary Drain in large scale projects.

2. Theory and fundamentals

This section is divided into five sub-sections. It aims to provide the reader with the basic knowledge and theory applied in the scope of the work.

Section 2.1 and 2.2 aims to provide the fundamentals of membrane technology, focusing on ultrafiltration, the important equations applied and membrane technology from inge GmbH.

Section 2.3 aims to explain fouling in terms of its trend, mechanism and modes.

Section 2.4 aims to provide the biological background related to biofouling and algal blooms.

Finally, Section 2.5 aims to provide the background in regression and statistics which was applied for feed water quality correlations.

2.1. Membrane technology

Quoted from M. Mulder [4],

"Membrane can be considered as a permselective barrier or interface between two phases, with Phase 1 usually considered as the feed and Phase 2 as the permeate. Separation is achieved as the membrane has the ability to transport one component from the feed mixture more readily than any other component(s). This may occur through various mechanisms and driving forces."

An example for the role of membrane is illustrated in Figure 1, where the blue component is transported more readily across the membrane. Pressure driven membranes such as Microfiltration (MF), Ultrafiltration (UF), Nanofiltration (NF) and Reverse Osmosis (RO) can be applied for water treatment applications. The terms "permeate" and "filtrate" can be used interchangeably. The types of rejection by different categories of membranes are summarized in Figure 2. inge® membrane belongs to UF category, which can reject material such as colloids and viruses.

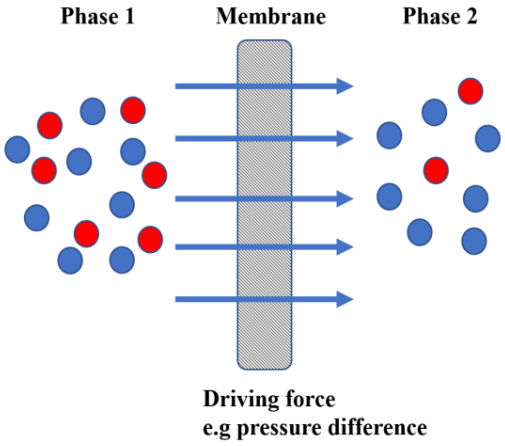

Figure 1: Membrane's role in separation of two components [5].

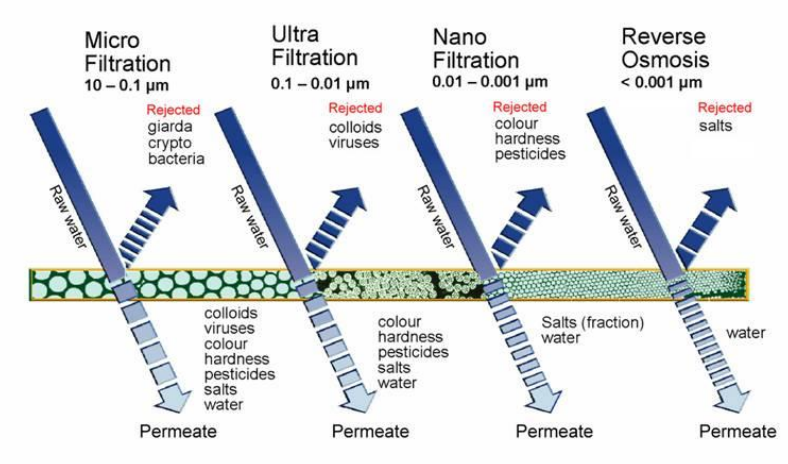

Figure 2: Various kinds of material rejection by different pressure driven membranes [6].

2.1.1. Portfolio of inge GmbH

In the scope of the Master's thesis, inside-out UF membrane from inge GmbH was used. inge GmbH was founded in 2000 and headquartered in Greifenberg (near Munich), Germany. In 2011, inge GmbH became part of BASF. inge® Multibore® membrane technology combines seven individual capillaries in a highly robust fiber of polyethersulfone nature. Commercially, capillaries with internal diameter of 0.9 mm (used in this work) and 1.5mm are available. The driving force is the pressure gradient, forcing feed water through the capillaries and dispersing laterally through the inner separation layer with pore diameter of 0.02µm. Suspended solids and germs can be retained, with 6 log and 4 log removal of bacterial and viruses, respectively. The honeycomb-style arrangement of the capillaries results in an extremely high stability of the membrane, with burst pressure of more than 14 bar [6].

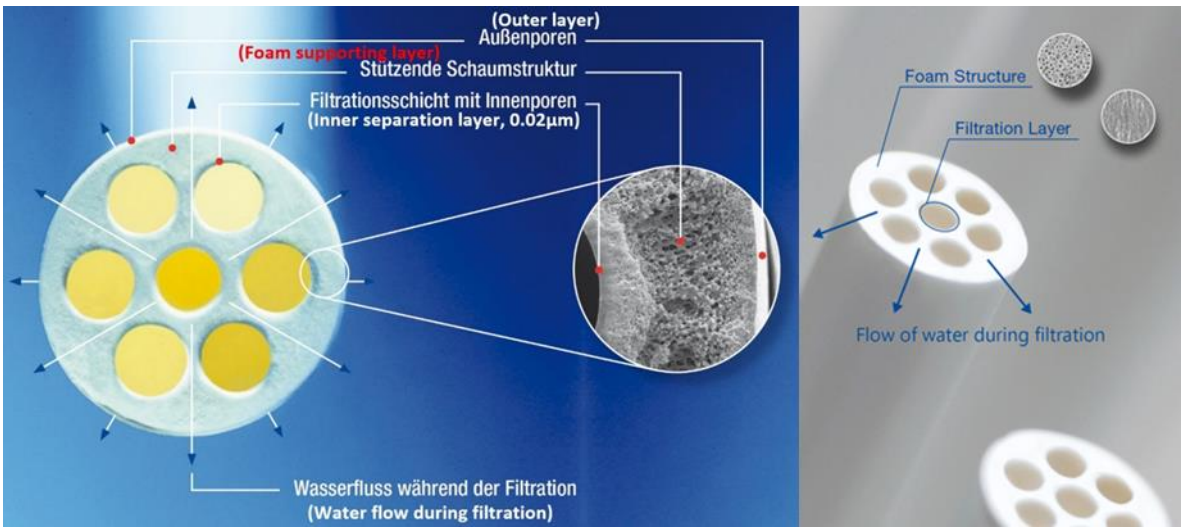

Figure 3: Details of different layers of inge® membrane fiber [6].

The hollow fibers are potted in modules and installed using the T-Rack®, a concept that offers unparalleled flexibility and helps keep investment and operating costs to a minimum [6]. The feed and drain pipes are integrated in the end caps of the headers, while the filtrate connections are welded to the module bodies and headers. There are no O-rings, and all the flanges of the header pipes are mounted in the same plane. The modules can be arranged in either two or four rows and each row can be operated as a separate filtration line.

Figure 4: T-rack® design

2.1.2. Ultrafiltration and its terminology

Membrane processes are typically characterized by flux (J_v) and permeability (Perm). In the scope of quantifying UF membrane performance, flux is defined as the flow per unit of membrane filtration area:

$$J_v = \frac{Q}{A_m} \qquad \text{Eq.1}$$

J_v: Flux [Litre of filtrate per square meter per hour, l/(m²·h)]

Q: Volumetric flow rate [l/h]

A_m: Total membrane effective surface area [m^2]

The driving force for the transport of water across UF is the pressure gradient across the membrane, better known as trans-membrane pressure (TMP).

For dead-end operation, TMP is defined as:

$$TMP = P_f - P_p \qquad \text{Eq.2}$$

P_f: Feed pressure [bar]

P_p: Permeate (or filtrate) pressure [bar]

To correct for hydrostatic pressure in the TMP measurement, inge® applied the following [6]:

$$\mathrm{TMP} = \left|\rho \times \mathrm{g} \times 10^{-5} \times \left(\frac{\mathrm{dh1+dh2}}{2} - \mathrm{dh3}\right) + \left[\left(\frac{\mathrm{PR200+PR201}}{2}\right) - \mathrm{PR300}\right]\right| \quad \text{Eq.3}$$

TMP: trans-membrane pressure [bar]

PR200, PR201, PR300: measured pressures [bar]

dh1, 2, 3: relative height of pressure sensor [m]

ρ: density of filtrated medium (for water ≈ 1000) [kg/m^3]

g: gravitational acceleration = 9.81 [m/s^2]

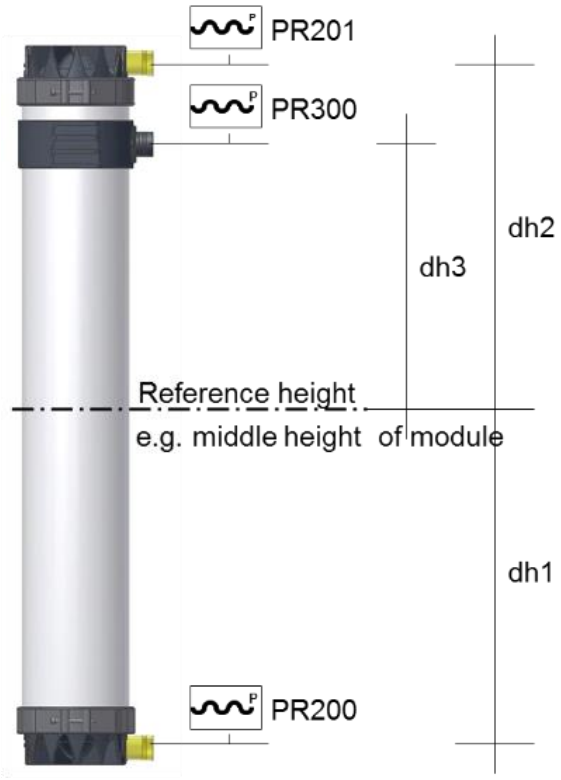

Figure 5: Reference height and positions of pressure sensors [6].

For simplification, the TMP data presented has already been corrected for the hydrostatic pressure using Eq.3.

Permeability (Perm), also known as the specific flux, is defined as:

$$\text{Perm} = \frac{J_V}{TMP} \qquad \text{Eq.4}$$

Perm: Permeability [l/(m²·h·bar)]

The value of permeability is affected by water viscosity (η), which varies at different temperatures. Thus, the following correction factor is applied to obtain a permeability normalized to 20°C.

$$\text{Perm}_{20°C} = \text{Perm} \cdot \frac{\eta(T)}{\eta_{20°C}} \qquad \text{Eq.5}$$

Viscosity, with units of Pa·s, is a function of temperature by the empirical equation, Eq. 6 [6],

$$\eta(T) = (17.91 - 0.6T + 0.017\,T^2 - 0.00017T^3) \cdot 10^{-4} \qquad \text{Eq.6}$$

For simplification, the permeability data presented has already been corrected to a reference temperature of 20°C but the symbol used will still be "Perm".

The specific volume (S_{vol}) and backwash specific volume ($S_{vol,bw}$) are the amount of filtrated permeate and permeate used for backwash, respectively, per unit of membrane filtration area:

$$S_{vol} = J_v \cdot t_{filt} \qquad \text{Eq.7}$$

$$S_{vol,bw} = J_v \cdot t_{bw} \qquad \text{Eq.8}$$

t_{filt} : total filtration time [h]

t_{bw} : total backwash time [h]

In the membrane process, recovery (θ) is the ratio between the final obtained filtrate quantity over the feed quantity, defined as:

$$\theta = \frac{V_{p,available}}{V_{feed,total}} = \frac{V_{feed} - (V_{p,BW} + V_{p,CEB})}{V_{feed} + V_{FF} + V_{pipe}} \qquad \text{Eq.9}$$

$V_{feed,total}$: total feed volume,

V_{feed}: feed volume,

$V_{p,BW}$: permeate volume used during backwash,

$V_{p,\,CEB}$: permeate volume used during Chemical Enhanced Backwash,

V_{FF}: feed volume used during forward flush,

V_{pipe}: feed volume used during pipe rinsing.

Availability (α), measures the ratio between the time during which permeate is produced over the total run time. α_{CD} is the availability taking in account conductance of Capillary Drain. Within a chemical cleaning cycle, the availabilities are defined as:

$$\alpha = \frac{n \cdot t_{filt}}{t_{chemical\ cleaning\ cycle}} = \frac{n \cdot t_{filt}}{n.(t_{filt} + t_{bw}) + t_{CEB}} \qquad \text{Eq.10}$$

$$\alpha_{CD} = \frac{n \cdot t_{filt}}{t_{chemical\ cleaning\ cycle}} = \frac{n \cdot t_{filt}}{n.\left(t_{filt} + t_{bw} + \frac{t_{CD}}{INT}\right) + t_{CEB}} \qquad \text{Eq.11}$$

n: the number of filtration cycles between two CEBs,

t_{filt}: filtration time,

$t_{chemical\ cleaning\ cycle}$: total time of one chemical cleaning cycle (between two CEBs),

t_{CD}: total time for conducting Capillary Drain,

t_{bw}: total time for backwash,

t_{CEB}: total time for CEB,

INT: interval of conducting the Capillary Drain (example, once every 6 filtration cycles)

The two availabilities are related by:

$$\alpha_{CD} = \frac{1}{\left(\frac{1}{INT}\frac{t_{CD}}{t_{filt}}\right) + \frac{1}{\alpha}} \qquad \text{Eq. 12}$$

The derivation of Eq. 12 is available in **APPENDIX A**.

2.2. Modes of Operation for inge® process

Membranes can be operated in either cross-flow or dead-end mode shown in Figure 6.

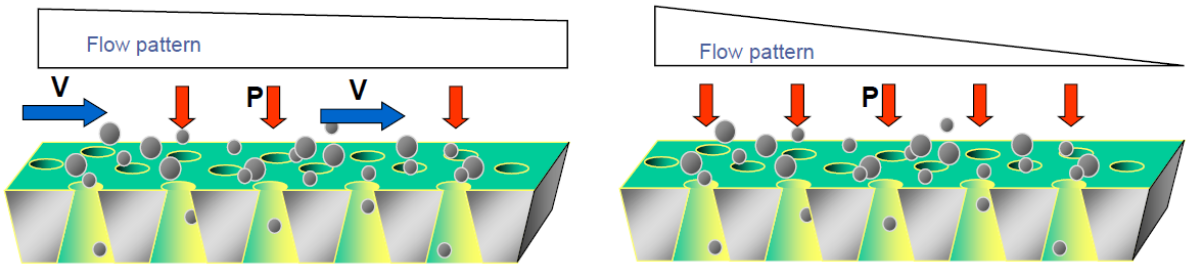

Figure 6: (Left) Cross flow filtration, where feed flows in tangential direction across the membrane surface and (right) dead-end filtration, where all the feed flows towards the membrane surface [6].

As inge® membranes were operated only in dead-end mode, the cross-flow operation will not be discussed in detail. In dead-end mode, the filtration flux and filtrate flux are equal.

2.2.1. Filtration

inge® membrane modules are operated in dead-end and filtration-bottom mode. Due to fouling (Section 2.3), physical and chemical cleaning of the membrane are required. Figure 7 shows the typical chemical cleaning cycle of ultrafiltration process.

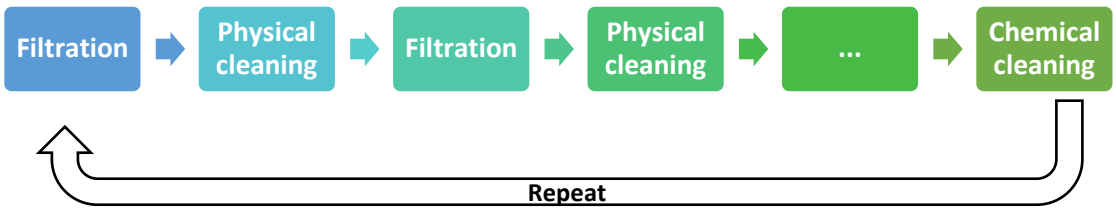

Figure 7: Chemical cleaning cycle of ultrafiltration process.

The two steps of filtration and physical cleaning (backwash) is commonly known as a unit cycle, and is repeated until a chemical cleaning is considered necessary. All process steps between two chemical cleanings are known as a chemical cleaning cycle. In a typical and standard filtration mode (which may be adjusted according to different clients' requirement), feed water is pressurized by the feed pump and enters the module from the bottom and permeate to the filtrate side while the top valve is closed, as illustrated in Figure 8.

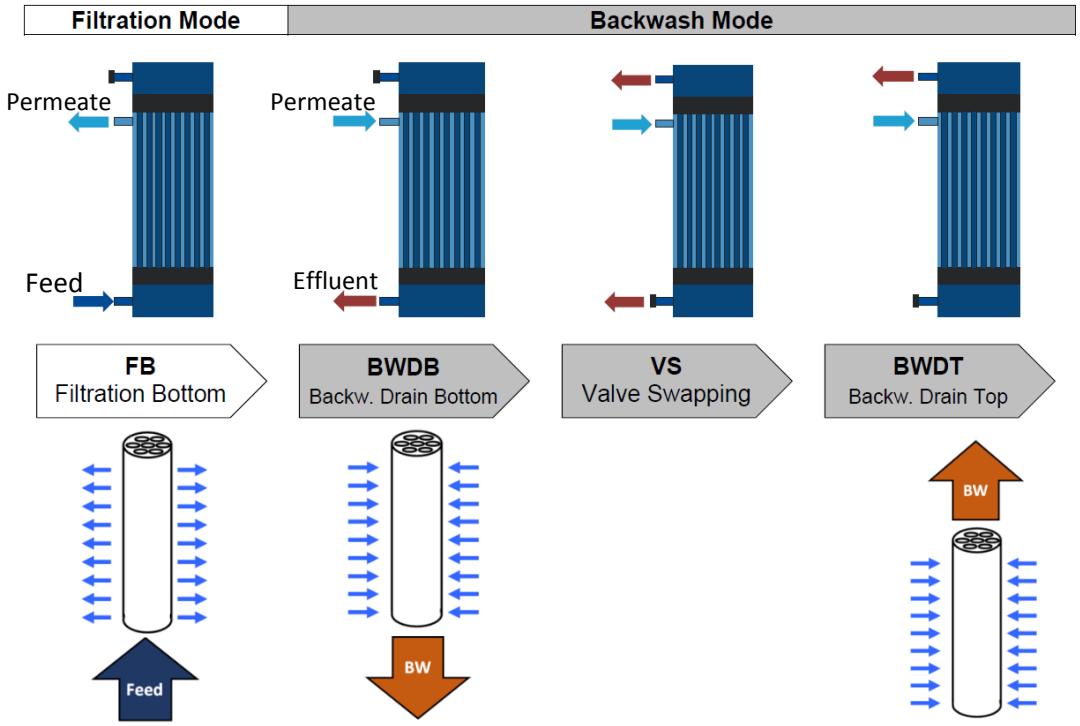

Figure 8: Procedure of filtration and reverse-combined-Backwash from inge GmbH, with illustration of feed and backwash effluent flow [6].

Depending on the quality of the feed water and flux, filtration time between 30 to 120 minutes can typically be expected before a rise in TMP is observed. This rise is due to fouling such as cake layer formation. Backwashes are performed at regular intervals to remove these foulant and recover the membrane permeability.

2.2.2. Backwash

The water required for backwash is drawn from the filtrate tank and pressurized by the backwash pump. The backwash stream passes through the membrane from the outside-in direction (opposite of the filtration mode) and detaches the accumulated foulant from the membrane surface. The backwash water is then rinsed out of the fiber capillaries and channeled through the module inlet connection to the drain.

During a typical physical cleaning or backwash, inge® implements the reverse-combined-Backwash (rcBW) strategy, where a backwash drain bottom was conducted for around two-third of the total backwash time and backwash drain top for around one-third of the total backwash time (Figure 8). Involving backwash drain top can help to remove potential plugging problem due to deposition of foulants at the dead-end side of the capillaries.

After rcBW is completed, pipe rinsing is carried out by isolating the membrane modules and flushing the pipes with feed water to remove remaining backwash water.

2.2.3. Chemical enhanced backwash

Chemical cleaning or Chemical Enhanced Backwash (CEB) is performed in a comparable way to a backwash with the addition of cleaning chemicals to boost the effectiveness of the process. Particularly, it helps to remove hydraulically irreversible foulants. Figure 9 shows the basic steps performed during a CEB.

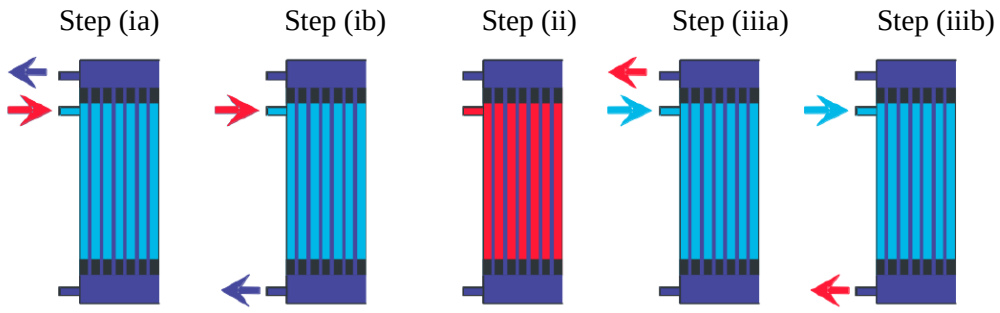

Figure 9: inge® CEB procedure [6].

Steps for conducting CEB are:

(i) Chemical injection
Done in two steps; (a) first in backwash drain top, (b) then in backwash drain bottom mode. A uniform distribution of chemicals can be established in this way.

(ii) Soaking
Soaking of chemicals in modules take place between 5-60 minutes.

(iii) Flushing of the modules
Done in two steps; (a) in backwash drain top, (b) followed by backwash drain bottom mode. Removes the chemical solution together with the fouling.

(iv) Short filtration
Clean the modules and piping from remaining chemicals.

(v) CEB can be repeated with different chemicals.

Typically, an alkaline CEB is conducted to first remove organic and/or particulate fouling. CEB can be conducted at pH up to 9.5 for seawater and pH up to 12 for surface water/wastewater. After, modules and piping are rinsed by rcBW with fresh permeate, before conducting an acidic CEB to remove inorganic fouling and/or potential precipitation due to high pH during alkaline CEB. Alkaline CEB chemicals include NaOH and NaOCl at pH 9.5 and acidic CEB chemical is H_2SO_4 or HCl at pH between 2.0 to 2.3.

2.3. Fouling

One major hurdle in the UF applications is fouling, which affect the overall performance of membrane processes over time. Explained by J. Crespo [7], fouling in membranes is a phenomenon caused by physical and/or chemical interactions between fluid, its composition and surface of membranes. Poor hydrodynamics may also contribute to membrane fouling. This results in the progressive deposition and/or adsorption of material on the membrane surface or within the membrane structure. The trend of fouling, fouling mechanisms and modes are explained in the following sub-sections.

2.3.1. Trend of fouling

Depending on the mode of operation, different trends can be seen. If the membrane process is operated in constant TMP mode, there will be a gradual loss of flux. If the membrane process is operated in constant flux mode, there will be a gradual increase of TMP. In both cases, the final result is the gradual loss of membrane permeability as seen in Figure 10.

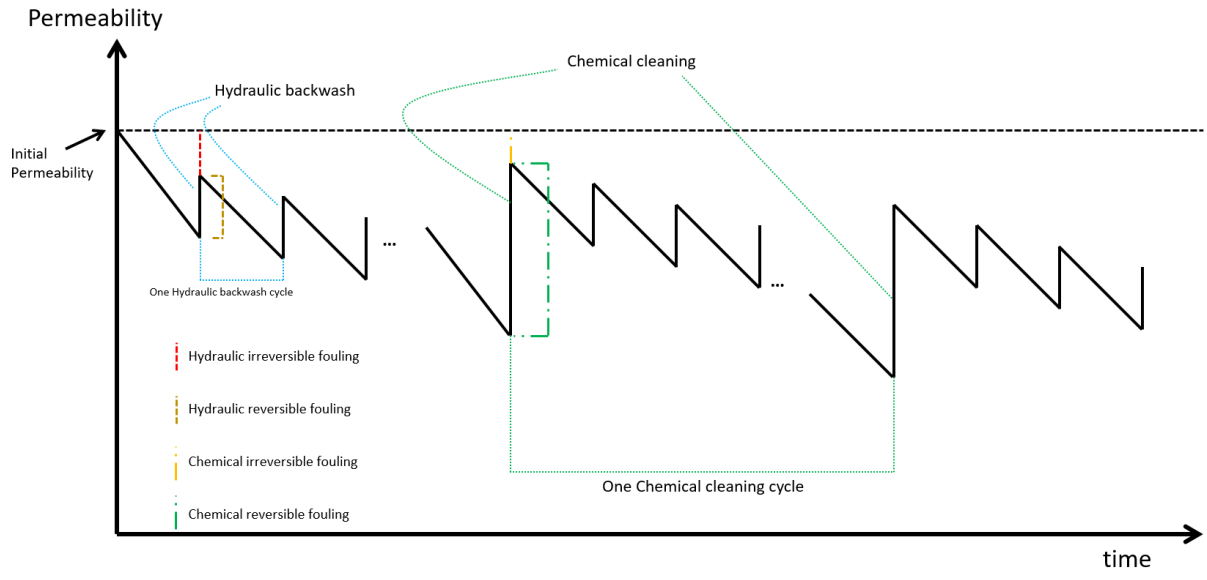

Figure 10: Trend of membrane permeability over time with hydraulic and chemical cleaning.

Materials which could cause membrane fouling include (but not limited to) solids, particulates, flocs, proteins, biological substances such as Extracellular Polymeric Substance (EPS), colloidal of organic and/or inorganic nature. Fouling which can be removed by certain methods of cleaning is commonly known as reversible fouling. Hydraulic and chemical reversible fouling can be removed by hydraulic backwash and chemical cleaning, respectively. Similarly, hydraulic irreversible and chemical irreversible fouling is left over as they cannot be removed by hydraulic backwash and chemical cleaning, respectively.

2.3.2. Fouling mechanisms and modes

In general, the main mechanisms of fouling observed are shown in Figure 11. It is also possible to have fouling from more than one mechanism, especially if the feed is complex.

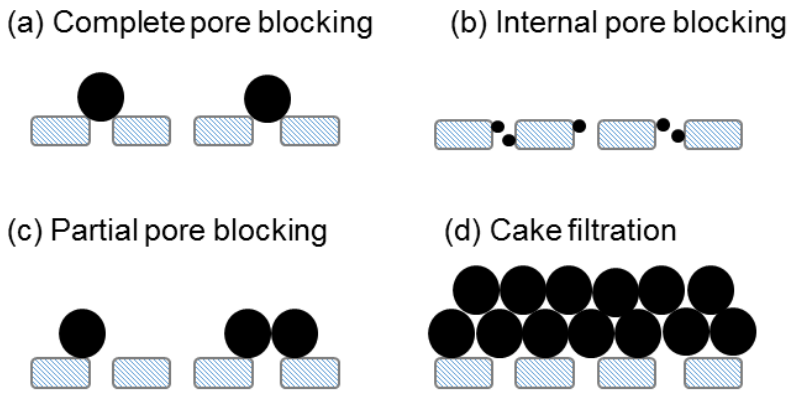

Figure 11: Fouling mechanisms of porous membranes adopted from S. Judd [8].

There are different fouling modes such as adsorption, chemical interactions, cake formation and pore blocking by diverse types of foulant [9]. Some examples are shown in Table 1:

Table 1: Fouling modes and the responsible constituents [8, 9].

Fouling modes	Responsible Constituents
Adsorption Foulants adsorbing onto membrane surface or in the pores. If the foulants are of organic nature, it is also known as organic fouling	Small molecules, Natural Organic Matter such as proteins or humic acids,
Chemical interactions pH or concentration increase can lead to precipitation of salts and/or hydroxides to form scaling (also known as inorganic fouling).	Soluble salts such as $CaCO_3$, $CaSO_4$ and $BaSO_4$, metal oxides
Cake formation & pore blocking Depositions of particles leading to cake filtration and/or blockage of pores (particulate fouling)	Small colloidal particles (Typically silica, silicates, and previously precipitated scales) Macromolecules Large suspended particles
Special case: **Biofouling** When biological substance, biological growth and biofilm are present. Biofouling may involve all four fouling modes.	Bacterial attachment on membrane surface, EPS released by bacteria, Biofilm formation

Although fouling cannot be avoided, membrane's permeability can be recovered to a certain extend with physical hydraulic or chemical cleaning as discussed previously in Section 2.3.2 and 2.3.3.

2.4. Biological background in feed water

One potential problem faced by water treatment plants is algal blooms, events which natural occurring microscopic algae experience a massive population growth. Algae are aquatic, plant-like organisms. They encompass a variety of simple structures, from single-celled phytoplankton floating in the water, to large seaweeds (macroalgae) attached to the ocean floor. Algal bloom is a result of changing environmental conditions, such as temperature, nutrient concentration and/or sunlight, in favor for one or more groups of algal [15].

Algal bloom may produce toxic compounds which can be harmful to human beings and animals in both land and sea. Additionally, it causes water discoloration, odor issues and can affect water treatment plants. An example was the "Red tide" bloom incident in the Gulf of Oman in 2008–2009.

Several Seawater Reverse Osmosis (SWRO) plants in the region were forced to shut down or reduce operation due to clogging of pretreatment systems and potential damage such as irreversible fouling problems in RO membranes. [10-13].

2.4.1. Algae classes

The main classes of algae which could cause algal bloom are identified by the Intergovernmental Oceanographic Commission of UNESCO, up to 300 species of microalgae were reported to cause blooms in aquatic environments [14]. Major algae groups often reported to cause severe blooms include diatoms, dinoflagellates, cyanobacteria, haptophytes, raphidophytes and chlorophytes. L. Villacorte [15] summarized the characteristics of common bloom forming species of microscopic algae in Table 2.

Table 2: List of common algal bloom forming species [15].

Bloom-forming algae	Cell size (µm)	Severe bloom (cells/ml)(*)	Potential adverse effect/consequences
Dinoflagellates			
Alexandrium tamarense	25-32	10,000	toxic bloom, red tide, O_2 depletion
Cochlodinium polykrikoides	20-40	48,000	toxic bloom, red tide, O_2 depletion
Karenia brevis	20-40	37,000	toxic bloom, red tide, O_2 depletion
Noctiluca scintillans	200-2000	1,900	red/pink/green tide, O_2 depletion
Prorocentrum micans	30-60	50,000	red/brown tide, O_2 depletion
Diatoms			
Chaetoceros affinis	8-25	900,000	O_2 depletion, fish gill irritation
Pseudo-nitzschia spp.	3-100	19,000	toxic bloom, O_2 depletion
Skeletonema costatum	2-25	88,000	O_2 depletion
Thalassiosira spp.	10-50	100,000	O_2 depletion
Cyanobacteria (blue-green)			
Anabaena spp.	3-12	10,000,000	toxic bloom, O_2 depletion
Microcystis spp.	2-7	14,800,000	toxic bloom, O_2 depletion
Nodularia spp.	6-100	605,200	toxic bloom, O_2 depletion
Haptophytes			
Emiliania huxleyi	2-6	115,000	O_2 depletion
Phaeocystis spp.	4-9	52,000	beach foam, O_2 depletion
Raphidophytes			
Chattonella spp.	10-40	10,000	toxic bloom, red tide, O_2 depletion
Heterosigma akashiwo	15-25	32,000	toxic bloom, red tide, O_2 depletion
Chlorophytes (green)			
Chlorella vulgaris	2-10	145,000	green tide, O_2 depletion
Scenedesmus spp.	2-25	820,000	green tide, O_2 depletion

(*) – Maximum recorded concentration reported in literature

2.4.2. Quantifying algae

Chlorophyll-a is a color pigment and molecule used in photosynthesis. It is found in plants, algae and phytoplankton. Six different chlorophylls have been identified [16, 17] in the form of chlorophyll-a, b, c, d, e and f. Each type reflects slightly different ranges of green wavelengths. chlorophyll-a is the primary molecule responsible for photosynthesis [16,18], meaning it is found in every single photosynthesizing organism from land plants to algae and cyanobacteria [16]. It is important to note that chlorophyll-a cannot be used to identify specific species, it can provide a rough estimate of biomass [19]. Nevertheless, chlorophyll measurements are recommended in Standard Methods for the Examination of Water and Wastewater to estimate algal populations [20].

Chlorophyll measurements rely on fluorimetry, based on the determination of the fluorescence spectrum of algae. When chlorophyll is exposed to a high-energy wavelength (approximately 470 nm), it emits a lower energy light (650-700 nm) [21]. This emission is measured to determine how much chlorophyll is in the water, which in turn estimates the algae concentration (units in µg/l). Total chlorophyll-a concentration above 15µg/l is considered problematic as recommended by New Hampshire Department of Environmental Services [22].

The instrument applied in this work is bbe AlgaeGuard®. Measurements in the bbe AlgaeGuard® are based not only on the fluorescence characteristics response of chlorophyll-a but also from different groups of algae. These responses are dependent on the colour and brightness of the excitation light. Comparing to laboratory methods, bbe AlgaeGuard® gives real time information about the concentration of chlorophyll-a in minutes [23].

Parameters which can be determined include:

- The total concentration of chlorophyll-a
- The concentration of up to 5 algae groups (algae differentiation)
- The transmission of 5 wavelengths (Option)
- Detection of yellow substances

Application of bbe AlgaeGuard® at the feed stream allowed real time monitoring of total chlorophyll-a, diatoms algae, green algae (Chlorophytes), blue-green algae (cyanobacteria) and cryptophyta concentrations.

These are useful information in making parameter changes (such as chemical concentration and soaking time) and during analysis of the performance data. A water correlation involving green algae and diatoms concentration against permeability were also conducted and discussed in detail in Section 6.

2.4.3. Potential problem of algae bloom on UF

Biofouling happens when biological substance, biological growth and/or biofilm are present on the membrane surface and/or structure via various fouling modes.

Several studies [24-27] on the performance of UF membrane, in relation to effects from algal blooms, tend towards membrane fouling caused by large macromolecules produced by the algae. These large macromolecules such as polysaccharides and proteins can be more problematic than the algal cell themselves. UF operation can be affected when there are high concentrations of sticky Algal Organic Matter (AOM) substances such as Transparent Exopolymer Particles (TEP) during algal blooms and intensify membrane fouling by particulate fouling, organic fouling and/or biofouling.

Particulate fouling in UF related to algal bloom develops when high amount of particulate materials such as AOM, algal cells and their debris form a heterogeneous and compressible cake layer on the membrane surface [15]. Capillaries of the UF membrane may be plugged when algae cells are transported and deposited at the dead-end side (Figure 12). The results can be an increase in resistance to permeate flow and/or loss of effective filtration area. When this happened during a constant flux operation mode, it is likely to observe a higher TMP. Conventional hydraulic cleaning may be less or not effective in removing the accumulated plugged material [28-31].

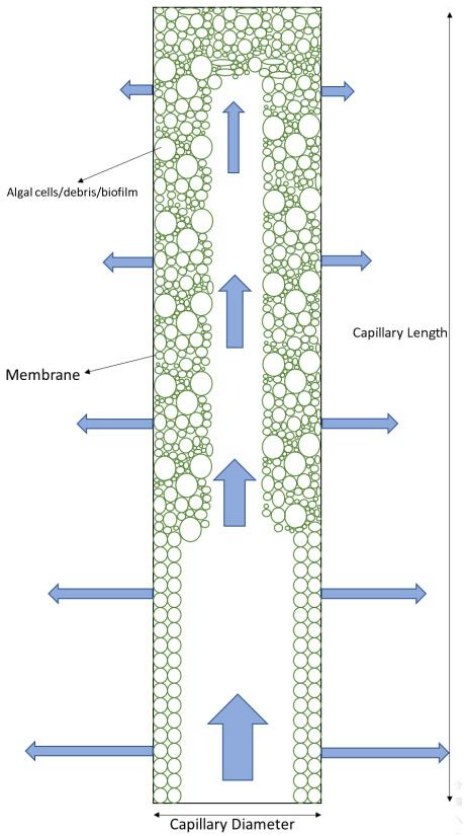

Figure 12: Plugging caused by algae cells adopted from L. Villacorte [15].

Organic fouling in UF related to algal bloom develops when algal blooms result in a large increase in AOM, particularly the sticky TEPs [32, 33]. TEPs are known to be hydrophilic materials that can absorb water up to 99% of their dry weight while allowing some water to pass through [34, 35]. TEPs can strongly adhere to UF's membrane surface and/or pores and are able to squeeze through the voids between algal cells and other accumulated solid particles. This is thought to increase the resistance to permeation. Several works [36, 37] showed that conventional hydraulic cleaning alone may be ineffective in removing the sticky fouling layer and restoring the membrane's initial permeability.

As explained previously in Section 2.4, biofouling can occur when bacteria attach themselves to the membrane or spacer components, and form biofilm. High concentration of TEPs during algal bloom can accelerate biofouling as its sticky nature can form a "conditioning layer" platform. This platform can enhance attachment and initial colonization of bacteria and they can effectively utilize nutrients from feed water [38, 39]

In general, biofouling is a considerable problem for NF/RO applications and is less concern for UF applications. This is due to periodic backwashing and chemical cleaning in dead–end UF applications, which leads to removal and/or dispersion of most accumulated bacteria and thus, hindering the biofilm formation [15].

2.5. Background in regression and statistics

This section describes the theory of linear regression and statistics, which is applied in the latter section of "Feed water correlation".

Minitab® 2017, a statistical program, is used for this work. An example is shown in Figure 13, where X-variable (also known as *predictor*) is plotted against Y-variable (also known as *response*) to determine potential relationship between them.

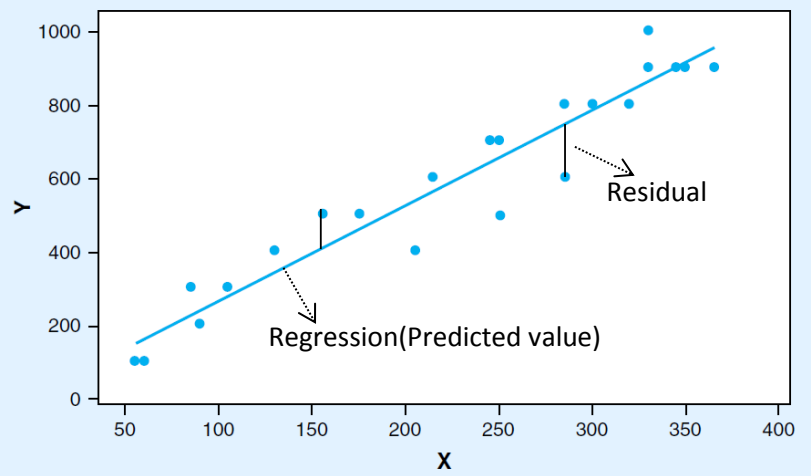

Figure 13: Example of linear regression.

Using the program helps to avoid tedious manual calculations of the regression. The regression model equation (right of Figure 13) can be obtained by input of data into the program and selecting the desired regression method. For example, a linear regression applies the least square method to minimize the residual (vertical distance from the response to the regression/predicted value).

R^2 value is known as the *coefficient of determination* and it represents proportion of the total variability in the dependent variable (in this case the Y-variable) that is explained by the regression model equation [40]. It is common for many to assume that a high R^2 value close to 1.0 indicates a good fit and that the regression model equation can describe very well the response (Y-variable) as a function of predictor (X-variable). However, this is not always true. In fact, R^2 is a comparison between two regression models; the obtained regression model (as per Figure 13) and the null model. The null model describes a horizontal line at the level of the mean of the responses (observed Y-values), which is the simplest possible model that could be fitted to any set of data. R^2 serves as a reference for comparison [40, 41].

Eventually, a high R^2 does not necessary assure a valid relation and a low R^2 does not mean the model is useless. G.J. Hahn [42] explained that with a hundred observations, a value of R^2 as low as 0.07 is

sufficient to establish statistical significance at the 1% level. What is also important is that reduction in R^2 can occur because the range of X-variable is restricted and not because the number of observed Y-variable is reduced.

"Fitted Line Plots" from Minitab® 2017 can provide important insights with the *p-values*, S-values of the regression model and availability of residual plots. The *p-value* shows if the regression is statistically significant within the chosen confidence level. It is common to use a confidence interval of 95%, and a *p-value* more than 0.05 means the regression model is not statistically significant [40, 41].

An example, not related to any variables and for illustration purpose only, is shown in Table 3 and Figure 14 and 15. The *p-value* is highlighted in red and the value is not actually zero but a value much lower than 0.001.

Table 3: Example of regression table from Minitab®.

The regression equation is
Turbidity Feed 10min avg (NTU) = 1,108 + 0,2507 Total chlo-a 10min avg (µg/l)

S = 0,917381 R-Sq = 5,1% R-Sq(adj) = 5,1%

Analysis of Variance

Source	DF	SS	MS	F	P
Regression	1	167,58	167,578	199,12	0,000
Error	3693	3107,98	0,842		
Total	3694	3275,56			

S-value is also known as the *Standard Error of the Regression*. It represents the average distance that the observed values are from the regression line and quantifies the precision of data [43]. From Figure 14, both regression lines have the same R^2 values but different S-values. S-value tells how wrong the regression model is on average, using the units of the response variable. Smaller values are indicators that the observations are closer to the fitted line.

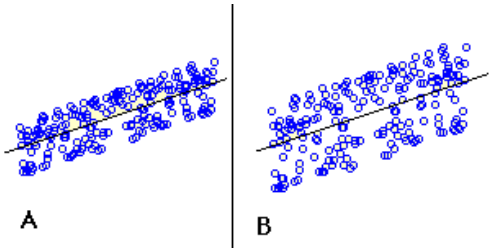

Figure 14: Example of regression with different S-values.

From Table 3, the Y-variable is "Turbidity Feed 10min avg (NTU)" and the X-variable is "Total Chlo-a 10min avg (µg/l)". The regression model equation of the example is Y = 1.108 + 0.2507X.

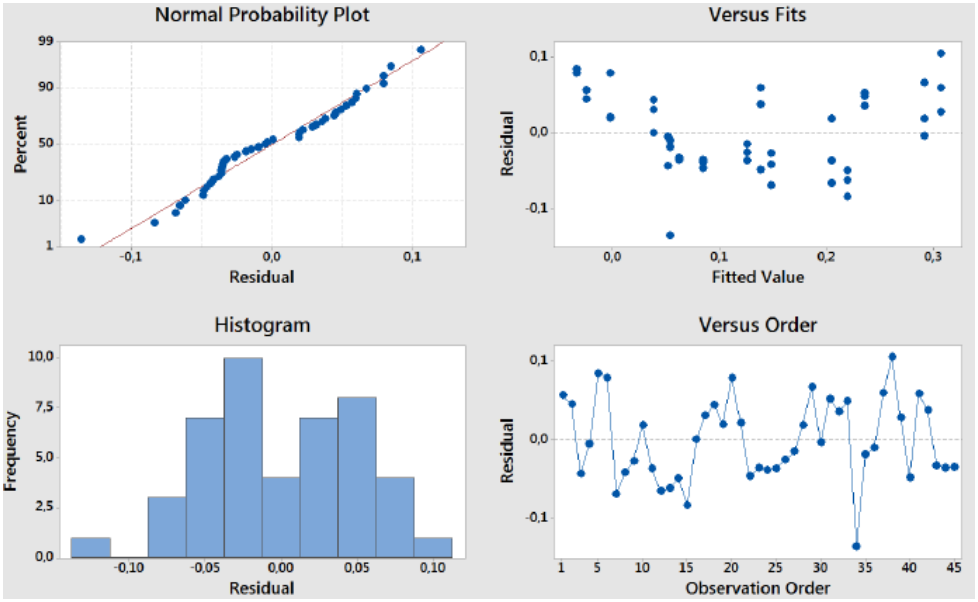

Figure 15: Example of residual plots from Minitab® 2017.

To make further analysis, one must always check the residual plots after regression is done due to the following assumptions [40]:

- The residuals are assumed to be normally distributed

  This can be checked by the "Normal Probability Plot" and "Histogram". If the residuals are normally distributed, it will lie along the red straight line in "Normal Probability Plot". The "Histogram" shows the range where the residuals lie and should ideally follow a Gaussian distribution.

- Residuals are assumed to be independent with a mean of zero

  This can be checked by the "Versus Order". If the residuals are independent, this plot should not show any particular trend. Residuals that are too large may be considered as "outliers".

- Residuals have variance that is constant for each residual and independent of any variable.

  This can be checked by the "Versus Fits" plot. It gives information about the variance of the residuals and should be equally spread around zero.

Any violation of these assumptions, especially violation of independence assumption, can cause problems and inaccurate conclusions about the regression model.

3. State-of-the-art

Through the experience of process development team from inge GmbH, it was observed that the permeability of inge® membrane seems to increase after an integrity-test is conducted. When 1 bar pressure of air is applied to the lumen of the membrane module, air cannot pass through the wetted pores of 0.02 µm due to air-liquid phase boundary of the surface tension of the membrane. These procedure steps are adjusted in the development of Capillary Drain procedure. Capillary Drain is a novel method proposed by the process development team to be applied regularly together with hydraulic backwash (rcBW) on membranes operated in inside-out filtration mode. The aims are to improve the cleaning and foulant removal efficiency. This section describes the Capillary Drain procedure in detail and to review the application of air in membrane processes.

3.1. Capillary Drain description

Before a rcBW, Capillary Drain is implemented in two steps; dewatering and pressure-hold as shown in Figure 16. Dewatering step send non-oil compressed air from the top valve into the lumen of the fibers, filtrating the remaining water in the module to the filtrate side (note that bottom feed valve is closed). Water permeates through the membrane while air is retained on the feed side due to the air-liquid phase boundary of the surface tension of the membrane, allowing pressure to be built up [6]. During the pressure-hold step, the top valve is closed and the pressure in the module is held. Finally, rcBW is conducted.

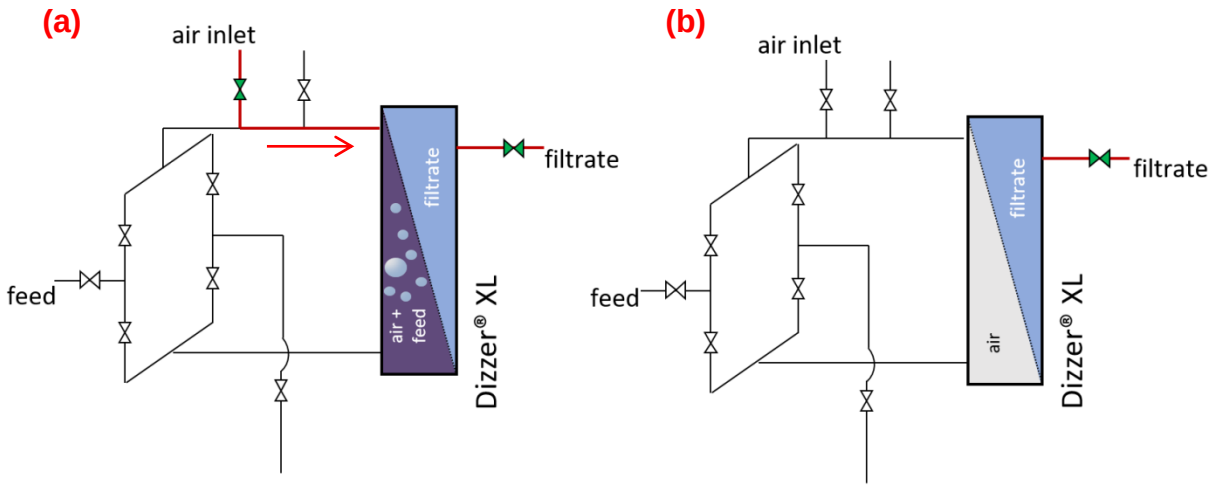

Figure 16: inge® concept of Capillary Drain (a) dewatering and (b) pressure-hold [6].

3.2. Application of air in membrane processes

In the literature review, the closest process to Capillary Drain may be the combination of air in membrane processes. Utilizing air in membrane processes is not entirely new. In the extensive literature review of Wibisono et. al. [44], research of 2-phase flow (air-liquid) in membrane

applications started as early as 1986. Commonly known as air-sparging, air can be injected during filtration to prevent surface fouling. It can also be applied during backwash to improve the removal of cake-form fouling.

As the Master's thesis work is focused on the proposed Capillary Drain during backwash, only the 2-phase flow used during backwash for inside-out membranes will be discussed.

Air Assisted Backwash (AABW) was proposed and investigated by C.Cabassud and co-workers at INSA, Toulouse, France [44]. Y.Bessiere et. al. [45] proposed a combination of AABW with rinsing to enhance UF performance for inside-out hollow-fiber modules. This procedure consisted of several steps, summarized in Table 4 in comparison with Capillary Drain. Backwashing with 2-phase flow greatly improved the removal of particulates leading to a reduction in cumulative fouling. P.J. Remize et. al. [46] showed that AABW lowered the amount of remaining-particulate-fouling (i.e. not yet removed at the end of the backwashes).

Table 4: Procedure comparison between Capillary Drain and AABW.

Capillary Drain	**AABW [45, 46]**
1) Dewatering Filtration of water in lumen of fibers through injection of air from the top.	1) Dewatering Removal of water by gravity
2) Pressure-hold After water in lumen is completely filtered, air supply is shut to hold the pressure	2) Air flushing Flushing of capillaries with air (direction and duration not stated)
3) Backwash rcBW using clean filtrate is conducted. -	3a) Backwash (mixed) Injection of air from concentrate compartment (top) while clean filtrate flow across membrane for about 20 seconds [46] 3b) Backwash (water-only) Using clean filtrate for about 20 seconds, with chlorine concentration of 5 ppm [46] -
	3c) Feed water flushing before start of filtration cycle to remove bubbles. (Duration not stated)

In addition, a comparison table of the membrane modules used is shown below.

Table 5: Comparison of membrane modules and operating specifications.

	inge® module [6]	**Module used in Y. Bessiere's work [45]**	**Module used in P.J. Remize's work [46]**
Brand	Inge GmbH	Not stated	Aquasource
Nominal pore size	0.02µm	0.01 µm	0.02 µm
Internal diameter	0.90 mm (of one capillary)	0.96 mm	0.96 mm
Membrane active surface area	80 m^2	6.5 m^2	6.5 m^2
Length	1.72 m (of fiber)	1.2 m (of module)	1.2m (of fiber)
Pre-filter	< 300 µm	150 µm	None
Initial module permeability	Line 1: 630 ± 20 l/(m²·h·bar) Line 2: 600 ± 60 l/(m²·h·bar)	400 l/(m²·h·bar)	400 ±50 l/(m²·h·bar)
Operational flux	76-92 l/(m²·h)	80 l/(m²·h)	85-90 l/(m²·h) at 20°C
Filtration cycle	45-60 min	25.5 min	30 min (Clay suspension) 20 min (natural surface water)
Backwash flux	230 l/(m²·h)	450 l/(m²·h)	384.6 l/(m²·h)
Backwash specific volume	2.1 L/m^2 3.0 L/m^2	7.5 L/m^2 For another experiment AABW + Rinsing 2.3 L/m^2	2.1 L/m^2
Superficial air flow	N/A	0.54 m/s	0.06 m/s 0.23 m/s 0.34 m/s
No. of filtration cycles	Every 14-15 before CEB	40 (and stopped) AABW applied for every cycle	130 (and stopped) AABW applied for every cycle
Chlorine concentration during backwash	0 ppm	5 ppm	5 ppm

**all membrane modules were inside-out, operated in dead-end and constant flux mode*

4. Materials and methods

This section describes the pilot plant, feed water quality, measurement instruments applied during the experiments. Methods to determine the efficiency of Capillary Drain are also introduced.

4.1. Pilot plant PU 22

The pilot plant located in Middle East was feed with direct seawater from the Arabic Gulf with no coagulation. The feed stream was divided into two lines, with both having an inge® Dizzer® XL module shown in Figure 17. They were operated at 76 l/(m²·h), 85 l/(m²·h), and 92 l/(m²·h) in April 2017 with a filtration time to 60, 50 and 45 minutes, respectively. This is to keep the recovery and thus, the feed loading to membrane constant. The full piping and instrumentation diagram is available in **APPENDIX B**.

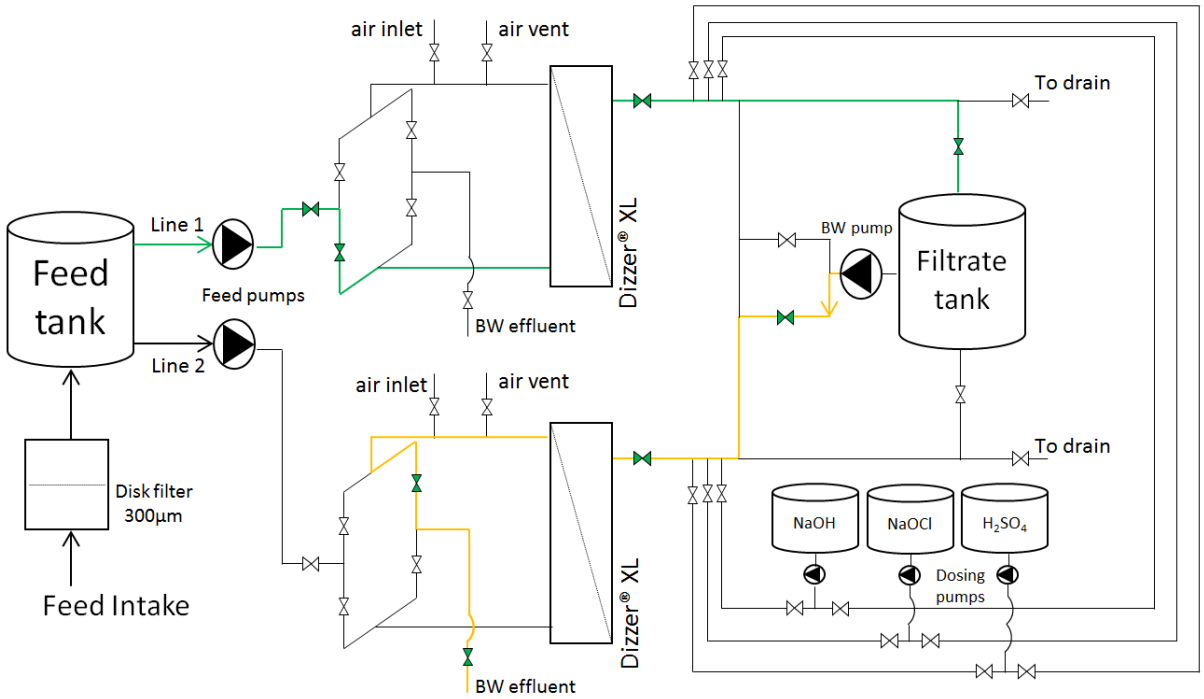

Figure 17: Simplified process flow diagram of PU 22, Line 1 in filtration mode (marked in green colour) and Line 2 in backwash mode (marked in yellow colour) [6].

4.2. Feed Water Quality

Temperature, pH, turbidity, feed flow rate, pressure at feed and filtrate sides were constantly monitored. Hourly averages of feed water quality for temperature, pH and turbidity are shown in Figure 18a.

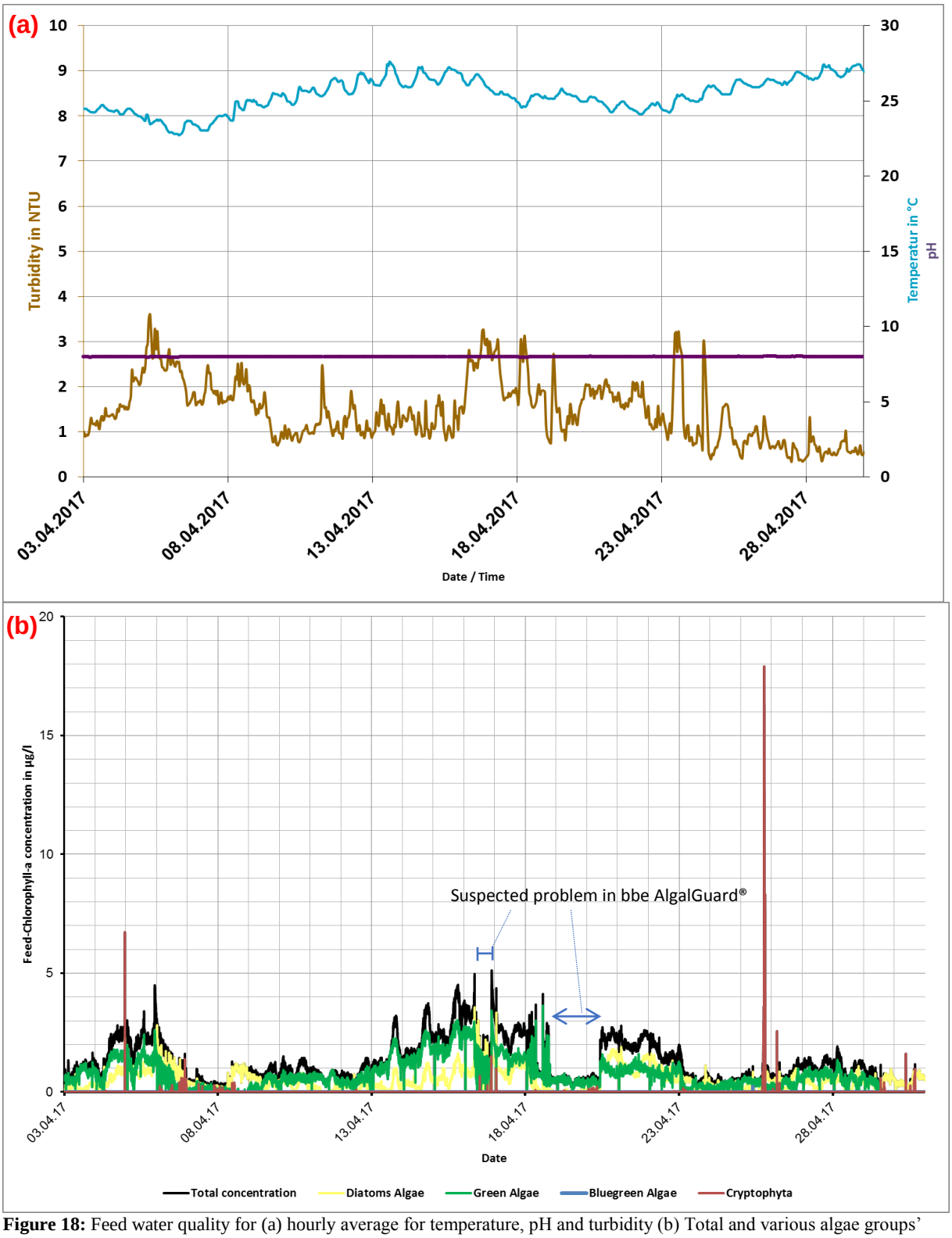

Figure 18: Feed water quality for (a) hourly average for temperature, pH and turbidity (b) Total and various algae groups' concentration.

The feed water quality was relatively good, with constant pH around 8.0, temperature between 22°C to 28°C, and turbidity less than 5 NTU. Table 6 shows a summary of the averages, standard deviation and range of values of the parameters.

Table 6: Feed water quality of PU 22.

Parameters	Units	Average	Standard Deviation	Range	Reference values [47]
Turbidity	NTU	1.47	1.99	0.08 - 11.05	2-10
pH	-	8.00	0.01	7.94 - 8.02	-
Temperature	°C	25.5	1.2	22.7 - 28.1	15.0 - 36.3
Total chlorophyll-a	µg/l	2.0	0.88	1.0 – 4.5	0.82 - 1.49 ± 0.33

Concentration of chlorophyll-a, diatoms algae, green algae (Chlorophytes), blue-green algae (cyanobacteria) and cryptophyta were measured and recorded by bbe AlgalGuard® every 97 seconds. It is considered an algal bloom event when the total chlorophyll-a concentration is more than 15 µg/l [22]. Referring to Figure 18b, there was no algal bloom during the period of experiment. However, certain trends were observed when the concentration was more than 4µg/L. The total chlorophyll–a concentration of feed water will be plotted alongside the performance chart. There was also some period of time where a problem in bbe AlgalGuard® was suspected to be not working. The data from these periods were removed during feed water correlation analysis.

The parameter settings for filtration, rcBW and CEB during the experiments can be found in **APPENDIX C**.

The methods used for analysis were (1) regression for Total Fouling and Hydraulic Irreversible Fouling Indices and (2) change in permeability. Both methods will be discussed in detail in the following section.

4.3. Methods used for determining the efficiency of cleaning

Being able to predict fouling in membranes is crucial, yet, highly complex as it depends on the feed water's physiochemical properties alongside the type of membrane used and the process parameters (TMP, filtration flux etc.) [48].

It is also challenging as certain feed water parameters such as Total Organic Carbon, Total Suspended Solids etc. are not measured constantly. Constantly sampling of feed water can be expensive and is not real-time monitoring. From the process point of view, it is useful to analyse the available parameters and fouling indices (calculated from the parameter data) which are measured constantly.

4.3.1. Fouling Indices

In general, feed water with high values of turbidity and TSS tends to cause severe fouling. However, the work of Zupancic et. al. [49] showed that turbidity is not directly correlated with fouling and is not sufficient as a sole indicator for fouling prediction.

Natural water sources containing high amount of Total Organic Carbon, Dissolved Organic Carbon and Natural Organic Matter (NOM) also tend to cause fouling. Different measures of NOM include Total Nitrogen, Dissolved Organic Nitrogen, ultraviolet absorbance, NOM molecular weight distribution, and NOM source have been found to have certain impacts on membrane fouling but no single characteristic has been demonstrated to control fouling [50-52].
The drawback of using these parameters is that they cannot be constantly monitored online and in real time easily. Constant sampling to test for these parameters will induce high operational cost. Over the years, simple, short and empirical filtration tests had been developed to obtain fouling indices to predict degree of membrane fouling.
The silt density index (SDI) and modified fouling index (MFI) are widely used in RO applications. Unfortunately, they have been reported to be insensitive to the presence of smaller particles and an unsatisfactory correlation with colloidal fouling has been observed for full-scale membrane installations [53, 54]. The MFI-UF (tested with a polyacrylonitrile 13 kDa UF membrane) was developed to account for the presence of smaller particles but at constant pressure [53, 54].
A group of researchers [52, 55-57] proposed a unified MFI for assessments of low pressure membrane performance at constant flux with the assumption that fouling is caused only by cake layer formation. It is in doubt if bench-scale or full-scale data can be compared with this unified MFI [48].

In the case of inge GmbH, the fouling index of Hydraulic Irreversible Fouling Index (HIFI) were chosen as the analysis tool. Together with Total Fouling Index (TFI) and Chemical Irreversible Fouling Index (CIFI), these indices were developed by A.H. Nguyen and co-workers [48] and were based on a resistance in-series model. The indices indicate the rate of increase in resistance due to fouling, i.e., smaller indices indicate slower rate of increase in resistance. The key feature of this development is that fouling is not attributed to a specific mechanism so the model is valid regardless of whether cake filtration, pore constriction, or a combination of fouling mechanisms occurring. The full derivation is available in **APPENDIX D** and the final form is summarized in Table 7.

Table 7: Summary of fouling indices developed by A.H. Nguyen et. al. [48].

Total Fouling Index (TFI)	**Hydraulic Irreversible Fouling Index (HIFI)**	**Chemical Irreversible Fouling Index (CIFI)**
Any single hydraulic backwash	Multiple hydraulic backwash cycles without any chemical cleaning (referred to as one chemical cleaning cycle)	Average values for all data for a series of chemical cleaning cycles
$\frac{1}{\text{Perm}'} = 1 + (\text{TFI})S_{vol}$	$\frac{1}{\text{Perm}'} = 1 + (\text{HIFI})S_{vol}$	$\frac{1}{\text{Perm}'} = 1 + (\text{CIFI})S_{vol}$

Perm': normalized permeability (or specific flux) [-]

S_{vol}: specific volume [m^3/m^2]

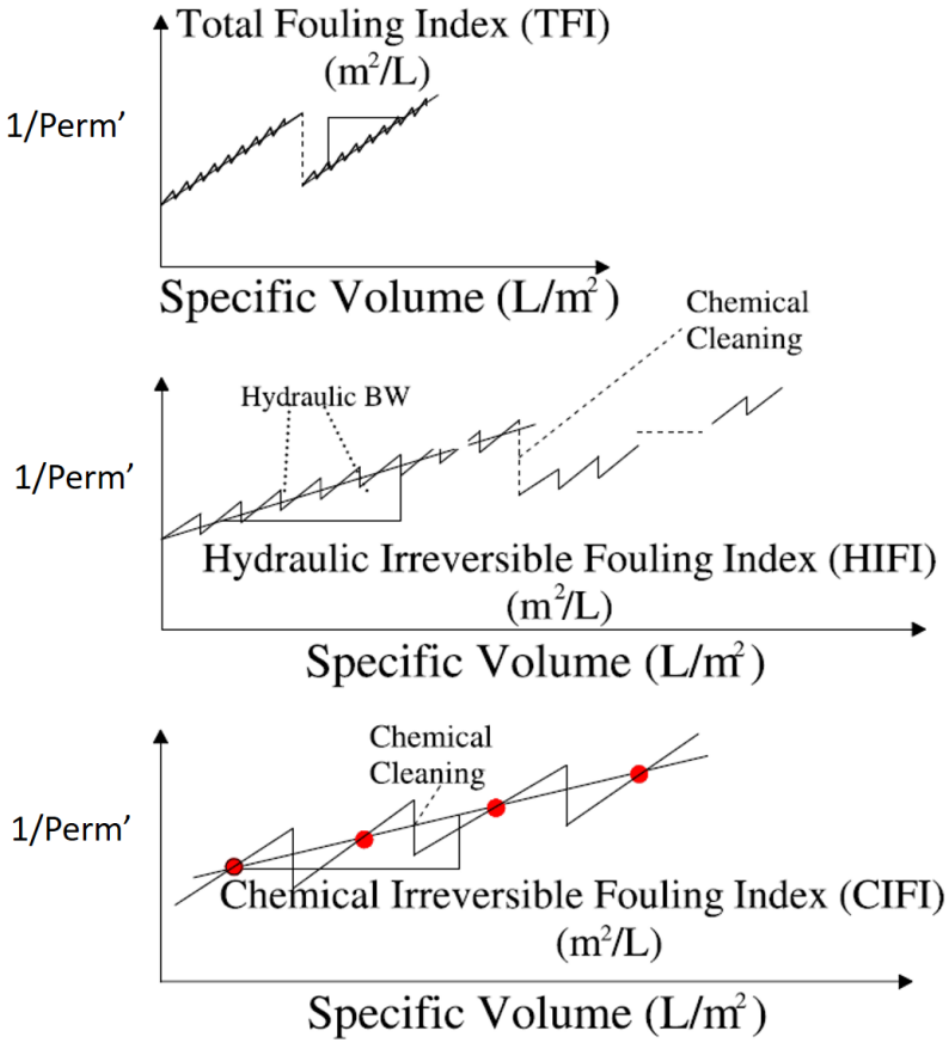

Figure 19: Illustration of fouling indices adopted from A.H. Nguyen et. al. [48].

4.3.2. Change in permeability

The most classical way for determining the physical cleaning's efficiency is to look at the permeability of the process. With reference to Figure 20, the permeability of the membrane process will drop over time due to fouling's additional resistance to permeation. The change in permeability (ΔPerm) before and after each rcBWs/CEBs gives a simple and general indicator on the removal of foulants.

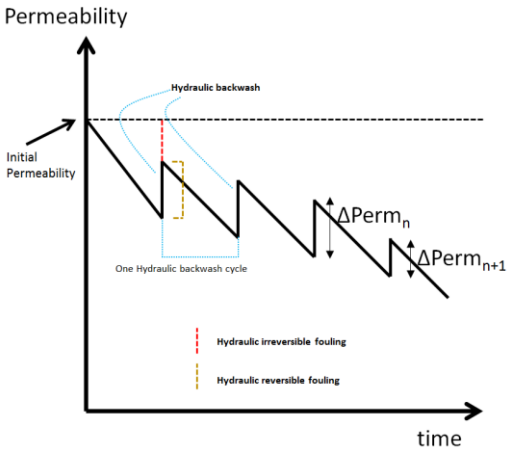

Figure 20: Illustration of ΔPerm.

Both methods of fouling indices and different in permeability will be used for comparison of the efficiency of Capillary Drain in this work.

4.4. Data Evaluation

The process of the data evaluation is illustrated in Figure 21.

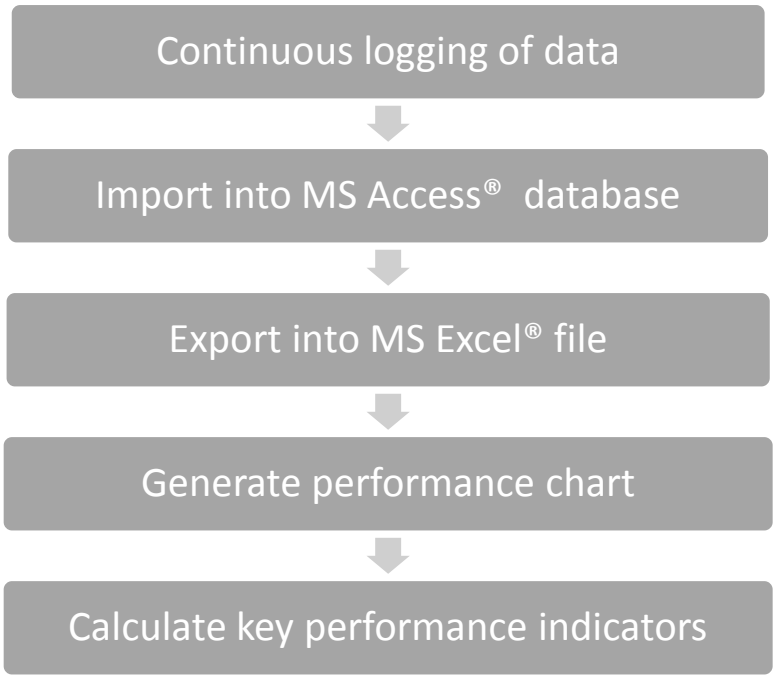

Figure 21: Steps of conducting data analysis.

Physical parameters of PU 22 pilot plant were logged. 44 of them were written into .csv files every 45 seconds during filtration and CEB. Backwash and Capillary Drain were written every second. These daily reports were imported into an MS Access® database, which can be exported to MS Excel® files for generation of performance charts. Flux was evaluated by dividing the recorded feed flow rate by the active membrane area of 80 m^2. TMP was evaluated by difference of pressure between the feed and filtrate side, with correction for the hydrostatic pressure using Eq.3. Permeability was evaluated by dividing the flux by TMP and then normalized to 20°C using Equations 5 and 6. Key performance indicators (Total Fouling and Hydraulic Irreversible Fouling Indices) were calculated using built-in regression function RGP in MS Excel®.

These data, together with parameters of feed water and filtrate, were fed into the statistical program Minitab® 2017 to investigate for potential correlations. Further details will be explained separately in Section 6.

5. Results and discussion

This section describes the results obtained from the pilot plant for discussion of effect of Capillary Drain.

5.1. Effect of Capillary Drain

Figure 22 illustrates the membrane process's performance of Line 2 with and without Capillary Drain. Blue-filled circles and yellow-filled circles represent the introduction of CEB and Capillary Drain, respectively. Unless otherwise stated, Capillary Drain was always conducted after one filtration cycle.

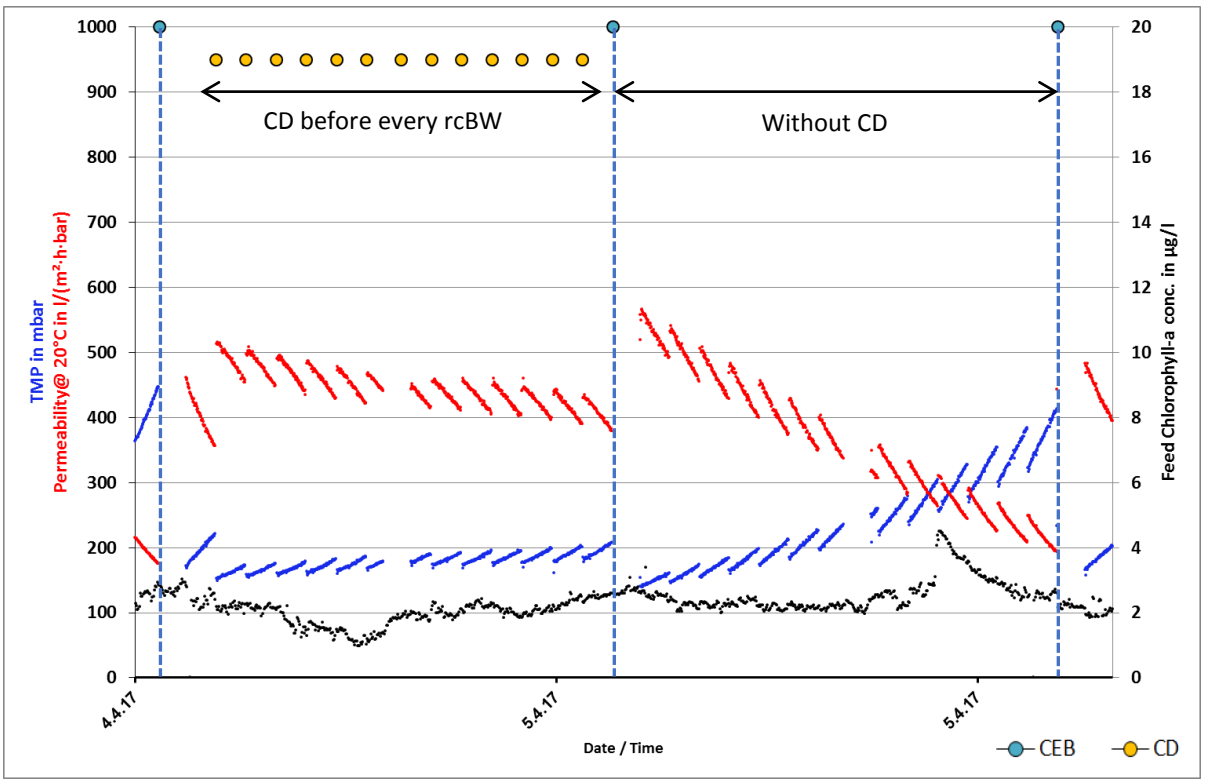

Figure 22: Performance of Line 2 at filtration flux and time of 85 l/(m²·h) and 50 minutes, BW flux and time of 230 l/(m²·h) and 35 seconds, CEB interval of 14.

Remarks for Figure 22

- *CEB interval of 14 means that CEB was conducted after 14 filtration cycles.*
- *A peak of more than 4 µg/L of chlorophyll-a was observed on 5 April 2017 around 2223 hours lasting around 1.5 hours. Despite of this, performance of Line 2 did not show abrupt changes for TMP and permeability.*

The positive effect of Capillary Drain is clearly shown in Figure 22. For the chemical cleaning cycle when Capillary Drain was introduced before every rcBW, the rate of permeability decrease was slower

than chemical cleaning cycle without Capillary Drain. To demonstrate this with Hydraulic Irreversible Fouling Index, "Normalized inverse permeability" was plotted against the specific volume in Figure 23 and the slope was determined. Without Capillary Drain, the Hydraulic Irreversible Fouling Index value is 1.3653 m^2/m^3 as compared to 0.2127 m^2/m^3 for Capillary Drain conducted before every rcBW. Clearly, Capillary Drain had slowed down the rate of increase in resistance. It is important to note that the regression of Total Fouling and Hydraulic Irreversible Fouling Indices follows the method proposed by A.H. Nguyen et. al. [48] using linear regression. This method for obtaining Total Fouling and Hydraulic Irreversible Fouling Indices are meant for interpretation of results and not trying to fit the best model with the experimental data.

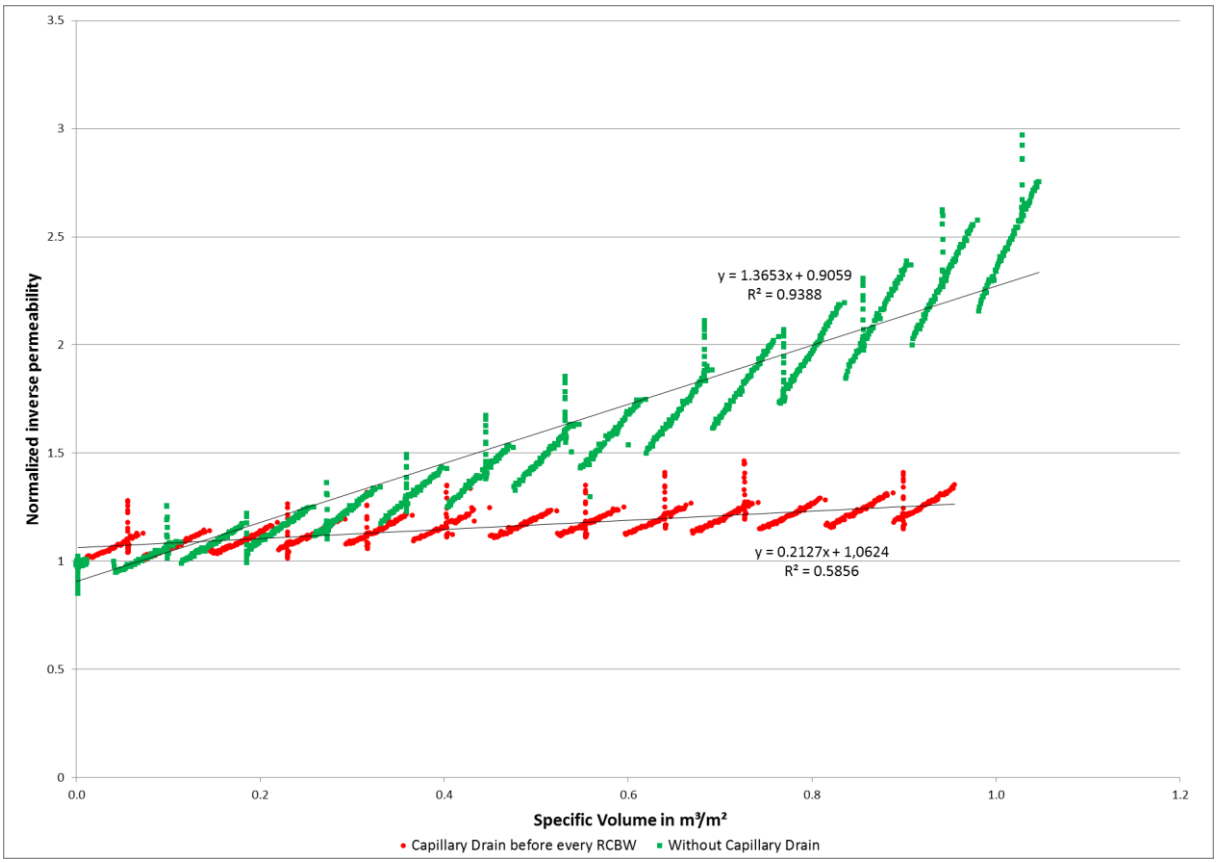

Figure 23: Hydraulic Irreversible Fouling Index plot for chemical cleaning cycle with Capillary Drain before every rcBW (red) and without Capillary Drain (green).

Remarks for Figure 23

- *The "high peaks" in the Hydraulic Irreversible Fouling Index plots were caused in one line when the other was in backwash mode.*
- *The change in R^2 was < 1% and change in Hydraulic Irreversible Fouling Index values were < 3% when these points were removed manually. This was deemed acceptable by inge GmbH and thus, the data points were kept.*

5.2. Effect of a single Capillary Drain after and in between CEBs

Conducting Capillary Drain after every filtration cycle can lower the availability of the membrane process. In this section, effect of conducting a single Capillary Drain was investigated. Figure 24 illustrates the membrane process's performance of Line 1 at 76 l/(m²·h) when a single Capillary Drain was introduced within a chemical cleaning cycle (i) one filtration cycle after CEB and (ii) in between the CEBs.

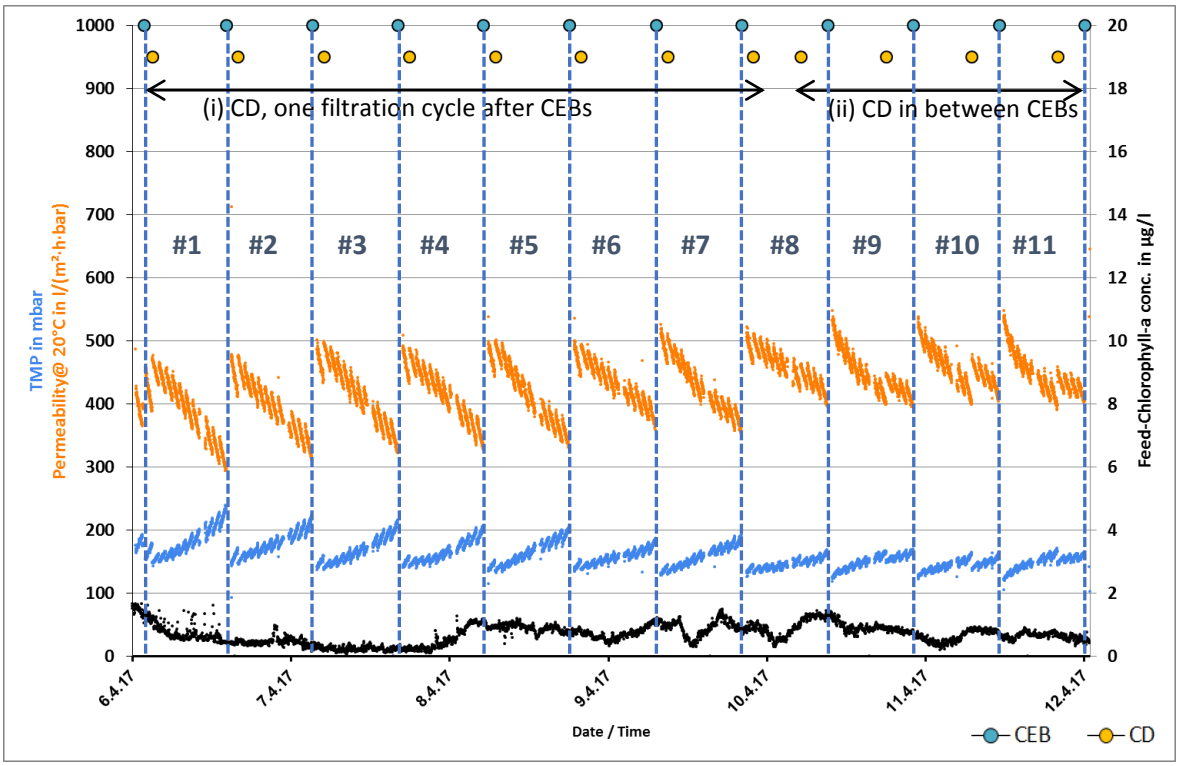

Figure 24: Performance of Line 1 at filtration flux and time of 76 l/(m²·h) and 60 minutes, BW flux and time of 230 l/(m²·h) and 35 seconds, CEB interval of 12.

In order to show the rate of increase in resistance were slowed down with the introduction of Capillary Drain, Total Fouling Indices for filtration cycles before and after conducting Capillary Drain, together with Hydraulic Irreversible Fouling Index were determined for chemical cleaning cycle #1 to #11. These fouling indices were determined in similar fashion as Figure 23 and thus, the values will be summarized in Figure 25 and 26 as bar charts.

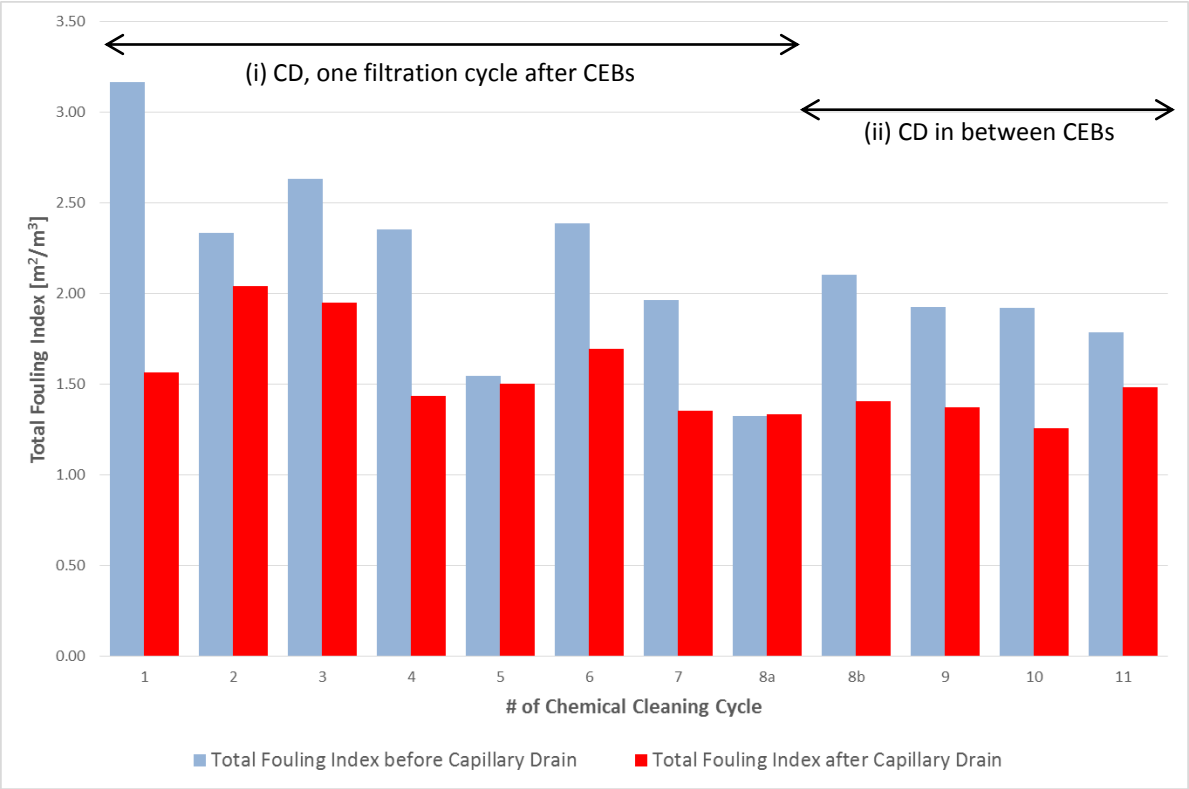

Figure 25: Summarized Total Fouling Indices for Line 1 at filtration flux and time of 76 l/(m²·h) and 60 minutes, BW flux and time of 230 l/(m²·h) and 35 seconds, CEB interval of 12.

Remarks for Figure 25

- *For chemical cleaning cycle #8, Total Fouling Indices for "Capillary Drain, one filtration cycle after CEB" and "in between CEB" were named as #8a and 8b respectively, due to parameter setting changes.*

From Figure 25, the Total Fouling Indices for filtration cycles after introduction of Capillary Drain were all lower than the Total Fouling Indices for filtration cycles before Capillary Drain, except for chemical cleaning cycle #8a (equal Total Fouling Indices). Clearly, the rate of increase in resistance was slowed down.

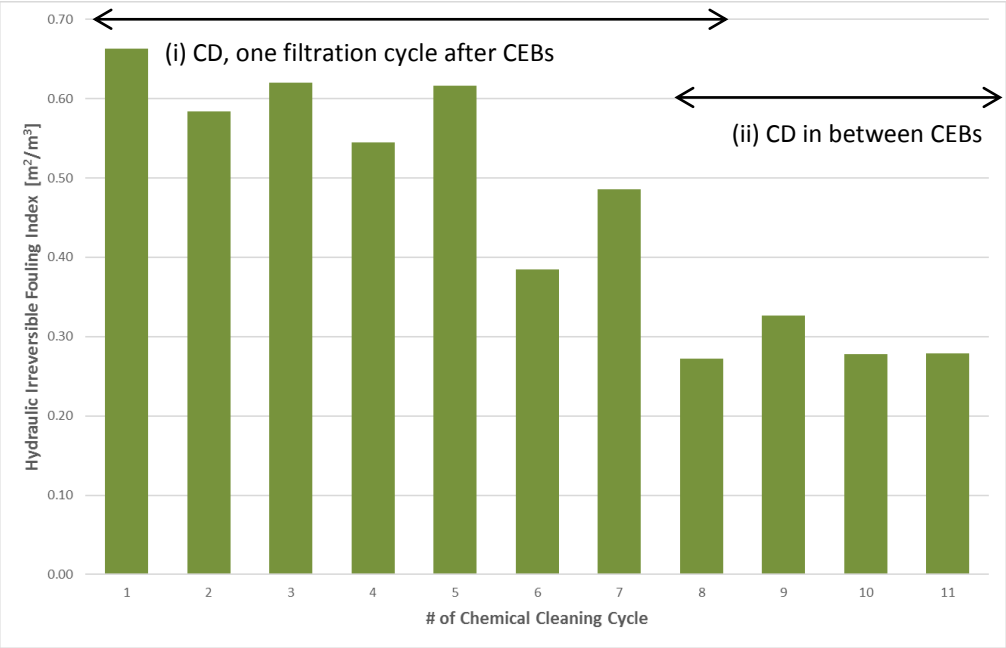

Figure 26: Summarized Hydraulic Irreversible Fouling Indices for Line 1 at filtration flux and time of 76 l/(m²·h) and 60 minutes, BW flux and time of 230 l/(m²·h) and 35 seconds, CEB interval of 12.

All values of Hydraulic Irreversible Fouling Indices from Figure 26 are lower than 1.365 m^2/m^3 (the Hydraulic Irreversible Fouling Index without Capillary Drain). When Capillary Drain was introduced in between CEBs (chemical cleaning cycle #9-11), the Hydraulic Irreversible Fouling Indices were lower than when Capillary Drain was introduced one filtration cycle after CEBs (chemical cleaning cycle #1-7). This showed that the rate of increase in resistance was slower when Capillary Drain was introduced in between CEBs. It is possibly due to the cumulative "available fouling" for removal. After a CEB, one can expect a large removal of foulants and thus, introducing a Capillary Drain after one filtration cycle probably did not enhance foulant removal because there was not enough "available fouling". Introducing Capillary Drain in between CEBs had shown to be more efficient as it first allowed some fouling to build up in the capillaries. After which, Capillary Drain can enhance the foulant removal by disrupting its fouling layer (cake formation, biofilm formation etc.). To verify this, ΔPerm, i.e. the change in permeability, before and after rcBWs/CEBs, was plotted against time shown in Figure 27.

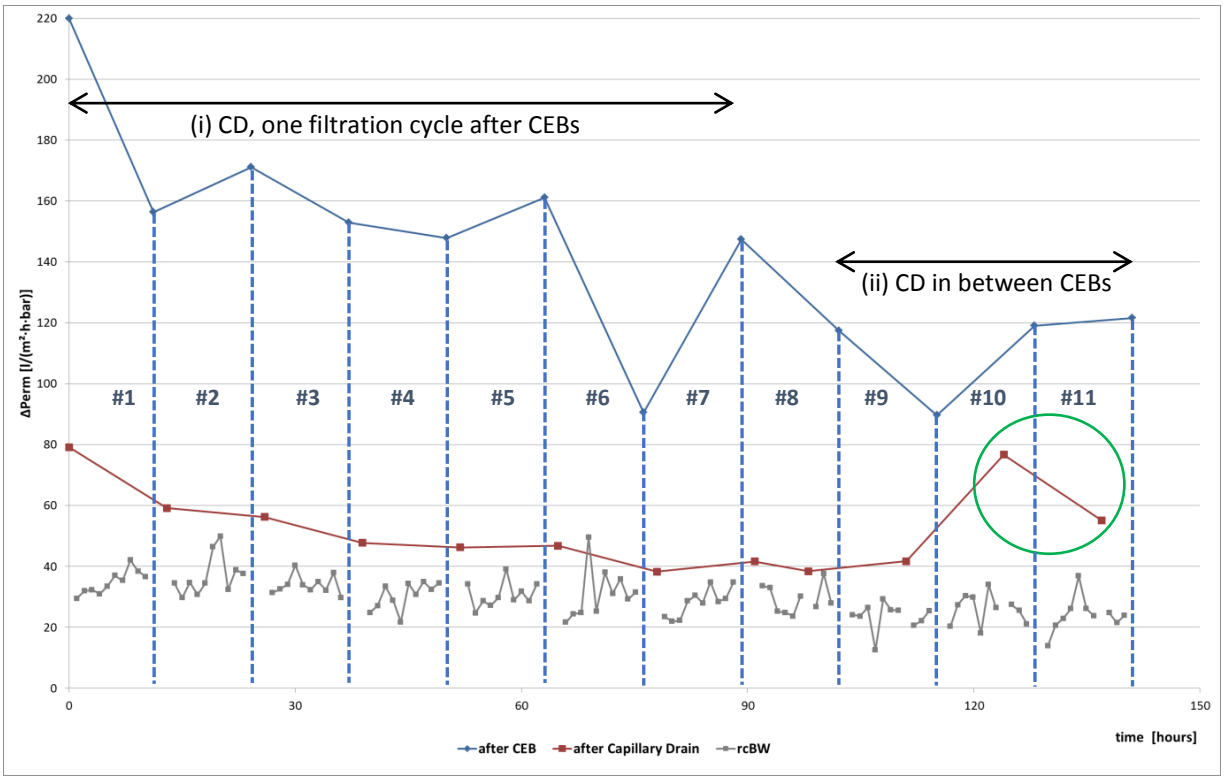

Figure 27: ΔPerm against time for Capillary Drain conducted right after and in between the CEBs for Line 1 at 76 l/(m²·h).

Highest ΔPerm values were observed when CEB was conducted as it removed hydraulically irreversible fouling. Interestingly, conducting a Capillary Drain helped rcBW to achieve a higher ΔPerm, shown as the red line named "after Capillary Drain". Physically, this indicates rcBW can remove some irreversible fouling with the help of Capillary Drain. The levels of ΔPerm was more or less around 50 l/(m²·h·bar) when Capillary Drain was introduced one filtration cycle after CEB. When Capillary Drain was switched in between CEBs, a higher ΔPerm can be achieved (circled in green). This agrees with the point that introducing Capillary Drain in between CEBs is more efficient as it first allowed some fouling to build up in the capillaries.

5.3. Effect of single Capillary Drain within a chemical cleaning cycle at different flux

Figure 28 and 29 illustrates the membrane process's performance when a single Capillary Drain was introduced within a chemical cleaning cycle in between the CEBs for (i) Line 2 at 85 l/(m²·h) and (ii) Line 1 at 92 l/(m²·h).

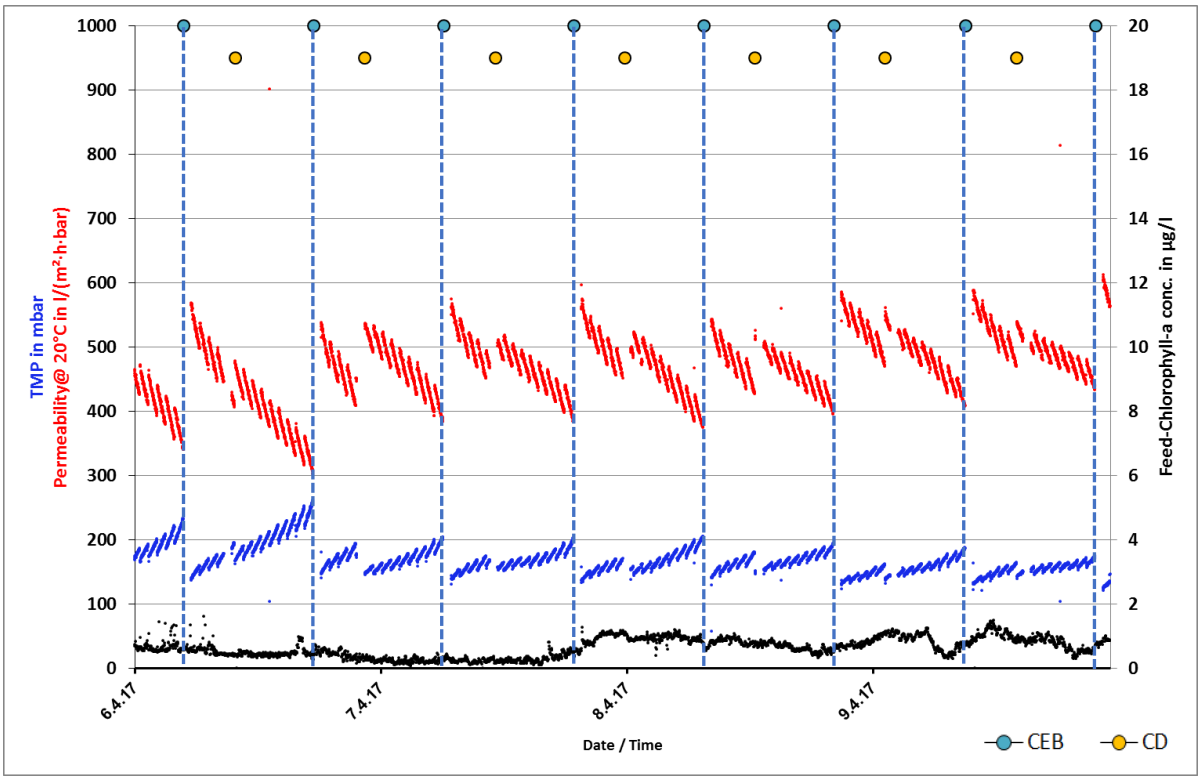

Figure 28: Performance of Line 2 at filtration flux and time of 85 l/(m²·h) and 50 minutes, BW flux and time of 230 l/(m²·h) and 35 seconds, CEB interval of 14.

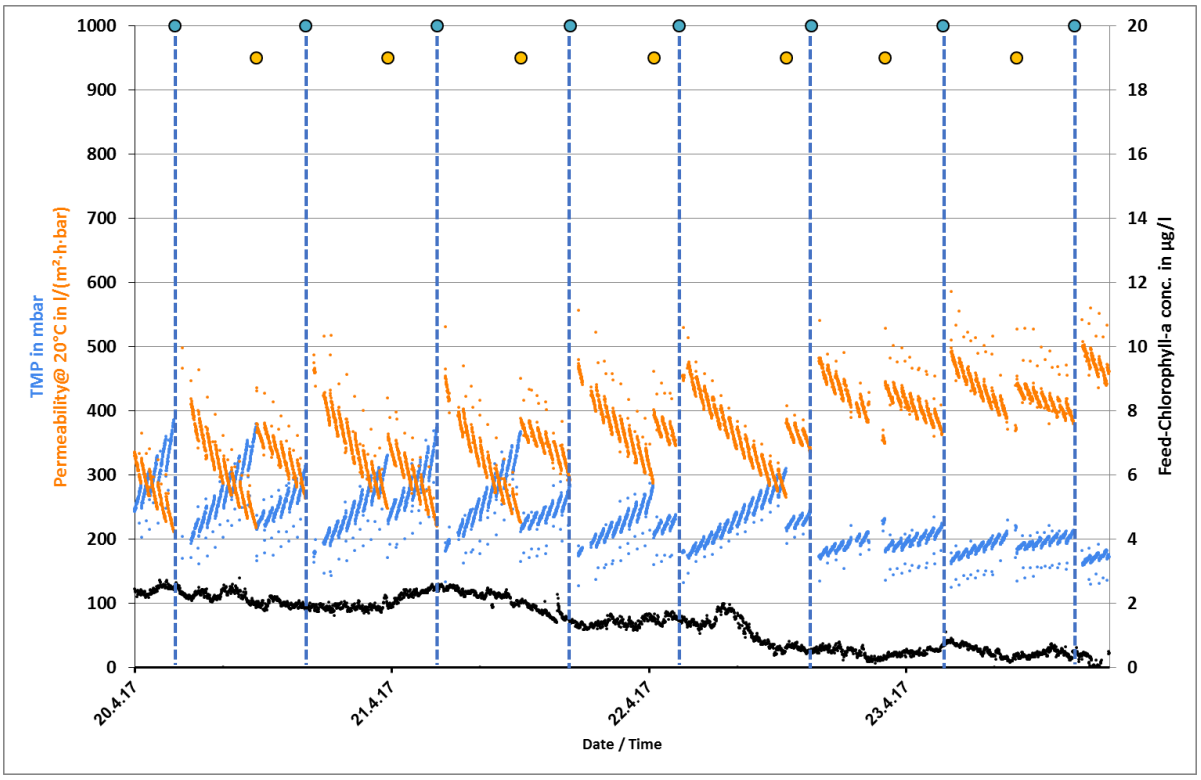

Figure 29: Performance of Line 1 at filtration flux and time of 92 l/(m²·h) and 45 minutes, BW flux and time of 230 l/(m²·h) and 35 seconds, CEB interval of 15.

Together with data for single Capillary Drain introduced within a chemical cleaning cycle at 76 l/(m²·h) (Section 5.2), the Total Fouling Indices for filtration cycles before and after introduction of Capillary Drain were determined for all chemical cleaning cycle. It was observed that all Total Fouling Indices for filtration cycles after introduction of Capillary Drain were lower than Total Fouling Indices for its respective filtration cycles before Capillary Drain. The beneficial effect from Capillary Drain is clear and the averages are shown in Figure 30.

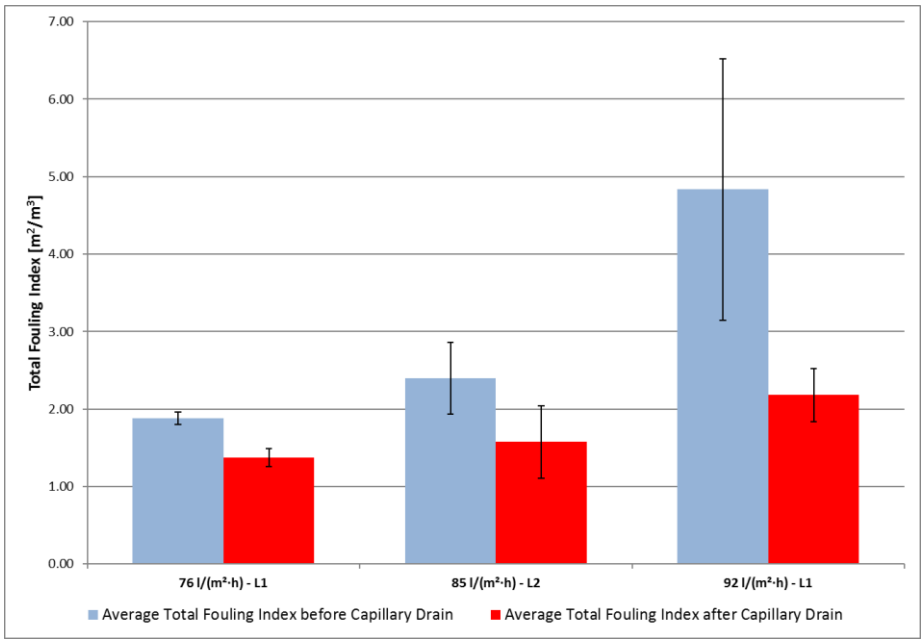

Figure 30: Average Total Fouling Indices of filtration cycles before and after conducting Capillary Drain, at different flux.

5.4. Effect of a single Capillary Drain during fluctuation of chlorophyll-a concentration

Figure 31 and 32 illustrates the membrane process's performance during a fluctuation of chlorophyll-a when a single Capillary Drain was introduced within a chemical cleaning cycle in between the CEBs for (i) Line 1 at 85 l/(m²·h) and (ii) Line 2 at 92 l/(m²·h).

Between 12th to 19th April 2017, chlorophyll-a concentration exceeded 4 µg/l (chemical cleaning cycle #2, #4-9). As a result, there was an impact on the performance of membrane process. The TMP increased from around 200mbar to 700mbar and 1000mbar for Line 1 and 2, respectively. The situation was brought under control after two days by doubling the concentration of chlorine and soaking duration. After which, the values of these chemical cleaning parameters were reset to their previous level. As such, direct comparison is not possible but in this section, the results will be presented to have a better understanding of what happened when Capillary Drain was introduced alongside a fluctuation in chlorophyll-a concentration.

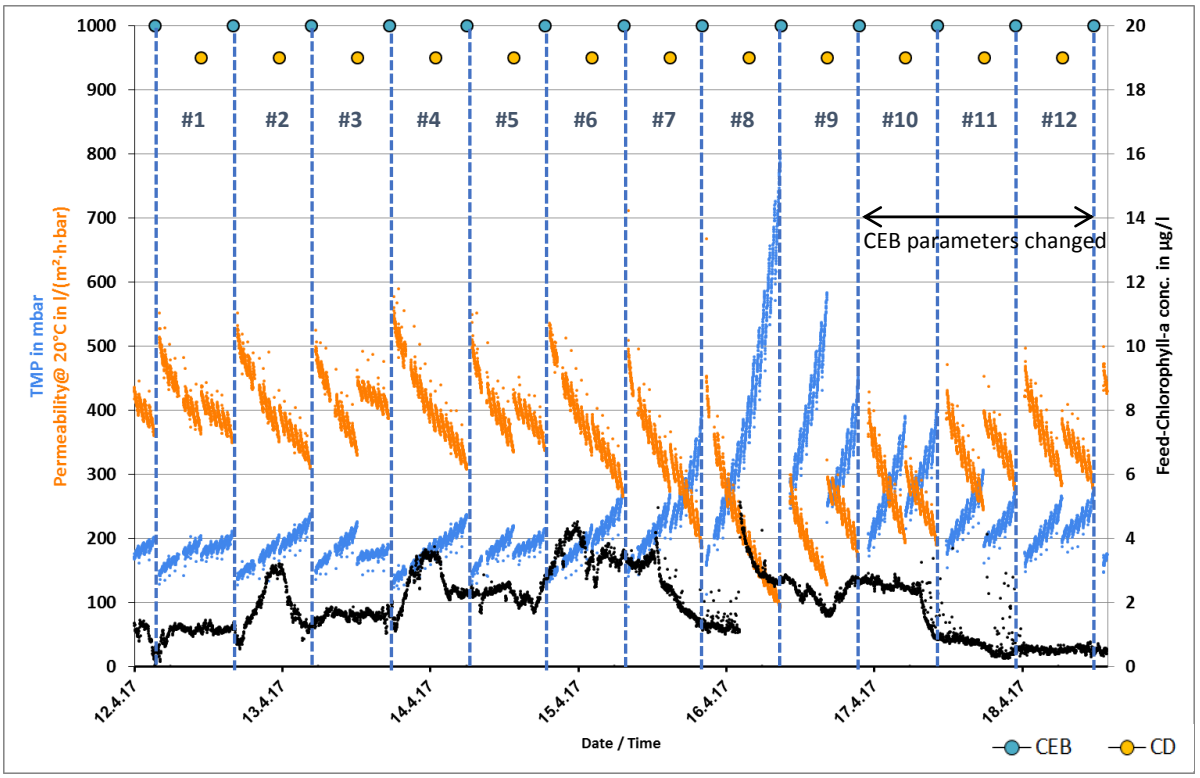

Figure 31: Performance of Line 1 at filtration flux and time of 85 l/(m²·h) and 50 minutes, BW flux and time of 230 l/(m²·h) and 35 seconds, CEB interval of 14.

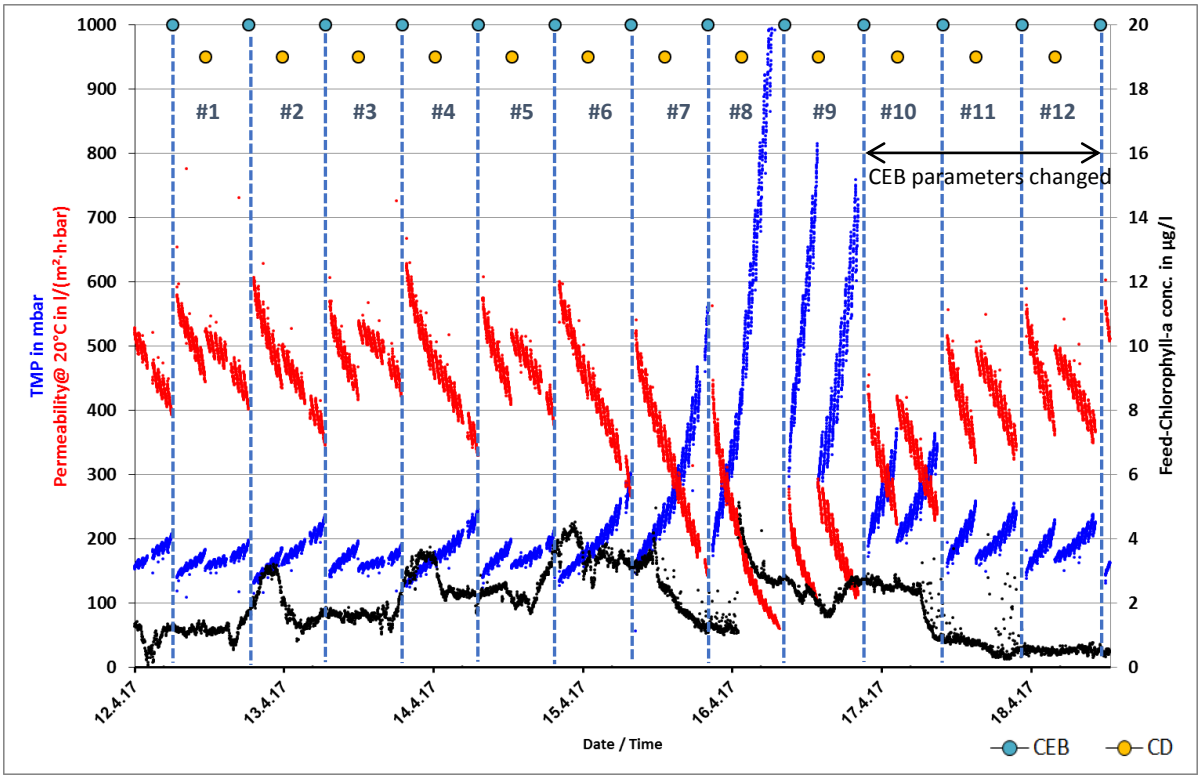

Figure 32: Performance of Line 2 at filtration flux and time of 92 l/(m²·h) and 45 minutes, BW flux and time of 230 l/(m²·h) and 35 seconds, CEB interval of 15.

An increasing trend of Hydraulic Irreversible Fouling Index can be observed when there was an increase in chlorophyll-a concentration. This is indicated in Figure 33 with blue and red lines. Therefore, Hydraulic Irreversible Fouling Indices can indicate a fluctuation of chlorophyll-a concentration in feed water. The concentration profile during fluctuation of chlorophyll-a from bbe AlgalGuard® is presented in Figure 34.

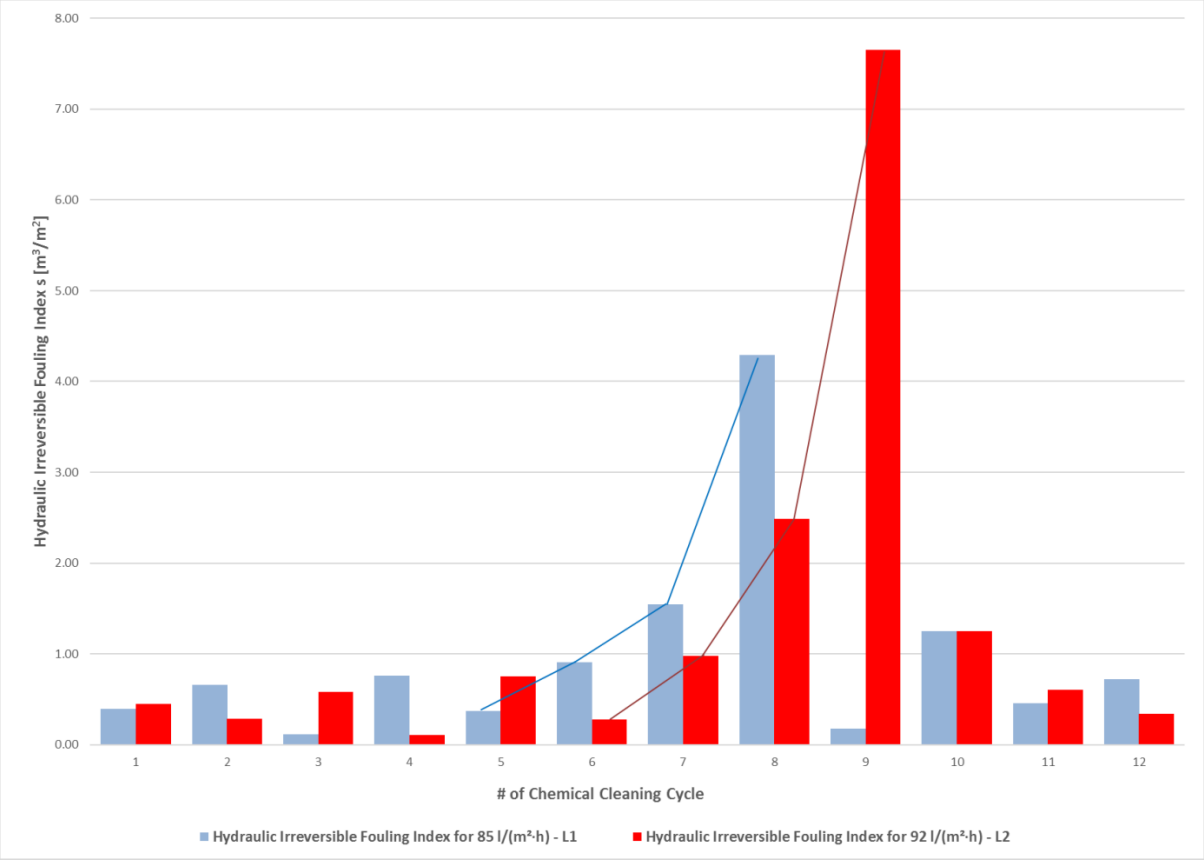

Figure 33: Hydraulic Irreversible Fouling Indices at 85 l/(m²·h) (Line 1) and 92 l/(m²·h) (Line 2) during fluctuation in chlorophyll-a concentration.

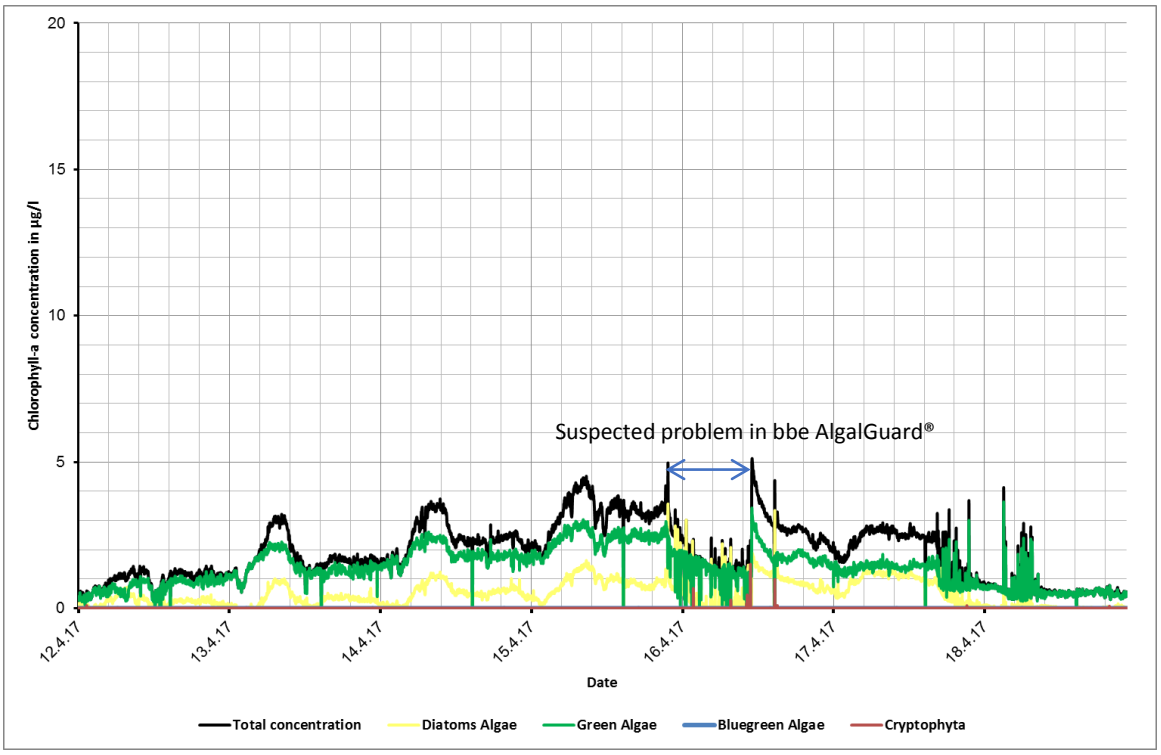

Figure 34: Concentration profile during fluctuation of feed chlorophyll-a concentration.

When the performance of both lines experienced high increase in TMP, the bbe AlgalGuard® seem to show a large contribution of chlorophyll-a concentration from green algae. There was also a period when the concentrations suddenly decreased. It is suspected that there might be too much algae clogging the inlet tubes of the bbe AlgalGuard® device and measurement was then not possible. The bbe AlgalGuard® needs regular cleaning and proper maintenance in order to avoid any possible clogging problem.

Both the performance curves and Hydraulic Irreversible Fouling Indices are not enough to explain the effect of Capillary Drain during fluctuation of chlorophyll-a concentration. ΔPerm plot (Figure 35 and 36) can be useful in this case. Before there was a fluctuation of chlorophyll-a concentration, a similar trend with Figure 27 is seen. The highest ΔPerm values were observed when CEB was conducted, due to removal of hydraulically irreversible fouling. Also, introducing a Capillary Drain helped rcBW to achieve a higher ΔPerm than just rcBW alone (circled in green).

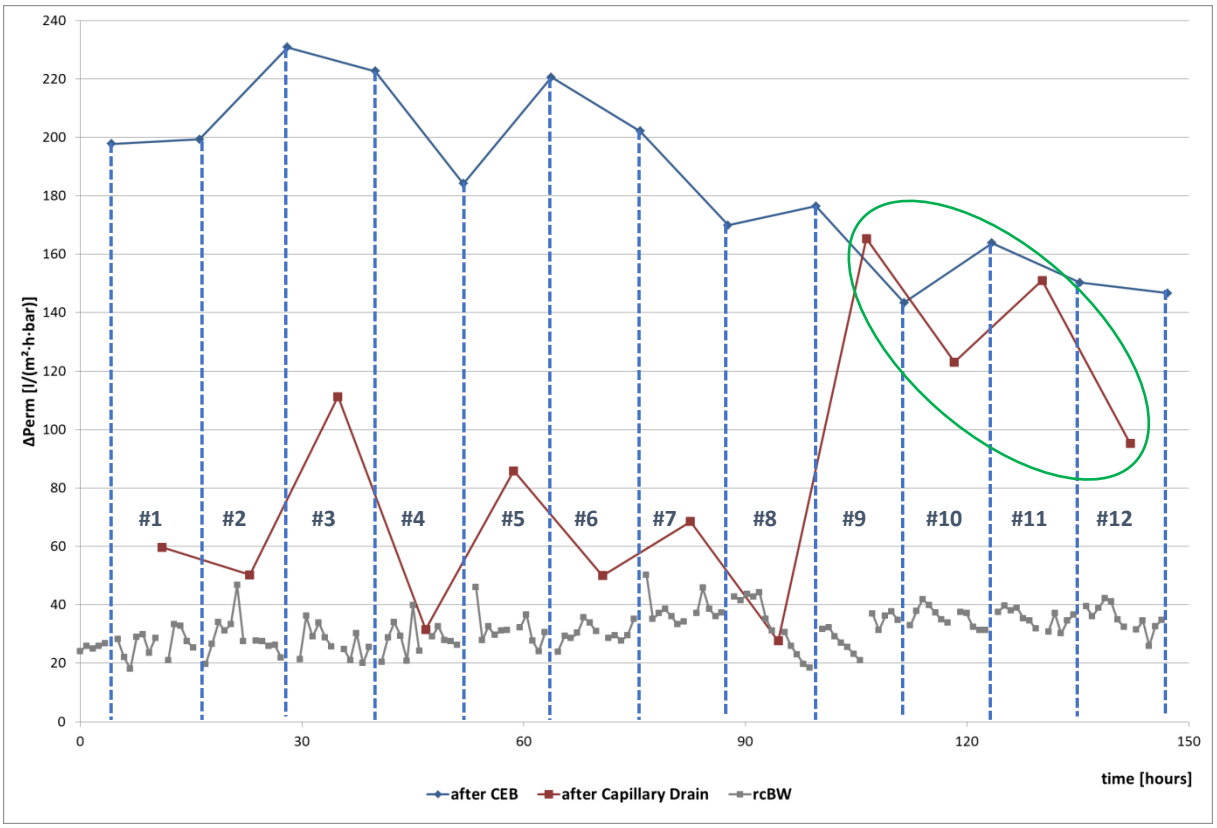

Figure 35: ΔPerm against time for Capillary Drain conducted in between the CEBs for Line 1 at 85 l/(m²·h) during fluctuation of chlorophyll-a concentration

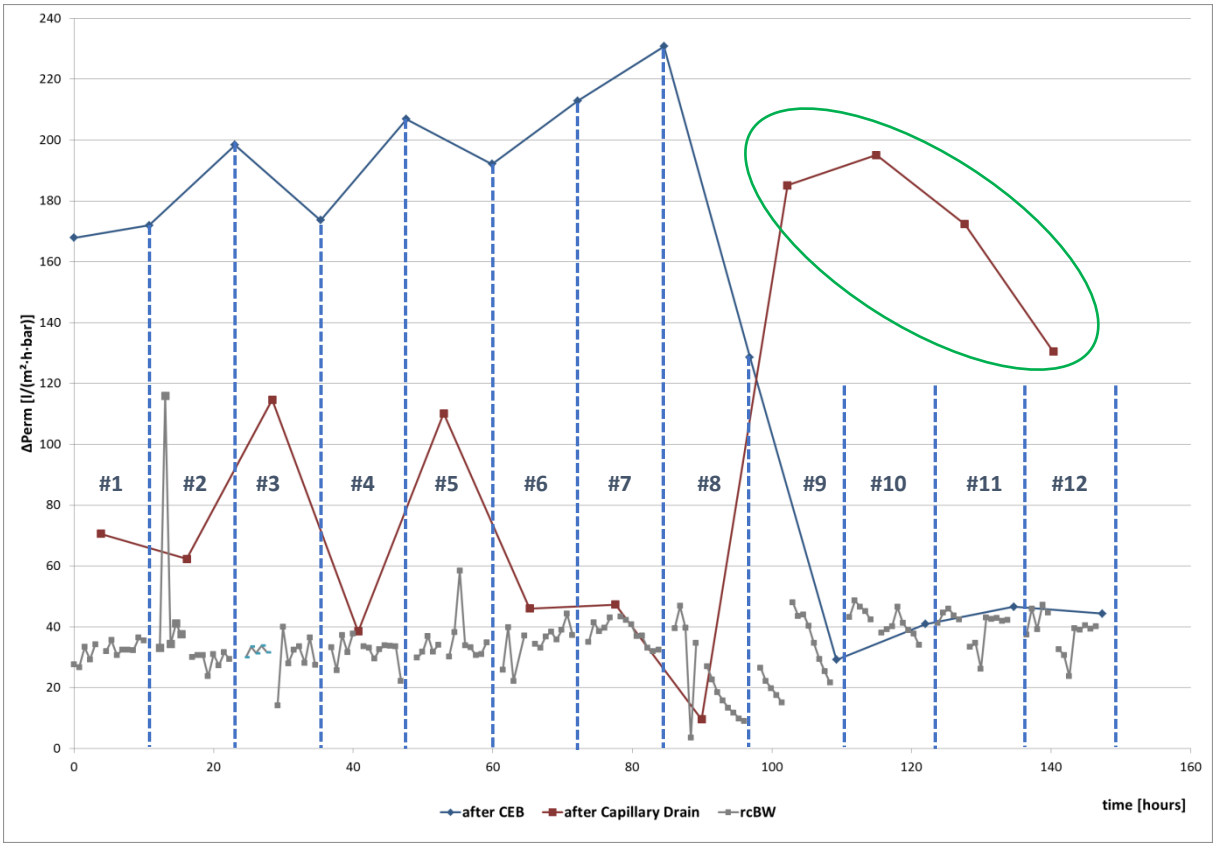

Figure 36: ΔPerm against time for Capillary Drain conducted in between the CEBs for Line 2 at 92 l/(m²·h) during fluctuation of chlorophyll-a concentration.

However, this trend changed after the chemical concentration (free chlorine) and soaking time were increased. Surprisingly, one can see a higher ΔPerm values after conducting Capillary Drain (chemical cleaning cycle #9 – 12) as compared to lower ΔPerm values from CEBs. Physically, this means that the CEBs did not seem to efficiently remove the fouling as compared to previous levels. Additionally, Capillary Drain helped to further improve the removal of fouling by rcBW as the chlorophyll-a concentration increased.

The increase of chemical concentration (free chlorine) and soaking time may also have assisted in improving Capillary Drain's performance for fouling removal. The CEB alone did not result in a better fouling removal but may have instead, "lossen" the fouling layer. As such, when Capillary Drain was introduced after a CEB with higher intensity, the combination improved the cleaning for fouling removal.

5.5. Possible explanation of beneficial effects from Capillary Drain

The reason behind the positive effect of Capillary Drain is probably due to brief period of 2-phase flow. Mentioned previously in Section 3.2, C. Cabassud and co-workers at INSA, (Toulouse, France) have been investigating inside-out hollow fiber membrane applications with air in both filtration and backwash since 1997 [44-46]. They demonstrated that 2-phase flow exists in capillary of membrane with inner diameter less than 1 mm when both air and water were injected into the capillary simultaneously at different velocities. It can exist as bubbles flow or slugs flow as shown below:

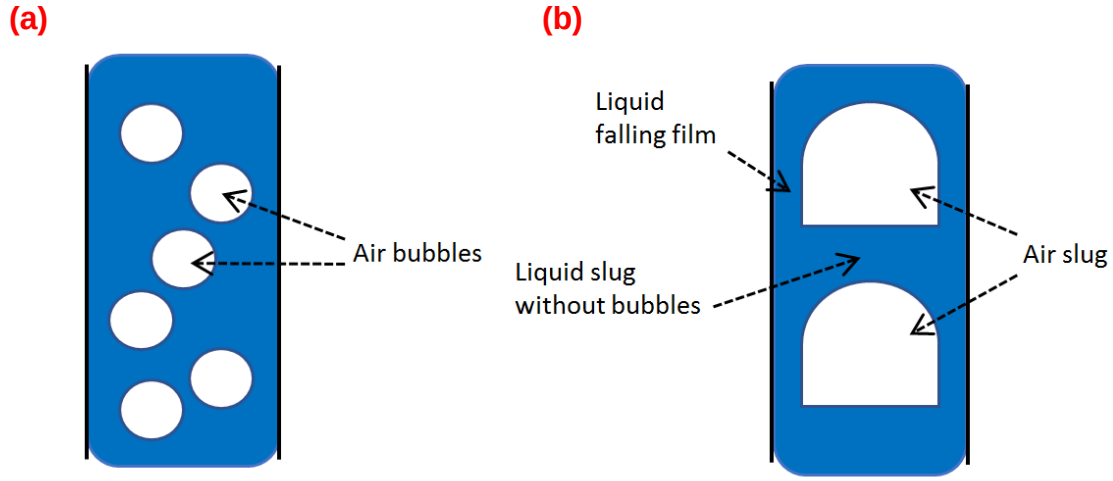

Figure 37: 2-phase flow in terms of (a) Bubbles flow (b) slugs flow, adopted from C. Cabassud [44-46].

The most important different between their work and the Capillary Drain proposed by process development from inge GmbH is that Capillary Drain has no simultaneous injection of air and water. Thus, it is not possible to predict accurately the type of 2-phase flow. However, there could be two possibilities to explain how Capillary Drain helps to improve the efficiency of hydraulic backwash.

5.5.1. Possibility 1 - Compressed air entered the fouling layer

During the dewatering step, compressed air with pressure of 1 bar entered the lumen of the fibers, allowing water to permeate through the membrane while air is retained. This is illustrated in Figure 38.

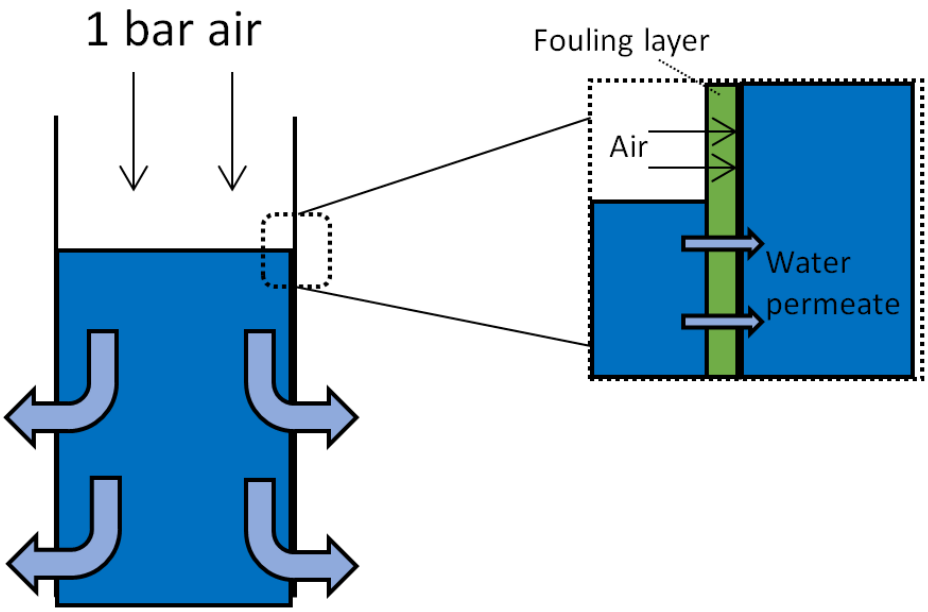

Figure 38: Air entering the porous fouling layer.

The compressed air could enter the voids of the porous fouling layer (such as the cake layer), causing a "loosening" effect. A hydraulic backwash can then be more efficient as fouling is "loosen". As fouling was removed more efficiently, subsequent fouling formation (such as cake layer) could take longer to be established. Thus, the Total Fouling and Hydraulic Irreversible Fouling Indices were observed to be lower after the introduction of Capillary Drain.

It is important to note that there is also a possibility that the porous fouling layer might also be compressed if the pressure-hold time is long.

5.5.2. Possibility 2 - Occurrence of bubble or slug flow

After the dewatering step, the capillaries of the membrane were filled with air before hydraulic backwash was conducted. Referring to Figure 39a, when backwash is conducted, the liquid enters the capillaries along the length of the membrane. There might be some "trapped" air trying to escape leave the capillaries while water entered capillaries. 2-phase flow in terms of either bubbles or slugs flow in nature could be established for a brief period and result in some kind of a shear stress along the wall. This could also make it easier to remove the fouling layer.

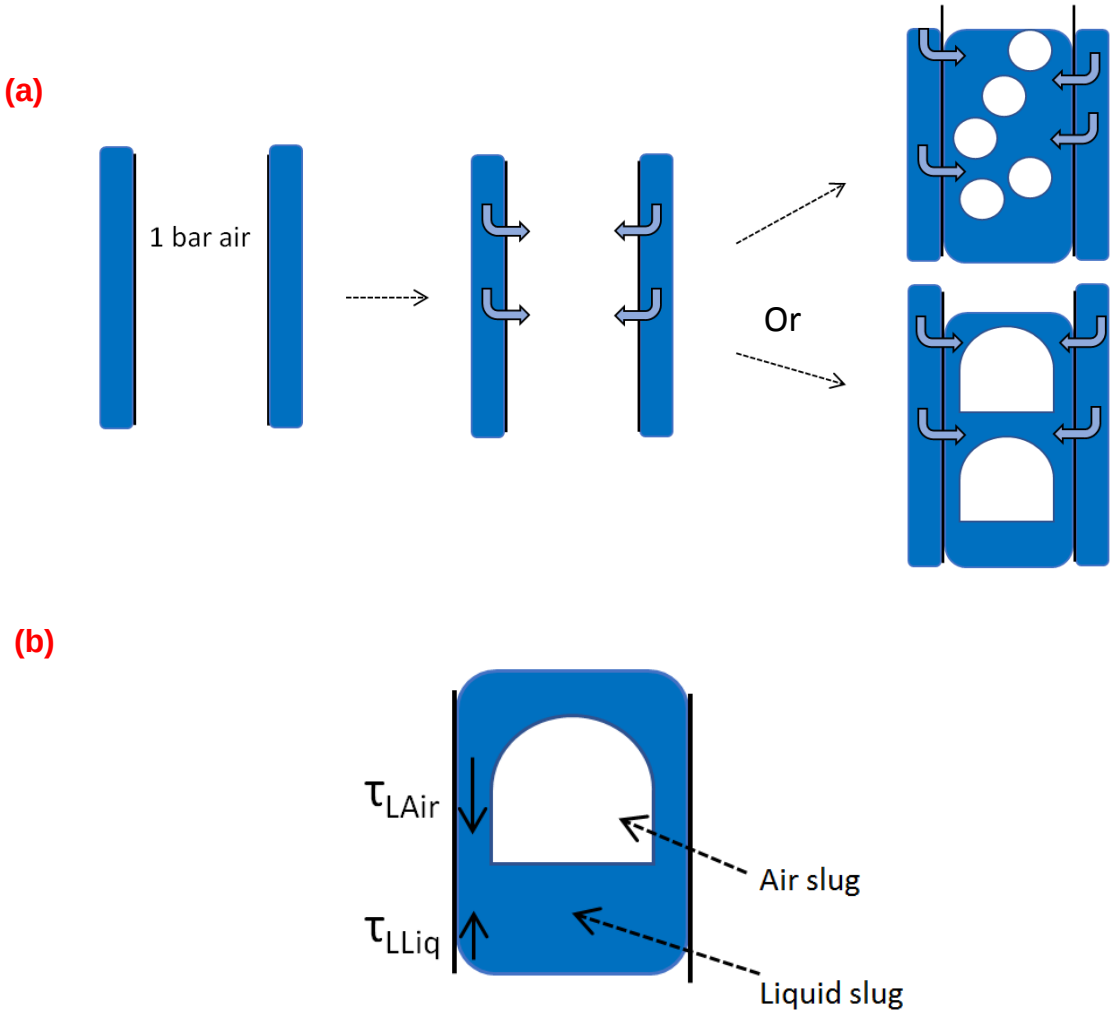

Figure 39: (a) Development of 2-phase flow (b) Shear stress on membrane surface [44-46].

In Figure 39b, the slug flow in particular can induce τ_{Lair} and τ_{LLiq}, the shear stresses on the wall by air slug and liquid slug respectively, and disrupt the cake formation. Recalling Figure 12 from Section 2.4.3, the shear stresses on the wall can also help to reduce particulate fouling by algal bloom.

6. Correlations between feed water parameters

In this section, parameters of feed water and filtrate were investigated for potential correlations. Minitab® 2017, a statistical program was used to check if two parameters have any statistically significant relationship. The parameters of interest are shown in Table 8 and grouped into X-variables and Y-variables. For each pair of variable, the "Fitted Line Plots" function, which uses the least square method for regression, was applied to see if the X-variable (predictor) can be fitted into a model to predict the Y-variable (response).

SDIs were not constantly measured. The foreign operators usually measured SDI once a day but there were times when SDI data is unavailable for some days. In February 2017, SDI data of feed stream came from the line with dissolved air flotation (DAF). From March to April 2017, SDI data of feed stream came directly from the seawater. Thus, regressions involving SDIs are done with "matching dates" of the available data.

Data for chlorophyll-a, green algae and diatoms concentrations were available from bbe AlgalGuard® with the time interval of every 97 seconds. Data for turbidity and permeability (filtration only) of both lines were available every 45 seconds. The different time interval is due to different measuring devices or sensors. Thus, these data from month of April 2017 were sorted into hourly and daily averages. Data during fluctuation of chlorophyll-a concentration were sorted into 10minutes-average in order to have a more detailed analysis. There were some periods when bbe AlgalGuard® was not working properly. Essentially, data from this period were deleted.

Data for Total Fouling Indices, during fluctuation of chlorophyll-a concentration, were sorted together with the "filtration cycle average" of total chlorophyll-a concentration. Due to the fact that Line 1 and Line 2 were operating at a filtration cycle of 50 and 45 minutes, respectively, hourly and 10minutes-averages is less suitable.

All data were sorted using MS EXCEL® before copying into Minitab® 2017 for "Fitted Line Plots" with a confidence interval of 95%. The results of R^2 and *p-values* are summarized in Table 8.

Table 8: Summary of regression variables, highlighted in red is not statistically significant as its *p-value* is more than 0.05.

Regression variables			**R^2**	***p-value* of regression**
Pair #	**Y-variable (Response)**	**X-Variable (Predictor)**	**-**	**-**
1	Perm L1 (hourly avg) [l/(m²·h·bar)]	Green algae (hourly avg) [µg/l]	0.095	<0.001
2	Perm L2 (hourly avg) [l/(m²·h·bar)]	Green algae (hourly avg) [µg/l]	0.047	<0.001
3	Perm L1 (hourly avg) [l/(m²·h·bar)]	Diatoms (hourly avg) [µg/l]	0.177	<0.001
4	Perm L2 (hourly avg) [l/(m²·h·bar)]	Diatoms (hourly avg) [µg/l]	0.124	<0.001
5	Perm L1 (10-min avg) [l/(m²·h·bar)]	Green algae (10-min avg) [µg/l]	0.002	0.310
6	Perm L2 (10-min avg) [l/(m²·h·bar)]	Green algae (10-min avg) [µg/l]	0.009	0.016
7	Perm L1 (10-min avg) [l/(m²·h·bar)]	Diatoms (10-min avg) [µg/l]	0.127	<0.001
8	Perm L2 (10-min avg) [l/(m²·h·bar)]	Diatoms (10-min avg) [µg/l]	0.099	<0.001
9	SDI (Feed-seawater, daily) [%/min]	Total chlorophyll-a (daily avg) [µg/l]	0.195	0.031
10	Turbidity of Feed, 10min avg [NTU]	Total chlorophyll-a (10 min avg) [µg/l]	0.029	<0.001
11	Turbidity of Feed, 10min avg [NTU]	Turbidity of Filtrate 10min avg [NTU]	0.001	0.078
12	SDI of Feed- seawater daily) [%/min] ***April only***	SDI of Filtrate (daily) [%/min] ***April only***	0.000	0.984
13	SDI of Feed- seawater (daily) [%/min] ***All available data***	SDI of Filtrate (daily) [%/min] ***All available data***	0.000	0.887
14	SDI of Feed-DAF (daily) [%/min] ***Different months***	SDI of Feed-seawater (daily) [%/min] ***Different months***	0.068	0.617
15	TSS [mg/l]	Total chlorophyll-a (daily avg) [µg/l]	0.093	0.695
16	Total Fouling Indices L1 [m^2/m^3]	Total chlorophyll-a (50-min filtration cycle avg) [µg/l]	0.026	0.063
17	Total Fouling Indices L2 [m^2/m^3]	Total chlorophyll-a (45-min filtration cycle avg) [µg/l]	0.023	0.066

At first hand, a quick glance of the R^2 column show all values of R^2 were low, with the highest value of 0.195 coming from Pair#9. These values of R^2 are not so useful to indicate any potential relationship between the two variables. Nevertheless, it is important to investigate the *p-values*. Pair#5 and Pair#11-17 have *p-values* of more than 0.05 and have no statistically significant relationship between each pair of variables at a confidence interval of 95%.

As for the other pairs of variables, the follow approach is applied to check for any potential relationship:

1) Educated guess if a potential relationship between the two variables is expected,
2) Check the "Normal Probability Plot" and "Histogram" to ensure residuals are normally distributed,
3) Check "Versus Order" for any trend to ensure that the residuals are independent,
4) Check if "Versus Fits" is equally spread around zero,
5) Check S-value.

6.1. Pair # 9 SDI (Feed-seawater, daily) and Total chlorophyll-a (daily average)

In theory, one can somewhat expect a relationship between these two parameters. SDI[1] is an empirical test for measuring the potential of influent water to foul an RO membrane with suspended solids and colloids. It uses a 0.45 µm filter paper for its measurement and is likely to remove some algae.

It is important to take note that SDI was measured only once a day at an unknown time. In order to perform a regression between SDI and chlorophyll-a concentration, daily average for the latter had to be used. Figure 40 below shows the fitting of the regression and the residual plots.

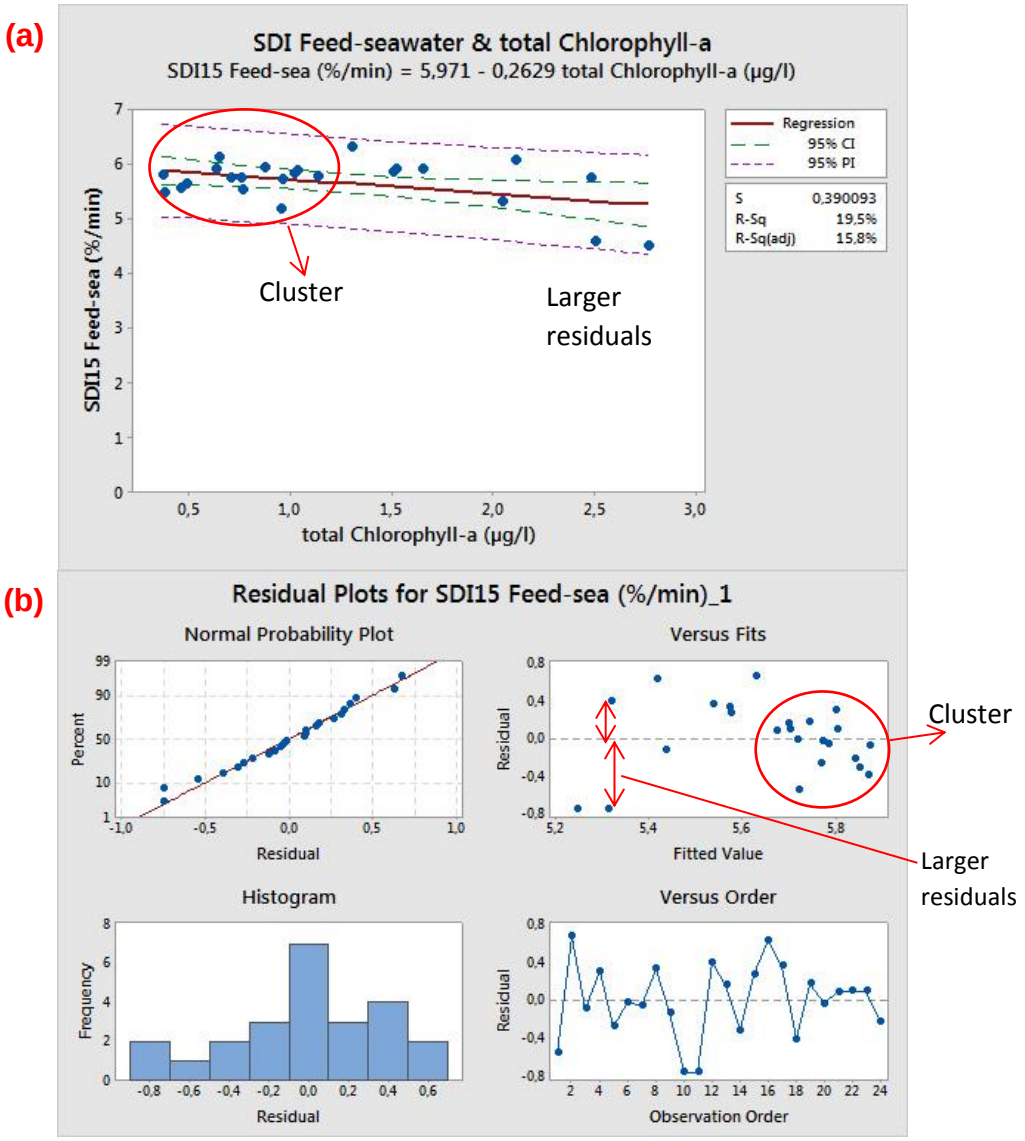

Figure 40: (a) Regression and (b) residual plots for Pair#9.

[1] SDI is determined by the time required to filter 500ml of feed water through a 0.45 µm filter paper at a feed pressure of 30 psig at start and after 15 minutes.

From Figure 40b, the "Normal Probability Plot" and "Histogram" showed that residuals were normally distributed. No particular trend can be seen from "Versus Order" plot. Interestingly, a trend was observed under "Versus Fits". Although the points looked kind of spread out, it has a cluster around fitted value from 5.6 to 5.8 %/min. This cluster of points has lower residual compared to the fitted values from 5.2 to 5.4%/min. A quick check against the regression plot (Figure 40a) shows exactly the same pattern. It seems like the regression plot is suitable to show a relationship between the two variables at a lower range of chlorophyll-a (0.5 to 1.2 µg/l). This kind of statistical phenomenon is known as **heteroscedasticity** [40].

Furthermore, low S-value of 0.39 %/min (the units of S-value is the same as the Y-variable) is 7% of the average mean of Y-variable of 5.65 %/min. In conclusion, for Pair#9 there seem to be a relationship at a lower range of chlorophyll-a concentration.

6.2. Pair # 10 Turbidity of Feed, 10min average and Total chlorophyll-a (10 min average)

In theory, one can somewhat expect a relationship between these two parameters. Turbidity measures the amount of light-scattering in the water sample. Having higher concentration of chlorophyll-a should theoretically increase the light-scattering. Figure 41 below shows the fitting of the regression and the residual plots.

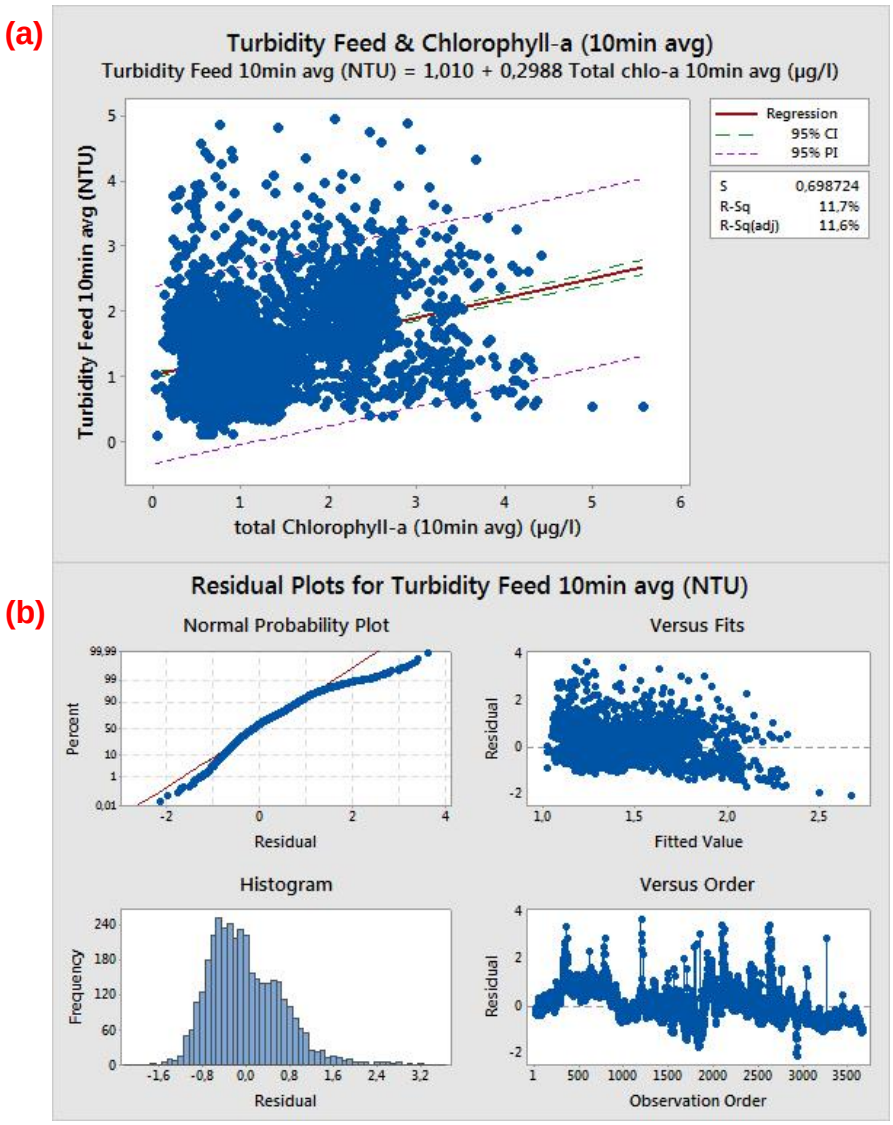

Figure 41: (a) Regression and (b) residual plots for Pair#10.

From Figure 41b, the "Normal Probability Plot" and "Histogram" showed that residuals were normally distributed. No particular trend can be seen from "Versus Order" plot. Interestingly, a trend was observed under "Versus Fits". There is a cluster around fitted value from 1.0 to 2.0. The same cluster of points is observed in the regression plot. Again, it seems like the regression plot is suitable to show a relationship between the two variables at a lower range of chlorophyll-a. On the other hand, S-value of 0.7 NTU may look small but it is 47.6% of the average mean of Y-variable of 1.47 NTU. In conclusion, for Pair#10, it is unlikely for a relationship between the pair of variables.

6.3. Pairs involving permeability

Pair #1 to 8 where the permeability was involved, a first look into their "Versus order" plots already shows a certain pattern. As an example, the figures for Pair# 5 are showed below.

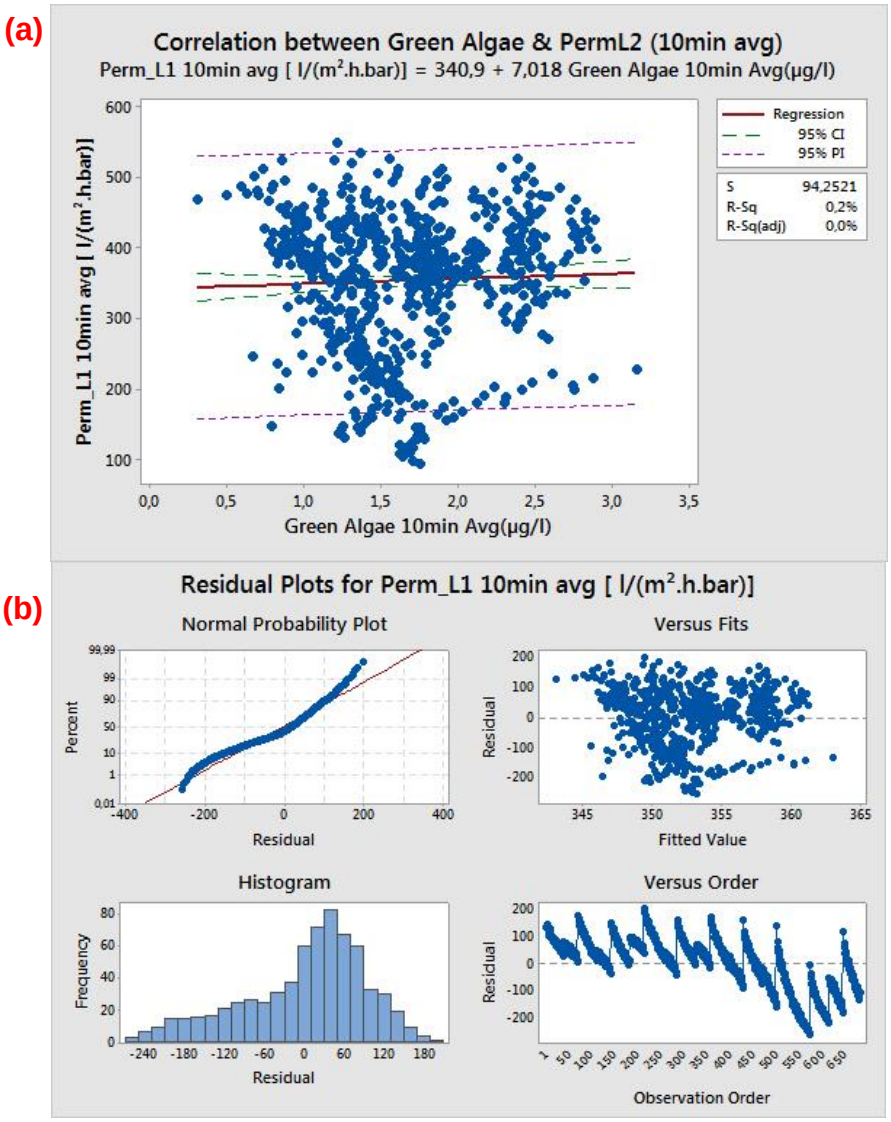

Figure 42: (a) Regression and (b) residual plots for Pair#5.

It is clear from the pattern of "Versus order" plots that the residual follow exactly the trend of a normal permeability performance curve. The permeability will always decrease with a downward trend due to fouling and a sharp increase after a backwash or chemical cleaning. Permeability is not dependent only on the algae concentrations. Any other non-algae substance which can cause fouling is also affecting its value. The complexity of permeability is that it is multi-variable dependent. To understand the variables which can affect permeability, one need to recall Eq.1 and Eq.4 for flux and permeability, respectively. Assuming the system is able to control feed at constant flux and has no problem with the equipment and process controls, permeability can still be affected by:

- Water quality
    - Algae concentration,
    - Constituents which might also contribute to fouling, such as Total suspended solids, Natural Organic Matter, Dissolved Organic Matter, Total Organic Matter, Turbidity etc.
    - Temperature (if permeability is not normalized)

- TMP, which is affected by fouling and the cleaning efficiency.
    - Hydraulic cleaning can be affected by introduction of new process such as Capillary Drain
    - Chemical cleaning can be affected by the kinds of chemicals used, quality of chemicals, soaking time, possibility of membrane degradation etc.

- Pre-treatment (if any)
    - Coagulation
    - Size of pre-filter

Therefore, it is a good initiative to try and find a correlation between permeability and algae concentrations but in terms of the outlook, multiple linear regressions can be considered in the future.

7. Capillary Drain for large scale UF-plant

The energy requirement and capital cost of implementing Capillary Drain for large scale UF-plant depends on the air compressor, which in turn depends on the pressure and amount of compressed air required. In this section, the dewater volume, which is also the volume of compressed air required, together with the size of reducer and energy requirement were calculated. Dewatering time was analysed and technical solutions to control the flux during Capillary Drain was proposed. In addition, availability of the process with and without Capillary Drain was investigated.

7.1. Dewater volume

In the first step of Capillary Drain, i.e. the dewatering step, compressed air is applied to fill the capillaries of the membrane modules. Before this can be achieved, water in the connection and T-pieces need to be removed before air reaches the capillaries as per Figure 43.

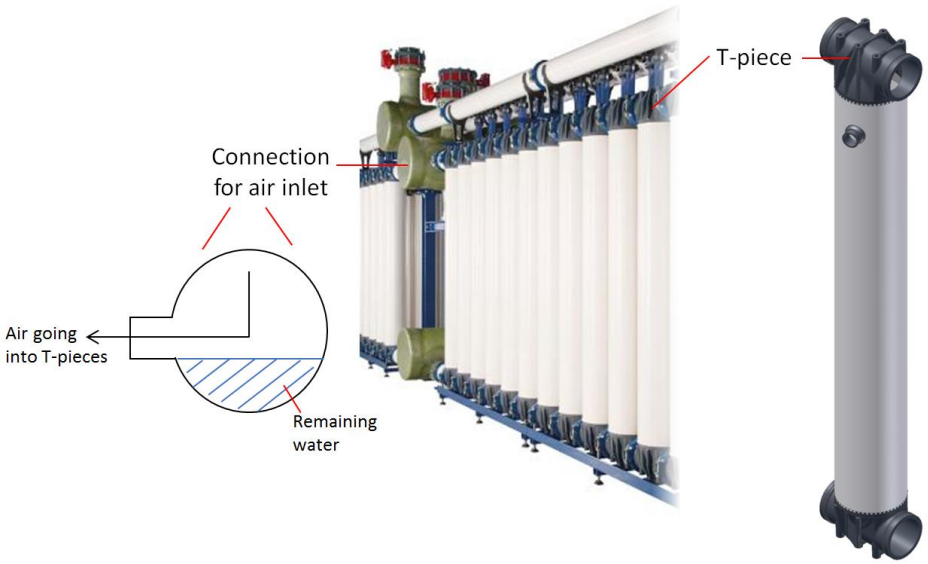

Figure 43: T-pieces and connection which needs to dewater.

Taking one rack with 120 modules as a basis, total volume of compressed air required is equal to the total dewatering volume:

Total dewatering volume = volume of capillaries + volume of T-pieces + volume of connection

Calculations were made based on the following conditions:

- T-piece's volume given as 7 litres per module
- Volume of connection given as 0.467 m^3
- Number of modules per rack given as 120
- Length of fibers given as 1.72 m
- 2500 fibers per module
- 7 capillaries per fibers
- Inner diameter of capillary is 0.9 mm
- Total membrane surface area

  $= 120 \text{ modules} \times 80 \frac{m^2}{\text{module}}$

  $= 9{,}600\ m^2$

For one rack, total volume of capillaries

$$= 120 \text{ modules} \times 2500 \frac{\text{fibers}}{\text{module}} \times 7 \frac{\text{capillaries}}{\text{fibers}} \times \left(\frac{\pi}{4} \times 0.0009^2\right) m^2 \times 1.72m = 2.298 m^3$$

Therefore, **total dewatering volume**

= volume of capillaries + volume of top headers + volume of T-pieces

$= 2.298\ m^3 + 0.467\ m^3 + \left(120 \times \frac{7}{1000}\right) m^3$

$= 3.605\ m^3$

7.2. Air flow requirement

By first assuming a dewatering time of 15 seconds, **Actual air flow**

$= 3.065\text{m}^3 \div 15\text{s} \times \frac{3600\text{s}}{\text{h}}$

$= 865\ \text{m}^3/\text{h}$

The air flow rate of 865 m^3/h is the "actual" air flow. Actual meters cubed per hour, or Am^3/h, is a terminology specifying the actual volumetric flow of gas at a given pressure and temperature. Inlet meters cubed per hour, or Im^3/h, is the volumetric flow at the compressor's suction. Normal meters cubed per hour, or Nm^3/h, is the volumetric flow with respect to P_{std} and T_{std}. The following equations were applied to convert the actual flow rate into normal flow rate:

$$Im^3/h = Am^3/h \left(\frac{P_{ref}}{P_s}\right)\left(\frac{T_s}{T_{ref}}\right)$$

$$Nm^3/h = Im^3/h \left(\frac{P_s}{P_{std}}\right)\left(\frac{T_{std}}{T_s}\right)$$

P_{ref}: reference pressure in bar absolute,

P_s: compressor suction pressure in bar absolute,

P_{std}: standard barometric pressure, equals to 1 bar absolute,

T_{ref}: reference temperature in K,

T_s: compressor suction temperature in K,

T_{std}: standard temperature, equals to 273K.

Applying the first equation with the following assumptions:

Temperature inside the system is constant at 293K

Temperature at suction of compressor is constant at 293K

Site elevation above sea level is 0 m

Required maximum pressure of compressed air is 2 bars absolute

Air flow at suction of compressor

$= Am^3/h \left(\frac{P_{ref}}{P_s}\right)\left(\frac{T_s}{T_{ref}}\right)$

$= 865\ Am^3/h \left(\frac{2\ \text{bar,a}}{1\ \text{bar,a}}\right)\left(\frac{293\text{K}}{293\text{K}}\right)$

$= 1{,}730\ Im^3/h$

Air flow in Nm^3/h

$= Im^3/h \left(\frac{P_s}{P_{std}}\right)\left(\frac{T_{std}}{T_s}\right)$

$= 1{,}730\ Im^3/h \left(\frac{1\ bar,a}{1\ bar,a}\right)\left(\frac{273K}{293K}\right)$

$= 1{,}612\ Nm^3/h$

With the calculated air flow rate and maximum desired pressure, one can approach a compressor company to ask for recommendation and quotation of compressors.

7.3. Piping diameter

A pressure reducer is required to reduce the compressed air's pressure and the outlet to the piping ensures a constant cross-flow velocity of the air entering the T-pieces. Given a maximum limit of 20 m/s for the cross-flow velocity [58], diameter of piping can be calculated by:

Cross sectional area of the pressure reducer

$$= \frac{\text{Actual air flow}}{\text{Max cross velocity}}$$

$$= \frac{865\ \frac{Am^3}{h}}{20\frac{m}{s}}$$

$= 0.012\ m^2$

Diameter of the piping

$$= \sqrt{\frac{4\times 0.012 m^2}{\pi}}$$

$= 0.124$ m

$= 124$ mm

7.4. Dewater time

Dewatering time

$= 3.605 m^3 \div [\text{Pemeability} \times 9600\ m^2 \times \text{Air pressure}]$

For calculations of dewatering time, one must consider that the flux is not constant over the entire Capillary Drain process. When the supply of compressed air can be constant, then the TMP during dewatering is almost constant. Nevertheless, first estimates can be calculated with assumptions of constant permeability. The following table shows various combinations which can be applied.

Table 9: Calculated values of flux and dewater time with assumption of constant permeability.

Permeability [l/(m²·h·bar)]	**100**		**200**		**500**	
Pressure [bar]	Flux rates [l/(m²·h)]	dewater time [s]	Flux rates [l/(m²·h)]	dewater time [s]	Flux rates [l/(m²·h)]	dewater time [s]
0.50	50	27.0	100	13.5	250	5.4
0.75	75	18.0	150	9.0	375	3.6
1.00	100	13.5	200	6.8	500	2.7

From the current pilot plant, the time for dewatering during Capillary Drain takes about 28 seconds. Therefore, assumption for permeability equals 500 l/(m²·h·bar)is not suitable because the dewater time seems too low. One must also take into consideration the available air volume, pressure and resistance of in-line components (especially pressure reducer). Typical filtration flux is 120 l/(m²·h) and this value should not be exceeded during Capillary Drain. The dewatering time should not be long or else it will lower the availability of the process.

In order to make a comparison, another way to estimate the permeability and air pressure is to set a target dewatering time of 15 seconds.

The "constant flux" for dewatering time of 15 seconds

$$= \frac{3605\text{L}}{15\text{s}} \times \frac{1}{9600\ \text{m}^2} \times \frac{3600\text{s}}{\text{h}}$$

$= 90$ l/(m²·h)

Again, estimates can be calculated by assuming constant air pressure or constant permeability shown in Table 10.

Table 10: Calculated values of permeability and pressure with dewater time of 15 seconds.

	Permeability [l/(m²·h·bar)]		**Pressure (bar) (Fixed)**
Fixed Pressure (bar)	-	**Fixed Permeability [l/(m²·h.bar)]**	-
0.50	180	**100**	0.90
0.75	120	**200**	0.45
1.00	90	**500**	0.18

Having a "constant flux" value of 90 l/(m²·h) is lower than typical filtration flux of 120 l/(m²·h). In terms of design, it is better to set the Capillary Drain time to 15 seconds and combine methods to control the flux at 120 l/(m²·h), which will be discussed in the next section.

7.5. Technical solutions for release of air during Capillary Drain

7.5.1. Controllable valve

One method is to have a controllable valve. With this method, the filtration flux during Capillary Drain can be controlled at 120 l/(m²·h) while keeping the dewatering time at 15 seconds. Figure 44 describes the flux with an assumption that the flux decreases linearly after a certain time t_a.

The total dewater volume of 3,605 liters is equal to $\mathbf{V_a + V_b}$, indicated in Figure 44. This assumption of linear flux decrease enables t_a to be calculated:

$\mathbf{V_a}$

$$= 120 \frac{l}{m^2 \cdot h} \times 9600\ m^2 \times t_a \times \frac{h}{3600s}$$

$= (320 \times t_a)\ l$

$\mathbf{V_b}$

$$= \frac{1}{2} \times 120 \frac{l}{m^2 \cdot h} \times 9600 m^2 \times (15 - t_a) \times \frac{h}{3600s}$$

$= (2400 - 160 \times t_a)\ l$

$V_a + V_b = 3605\ l$

$(320 \times t_a) + (2400 - 160 \times t_a) = 3605$

$\mathbf{t_a} = 7.5$ seconds

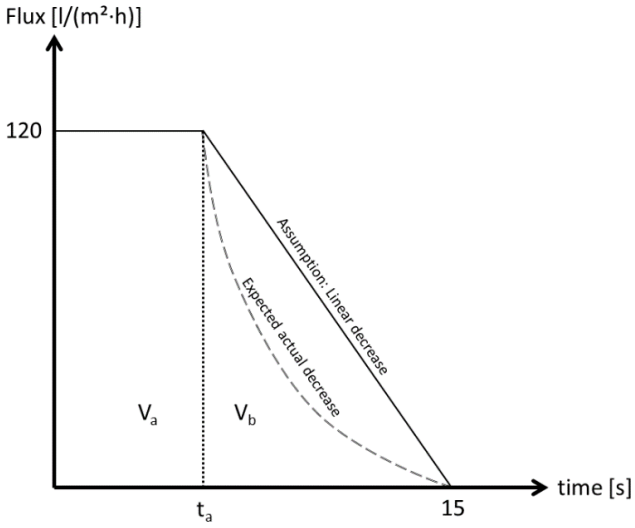

Figure 44: Scenario of flux and TMP during Capillary Drain with 1 bar compressed air using controllable valve.

The option of having a controllable valve seems to be able to control flux during Capillary Drain. However, the controllable valve can be expensive and requiring a considerable amount of effort to set up. An alternative is explored in the next sub-section.

7.5.2. Application of air buffer tanks

An alternative proposed solution is to have a buffer tank to allow release of compressed air with constant pressure as illustrated below.

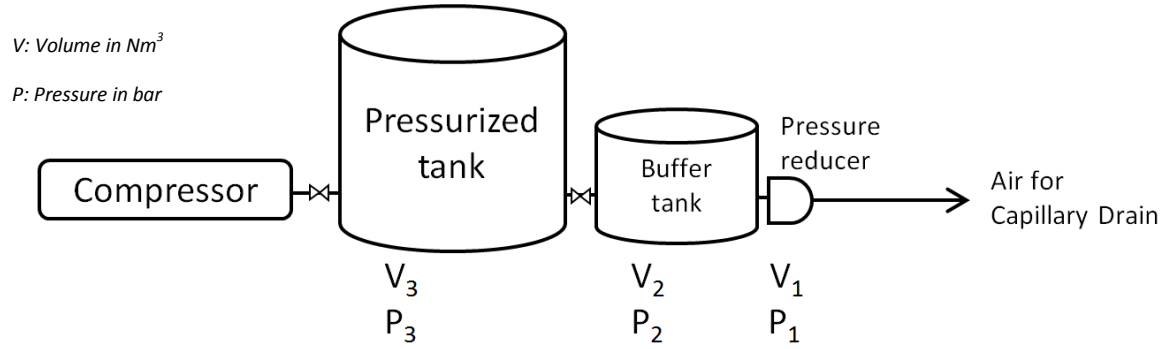

Figure 45: Setup with pressurized and buffer tanks for release of compressed air through pressure reducer.

The buffer tank's volume should have the amount of air required for one Capillary Drain while the pressurized tank should have the amount of air required for three Capillary Drains within an hour as a safety factor. It is an industrial practice to have compressed air at a pressure higher than its requirement. Considering that standard pressure tanks comes in pressure limit of 11 bar,a and 8 bar,a, the following volume of the tanks are proposed. Calculations are based on the ideal gas law.

i	V_i	P_i
1	6.7 Nm^3	2 bar,a
2	1.68 Nm^3	8 bars,a
3	(1.22 Nm^3 x 3) = 3.65 Nm^3	11 bars,a

To have the calculated volume of pressurized tank within an hour, the energy requirement is 0.052 kWh. The detailed calculations are available in **APPENDIX E**.

Using the current pilot plant's reference value of 120 l/(m²·h) and 0.34 bars for flux and TMP respectively, the flux when TMP is at 1 bar can be calculated using $J_v = \frac{TMP}{\mu R}$.

$$\frac{J_1}{TMP_1} = \frac{J_2}{TMP_2}$$

$$\frac{120\ l/(m^2 \cdot h)}{0.34\ bars} = \frac{J_2}{1\ bars}$$

$$J_2 = 353\ l/(m^2 \cdot h)$$

As mentioned previously, a flux over 120 l/(m²·h) is too high for the membrane process. Figure 46 below describes flux and TMP when Capillary Drain is conducted.

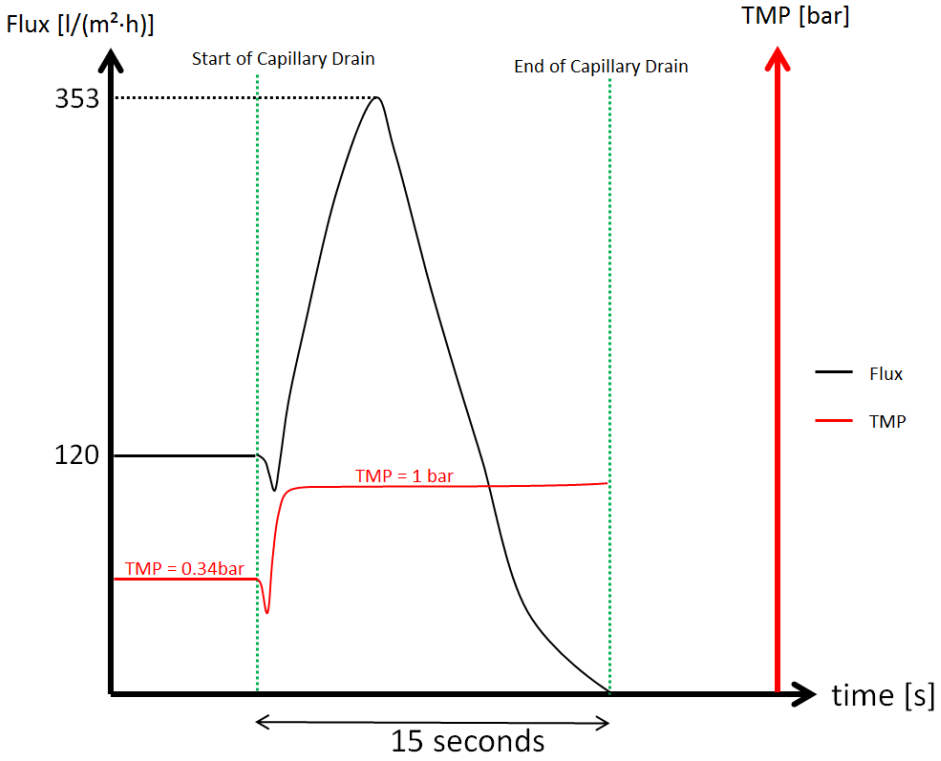

Figure 46: Scenario of flux and TMP during Capillary Drain with controlled release of air.

The drop in TMP is due to response time and valves switching when the feed pump stopped and air valves are opened. Flux changes accordingly with the change in TMP. It is important to note that the peak flux of 353 l/(m²·h) is not constant. This peak value can decrease over time (in magnitude of years) during the operation lifespan of the membrane due to fouling (increase of total resistance, R). Thus, the application of air buffer tank can be done in conjunction with manual adapting the pressure on the regular basis. An operator can be there physically to adjust the pressure of the compressed air starting from a lower pressure, say 0.5 bar. The time for dewatering can be checked and the air pressure can be increased manually step wise to reach a suitable solution.

7.6. Effect on availability

The availability of process with six, eight and ten racks were checked with inge® system design or iSD® 2014, a design program developed by inge GmbH. The following parameters were entered into the program to obtain availability without Capillary Drain.

Table 11: Conditions applied into iSD®.

Average feed flow for 6 racks	4,600	m^3/h
Average feed flow for 8 racks	6,000	m^3/h
Average feed flow for 10 racks	7,505	m^3/h
Filtration time	60	min
Backwash		
Backwash time	30	s
time for pause/response/ramp	19	s
Total of one backwash	0.82	min
CEB		
Injection	90	s
soak	15	min
rinsing	1	min
pause/response/ramp	19	s
total for 1 CEB (base + acid)	35.6	min
no. of CEB per day	2	
no. of BW per day	22.3	
Capillary Drain		
time per Capillary Drain	15	s
time for pause/response/ramp	19	s
Total time for each CD	34	s

After which, Eq. 12 is applied to obtain the availability when Capillary Drain is conducted every 6th interval (i.e. after 6 filtration cycles). The results are summarized in Table 12.

$$\alpha_{CD} = \frac{1}{\left(\frac{1}{INT}\frac{t_{CD}}{t_{filt}}\right)+\frac{1}{\alpha}} \quad \text{Eq. 12}$$

Table 12: Results of availability of plant with and without Capillary Drain.

	6 racks	**8 racks**	**10 racks**
α (without CD)	93.09%	92.10%	91.99%
α_{CD}	92.96%	91.97%	91.86%
Differences	0.13%	0.13%	0.13%

The difference with and without Capillary Drain is only 0.13%. Overall, the introduction of Capillary Drain in large scale plants only lowers the availability at a modest amount.

8. Recommendations and outlook

This section provides recommendations which can be explored to further understand Capillary Drain and the outlook of the Master's thesis work.

(i) Pressure-hold time

Pressure-hold is the second step of Capillary Drain to ensure water inside the capillaries is fully drained. Also, during the initial development of the Capillary Drain process, it was thought to have some "drying effect" on the fouling layer. The potential effects of pressure-hold time remain unclear. Nevertheless, draining of capillaries can be verified by checking the filtrate pressure. When all the water is fully drained in the capillaries, there should not be any more filtration and the filtrate pressure should be constant and close to zero.

It is important to point out that long pressure-hold time will lower the process's availability and might even compress the fouling layer. The latter can result in a higher level of irreversible fouling. Since its potential effects are unclear, investigation is recommended to find out if the pressure-hold time should be lowered.

(ii) Backwash flux during rcBW

It will be interesting to check if backwash flux can be lowered from the levels of 230 $l/(m^2 \cdot h)$ to achieve the same cleaning efficiency. With the same backwash time, lower backwash flux can increase the recovery of the process.

(iii) Effect of conducting Capillary Drain in between rcBW

rcBW involves two parts, a backwash drain bottom for around two-third of the total backwash time and backwash drain top for around one-third of the total backwash time. In the current settings, Capillary Drain is conducted before the rcBW. It is suggested to explore applying Capillary Drain before a backwash drain bottom in combination with another Capillary Drain before backwash drain top to determine the fouling removal efficiency.

(iv) Effect of conducting Capillary Drain before CEB

The effects of Capillary Drain before CEB can be explored and compared to the effects from conducting Capillary Drain after and in between CEB. The "best position" can be determined.

(v) Design of Experiment

Conventionally, experiments can be conducted by changing one-factor-at-a-time. Not only is this time and resource consuming, this method also assumes that there are no interactions between various factors. There could be a possibility that the effects of one factor are dependent on the factor level of other factors [40, 41]. In fact, applying one-factor-at-a-time in the presence of interaction can lead to

serious misunderstanding of how the response varies as a function of the factors. The Design of Experiment strategy can be applied using factors from Point (i) to (iv), or more factors identified later to look at multi factors and levels interactions. Examples can be a full factorial design or fractional factorial design.

(vi) Investigating Capillary Drain using bench-scale modules with transparent connections

Capillary Drain experiments can be conducted using a smaller, "broom-stick" bench-scale modules containing 5 to 10 hollow fibers. Currently, "broom-stick" bench-scale modules from inge GmbH have PVC connections. It is suggested to have a transparent connection to observe the bubbles characteristics leaving the lumen when conducting Capillary Drain. Physical observations can help to better understand if Capillary Drain improves foulant removal with occurrence of 2-phase flow.

(vii) Chlorophyll-a concentration above levels of 15µg/l

Within the time frame of the Master's thesis, the concentration of chlorophyll-a did not reach the levels of an algal bloom. One can wait for potential algal bloom events as the current plant is still in operation. Alternatively, experiments with artificial feed water can be conducted to explore Capillary Drain effect during real or induced algal bloom.

(viii) Capillary Drain effect in other applications

The type of fouling modes is different in different applications (wastewater, river water etc.). Capillary Drain's effects are expected to be different as well and investigations can be conducted using different source of feed water to compare the effects of Capillary Drain in these applications.

(ix) Long-term applications of the fouling indices

The operation of the current pilot plant can continue to gather information to observe the long-term effects of Capillary Drain on the process using the fouling indices.

9. Conclusions

In conclusion, the objectives of this work were met. The biological background of different algae classes were reviewed and the effect of Capillary Drain was investigated with a pilot plant in the Middle East using inge® Dizzer® XL modules with non-treated seawater. Capillary Drain involves two steps, dewatering and pressure-hold with non-oil compressed air. A hydraulic cleaning of reverse-combined Backwash (rcBW) is conducted after. They were operated at 76 l/(m²·h), 85 l/(m²·h), and 92 l/(m²·h) in April 2017 with a filtration time to 60, 50 and 45 minutes, respectively, to keep the recovery and feed loading constant. Fouling indices developed by A.H. Nguyen [48] (Total Fouling and Hydraulic Irreversible Fouling Index) and the change in permeability were used for comparison of the efficiency of Capillary Drain.

Membrane process performance with and without Capillary Drain resulted in a Hydraulic Irreversible Index of 0.213 m^2/m^3 and 1.365 m^2/m^3, respectively. The former indicated that Capillary Drain slowed down the rate of increase in resistance due to fouling. Availability of the membrane process will decrease if Capillary Drain were conducted after every filtration cycle. Thus, effects of single Capillary Drain within the chemical cleaning cycle at different flux were further investigated.

The Total Fouling Indices for filtration cycles after conducting Capillary Drain were lower than the Total Fouling Indices for its respective filtration cycle before Capillary Drain. This is true in two situations, when Capillary Drain was introduced one filtration cycle after a CEB, and when it was introduced in between CEBs. Better results were seen when Capillary Drain was introduced in between CEBs due to lower Hydraulic Irreversible Fouling Indices. Applying the same concept to compare the Total Fouling Indices, Capillary Drain also proved to be effective at higher operating flux of up to 92 l/(m²·h).

The pilot plant experienced a tremendous increase of TMP when chlorophyll-a concentration reached levels of 4 µg/l. TMP increase from around 200mbar to 700mbar and 1000mbar for Line 1 and 2, respectively. The concentration of chlorine and soaking duration were doubled in order to bring the situation under control. Higher change in permeability (ΔPerm) was observed for Capillary Drain as compared to CEB, which indicated that Capillary Drain seemed to be able to remove fouling better than just CEB alone.

Possible explanations for Capillary Drain's positive effect are (i) the "loosen" effect when air entered the porous fouling layer and/or (ii) occurrence of 2-phase flow resulting in shear stress along the capillaries wall. Capillary Drain performed well as an advanced physical cleaning method for seawater applications with no coagulation.

The application of Fouling Indices by A.H. Nguyen et. al. [48] for comparison of cleaning efficiency is useful when investigating new methods and/or new parameter setting in the process. Performance

affected by changes in feed water quality can also be detected. Long term trend of membrane process's performance can be established if one compared the current and initial Fouling Indices values.

Correlations between algae occurrence, process stability and feed water parameters were also investigated using a statistical program, Minitab® 2017. SDI of feed seawater (daily) seems to have a relationship with total chlorophyll-a (daily average) at lower range of chlorophyll-a (between 0.5 to 1.2 µg/l). Other parameters compared seem to have no statistically significant relationships between them at a confidence interval of 95%.

The feasibility of Capillary Drain application in large scale UF-plant was analyzed. Calculations were made to determine the energy requirement of compressor to produce the necessary amount of compressed air for one rack with 120 modules. It will require 0.052 kWh to conduct three Capillary Drain within an hour. Two technical solutions; application of controllable valve and air buffer tanks, were proposed to control the filtration flux during Capillary Drain. Availability of the process with and without Capillary Drain was also calculated with the derived formula. The introduction of Capillary Drain in large scale plant only lowers the availability at a modest amount of 0.13%.

Finally, recommendations were made to investigate the pressure-hold time, backwash flux, applying Capillary Drain within a rcBW and before CEB, possibly with Design of Experiment strategy. Conducting Capillary Drain on bench-scale modules with transparent connections allows physical observe for any occurrence of 2-phase flow. Applications of Capillary Drain in areas such as wastewater, river water, during algal bloom and the long-term application of Fouling Indices should also be considered.

References

[1] United Nations Population Fund, Extracted on April 2017. From: http://www.unfpa.org/ (2016)

[2] World Health Organization, *Drinking-water Fact sheet*, Extracted on April 2017. From: http://www.who.int/mediacentre/factsheets/fs391/en/ (2016)

[3] Xiafu Shi, Galit Tal, Nicholas P. Hankins, Vitaly Gitis, *Fouling and cleaning of Ultrafiltration membrane: A Review*, Journal of Water Process Engineering, 1 (2014) 121-138

[4] Marcel Mulder, *Basic Principles of Membrane Technology*, Kluwer Academic Publishers, Netherlands (1996)

[5] APEC Water, Extracted on April 2017. From: http://www.freedrinkingwater.com/water_quality/quality1/43-08-ultrafiltration-membrane-filter-tech.htm

[6] inge GmbH, Resources from the company (2010 – 2017)

[7] J. Crespo, *Lecture on Pressure driven processes*, Universidade Nova de Lisboa (2016)

[8] S. Judd, *The MBR Book: Principles and Applications of Membrane Bioreactors in Water and Wastewater Treatment***,** Elsevier Ltd (2006)

[9] Z.F. Cui and H.S. Muralidhara, *Membrane Technology: A Practical Guide to Membrane Technology and Applications in Food and Bioprocessing*, Elsevier Ltd, Oxford (2010)

[10] A. Berktay, *Environmental approach and influence of red tide to desalination process*

in the middle-east region, International Journal of Chemical and Environmental Engineering 2, 3 (2011) 183–188

[11] N. Nazzal, *Red tide' shuts desalination plant. Gulf News, Dubai, UAE*. Extracted on April 2017. From: http://gulfnews.com/news/gulf/uae/environment/red-tide-shuts-desalinationplant-1.59095 (2009)

[12] T. Pankratz, *Red tides close desal plants*, Water Desalination Report 44 (2008).

[13] M.L. Richlen, S.L. Morton, E.A. Jamali, A. Rajan, D.M. Anderson, *The catastrophic 2008–2009 red tide in the Arabian Gulf region, with observations on the identification and phylogeny of the fish-killing dinoflagellate Cochlodinium polykrikoides*, Harmful Algae 9 (2) (2010) 163–172

[14] IOC-UNESCO, *What are harmful algae?* Extracted on April 2017, From: http://hab.ioc-unesco.org/ (2013)

[15] L. Villacorte, *Algal Blooms and Membrane Based Desalination Technology*, CRC Press/Balkema, Netherlands (2014)

[16] R. G. Wetzel, *Limnology: Lake and River Ecosystems 3rd ed.*, CA: Academic Press, San Diego (2001)

[17] E. Callaway, A new kind of chlorophyll – and it only took 67 years to find, Extracted on April 2017. From: http://blogs.nature.com/news/2010/08/a_new_kind_of_chlorophyll_and.html (2010)

[18] B. R. Speer, *Photosynthetic Pigments in Glossary*, Extracted on April 2017. From http://www.ucmp.berkeley.edu/glossary/gloss3/pigments.html (1997)

[19] K. Schulz, *Phytoplankton Measuring and Culture Techniques. In Phytoplankton Ecology (Lecture)*, Extracted on April 2017. From: http://www.esf.edu/efb/schulz/phytotechniques.doc

[20] American Public Health Association, American Water Works Association & Water Environment Federation, *Standard Methods for the Examination of Water and Wastewater 20th ed.*, Baltimore, MD: American Public Health Association (1999)

[21] YSI Incorporated, *The Basics of Chlorophyll Measurement*, YSI Environmental Tech Note, Extracted on April 2017. From: http://www.ysi.com/media/pdfs/T606-The-Basics-of-Chlorophyll-Measurement.pdf

[22] NHDES, *Description of River Water Quality Parameters*, Department of Environmental Services, Extracted on April 2017. From: http://des.nh.gov/organization/divisions/water/wmb/vrap/documents/wq-resultsinfo.pdf

[23] bbe Moldaenke GmbH, *bbe AlgaeGuard® User Manual* (2012)

[24] S.H. Kim, J.S.Yoon, *Optimization of microfiltration for seawater suffering from red-tide contamination*, Desalination, 182(1–3), (2005) 315–321

[25] D. A. Ladner, D. R. Vardon, M.M. Clark, *Effects of Shear on Microfiltration and Ultrafiltration Fouling by Marine Bloom-forming Algae*, Journal of Membrane Science, 356, (2010) 33–43.

[26] R. Schurer, A. Tabatabai, L. Villacorte, J.C. Schippers, M.D. Kennedy, *Three years operational experience with ultrafiltration as SWRO pre-treatment during algal bloom*, Desalination & Water Treatment, 51(4-6), (2013) 1034-1042

[27] R. Schurer, A. Janssen, L. Villacorte, M.D. Kennedy, *Performance of ultrafiltration & coagulation in an UF-RO seawater desalination demonstration plant*, Desalination & Water Treatment 42 (1-3), (2012) 57-64

[28] S. G. J. Heijman, M. D. Kennedy, G. J. van Hek, *Heterogeneous fouling in dead-end ultrafiltration*, Desalination, 178(1-3), (2005) 295-301

[29] S. G. J. Heijman, M. Vantieghem, S. Raktoe, J. Q. J. C. Verberk, J. C. van Dijk, *Blocking of capillaries as fouling mechanism for dead-end ultrafiltration*, Journal of Membrane Science, 287(1), (2007) 119-125

[30] A. Lerch, W. Uhl, R. Gimbel, *CFD modelling of floc transport and coating layer build-up in single UF/MF membrane capillaries driven in inside-out mode*, Water Science and Technology: Water Supply, 7 (4), (2007) 37-47.

[31] S. Panglisch, *Formation and prevention of hardly removable particle layers in inside-out capillary membranes operating in dead-end mode*, Water Science and Technology: Water Supply, 3 (5-6), (2003) 117-124.

[32] S. M. Myklestad, *Release of extracellular products by phytoplankton with special emphasis on polysaccharides*, Science of the Total Environment, 165, (1995)155-164.

[33] L. Villacorte, Y. Ekowati, H. Winters, G.L. Amy, J.C. Schippers, M.D. Kennedy, *Characterisation of transparent exopolymer particles (TEP) produced during algal bloom: a membrane treatment perspective*, Desalination & Water Treatment, 51 (4-6), (2013) 1021-1033

[34] U. Passow, *Formation of transparent exopolymer particles (TEP) from dissolved precursor material*,Marine Ecology Progress Series, 192 (2000) 1-11

[35] P. Verdugo, A.L. Alldredge, F. Azam, D.L. Kirchman, U. Passow, P.H. Santschi, *The oceanic gel phase: a bridge in the DOM–POM continuum*, Marine Chemistry, 92 (2004) 67-85

[36] L. Villacorte, R. Schurer, M. Kennedy, G. Amy, J.C. Schippers, *The fate of transparent exopolymer particles in integrated membrane systems: a pilot plant study in Zeeland, The Netherlands*, Desalination & Water Treatment, 13 (2010) 109-119

[37] L. Villacorte, R. Schurer, M. Kennedy, G. Amy, J.C. Schippers, *Removal and deposition of Transparent Exopolymer Particles (TEP) in seawater UF-RO system*, IDA Journal, 2 (1), (2010) 45-55

[38] T. Berman, M. Holenberg, *Don't fall foul of biofilm through high TEP levels*, Filtration & Separation, 42 (4), (2005) 30-32

[39] H. Winters, I. R. Isquith, *In-plant microfouling in desalination*, Desalination, 30 (1), (1979) 387-399

[40] T.P. Ryan, *Modern Engineering Statistics*, John Wiley & Sons Inc, New Jersey (2007)

[41] P. M. Berthouex, L.C. Brown, *Statistics for Environmental Engineers 2nd ed.*, Lewis Publishers, Florida (2002)

[42] G.J Hahn, *The Coefficient of Determination Exposed*, Chemtech,(1973) 609–611

[43] The Minitab blog, *Regression Analysis: How to Interpret S, the Standard Error of the Regression*, Extracted on April 2017. From: http://blog.minitab.com/blog/adventures-in-statistics-2/regression-analysis-how-to-interpret-s-the-standard-error-of-the-Regression (2014)

[44] Y.Wibisono, E. R. Cornelissen, A.J.B. Kemperman, W.G.J. van der Meer, K. Nijmeijer. *Two-phase flow in membrane processes: A technology with a future*. Journal of Membrane Science, 453 (2014) 566–602

[45] Y.Bessiere, C. Guigui, P.J. Remize, C. Cabassud, *Coupling air-assisted backwash and rinsing steps: a new way to improve ultrafiltration process operation for inside-out hollow fibre modules*. Desalination, 240 (2009) 71–77

[46] P.J. Remize, C. Guigui, C. Cabassud, *Evaluation of backwash efficiency, definition of remaining fouling and characterisation of its contribution in irreversible fouling: Case of drinking water production by air-assisted ultra-filtration*, Journal of Membrane Science, 355 (2010) 104-11

[47] Mohamed. O. Saeed, Essam S. Al-Thobaiti, Mohammad A. Daili, A. Al-Hamzah, *Biofouling potential in Al-jubail intake bay with reference to the 24MGD SWRO Plant*, Saline Water Conversion Corporation, Technical report No. APP 3805/97005 (2001)

[48] A.H. Nguyen, J.E. Tobiason, K.J. Howe, *Fouling indicies for low pressure hollow fiber membrane performance assessment*, Water Research, 45 (2011) 2827-2637

[49] M. Zupancic, D. Novak, J. Diacum I. Golobic, *An evaluation of industrial ultrafiltration systems for surface water using fouling indices as a performance indicator*, Desalination, 344 (2014) 321–328

[50] N. Lee, G. Amy, J.P. Croue, H. Buisson, *Identification and understanding of fouling in low-pressure membrane (MF/UF) filtration by natural organic matter (NOM)*, Water Research, 38 (2004) 4511-4523

[51] N. Lee, G. Amy, J.P. Croue, Low-pressure membrane (MF/UF) fouling associated with allochthonous versus autochthonous natural organic matter, Water Research, 40 (2006) 2357-2368

[52] J. Lozier, L. Cappucci, N. Lee, G. Amy, J. Jacangelo, H. Huang, T. Young, C. Mysore, C. Emeraux, J. Clouet, J. Croue, B. Heijmann, 2008. *Natural Organic Matter Fouling of Low-Pressure Membrane Systems*, Water Research Foundation Report, (2008) USA.

[53] S. Boerlage, M. Kennedy, A. Meseret, A.Elhadi, G. Gilbert, J. Schippers, *Monitoring particulate fouling in membrane systems*, Desalination 118 (1998) 131-142.

[54] S. Boerlage, M. Kennedy, A. Meseret, A.Elhadi, G. Gilbert, T. Zeyad, J. Schippers, *The MFI-UF as a water quality test and monitor*, Journal of Membrane Science, 211 (2003) 271-289

[55] H. Huang, Y. Thayer, J. Jacangelo, *Unified membrane fouling index for low pressure membrane filtration of natural waters: principles and methodology*, Environmental Science and Technology, 42 (2008) 714-720

[56] H. Huang, R. Spinett, C.R. O'Melia, *Direct-flow microfiltration of aquasols - Impacts of particle stabilities and size*, Journal of Membrane Science, 314 (2008) 90-100

[57] H. Huang, Y. Thayer, J. Jacangelo, *Novel approach for the analysis of bench-scale, low pressure membrane fouling in water treatment*, Journal of Membrane Science, 334 (2009) 1-8

[58] C.Staaks, inge GmbH (2017)

[59] Alia Unit converter, Extracted on May 2017. From: http://www.alia-inc.com/en/Unit_converter4.asp#2 (2007)

[60] Kaeser Technical Specification, Extracted on May 2017. From: http://us.kaeser.com/Images/USSXSMSK_SX-SM-SK-Series_03-2014-tcm9-497993.pdf (2017)

[61] SCE&G, Calculating Energy cost to operate a compressor Extracted on May 2017. From: http://www.scegbusiness.com/Article.aspx?userID=351124&articleID=226 (2011)

APPENDIX A - Derivation of relation between availability with and without Capillary Drain

Availability without Capillary Drain is defined as:

$$\alpha = \frac{n \,.\, t_{filt}}{n.\,(t_{filt} + \ t_{bw}) + t_{\,CEB}}$$

Inverse the above equation,

$$\frac{1}{\alpha} = \frac{n.\,(t_{filt} + \ t_{bw}) + t_{\,CEB}}{n \,.\, t_{filt}}$$

$$\frac{1}{\alpha} = \frac{n.\,(t_{filt} + \ t_{bw})}{n \,.\, t_{filt}} + \frac{t_{\,CEB}}{n \,.\, t_{filt}}$$

$$\frac{1}{\alpha} = \frac{(t_{filt} + \ t_{bw})}{t_{filt}} + \frac{t_{\,CEB}}{n \,.\, t_{filt}}$$

Availability with Capillary Drain is defined as:

$$\alpha_{CD} = \frac{n \,.\, t_{filt}}{n.\left(t_{filt} + t_{bw} + \frac{t_{CD}}{INT}\right) + t_{\,CEB}}$$

Inverse the above equation,

$$\frac{1}{\alpha_{CD}} = \frac{n.\left(t_{filt} + t_{bw} + \frac{t_{CD}}{INT}\right) + t_{\,CEB}}{n \,.\, t_{filt}}$$

$$\frac{1}{\alpha_{CD}} = \frac{n.\left(t_{filt} + t_{bw} + \frac{t_{CD}}{INT}\right)}{n \,.\, t_{filt}} + \frac{t_{\,CEB}}{n \,.\, t_{filt}}$$

$$\frac{1}{\alpha_{CD}} = \frac{\left(\frac{t_{CD}}{INT}\right)}{t_{filt}} + \underline{\frac{(t_{filt} + t_{bw})}{t_{filt}} + \frac{t_{\,CEB}}{n \,.\, t_{filt}}}$$

Underlined in red is equal to the first inversed expression,

$$\frac{1}{\alpha_{CD}} = \frac{\left(\frac{t_{CD}}{INT}\right)}{t_{filt}} + \frac{1}{\alpha}$$

$$\alpha_{CD} = \frac{1}{\left(\frac{1}{INT}\,\frac{t_{CD}}{t_{filt}}\right) + \frac{1}{\alpha}}$$

APPENDIX B - Piping and Instrumentation diagram of PU 22

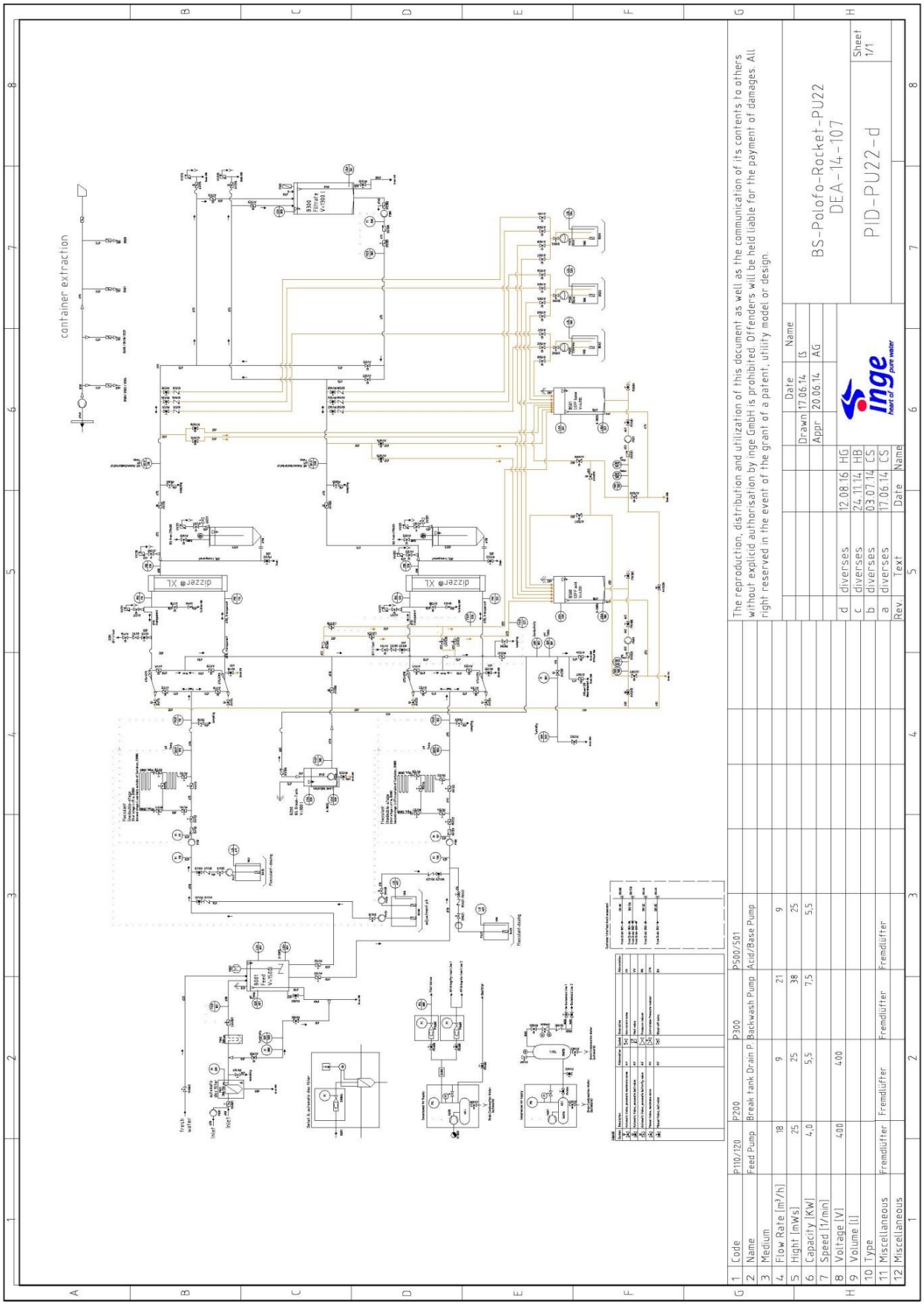

APPENDIX C - Summary of operating parameters

			Line 1			Line 2	
Filtration	**Flux**	**l/(m²·h)**	76	85^	92	85	92^
	Time	**min**	60	50	45	50	45
Reverse Combined Backwash	**Flux**	**l/(m²·h)**	230				
	Backwash time	**s**	35				
	BW Distribution	**Drain Bottom**	25				
		both	5				
		Drain Top	10				
Capillary Drain	**Interval**	**cycles**	12	14	15	14	15
	Dewatering pressure	**bar**	1				
	Dewatering time	**min**	0.5				

^ *fluctuation of chlorophyll-a concentration*

CEB1.1							
Chemical	**-**	NaOH (30%)					
Additional Chemical	**-**	NaOCl (10-12%)					
Interval	**cycles**	12	14	15	14	15	
Frequency	**per day**	2					
Set point pH value in rack	**-**	9.5					
Measured free Chlorine	**mg/l**	148					
Soaking time	**min**	15					
CEB1.2							
Chemical	**-**	HCl (30%)					
Interval	**cycles**	12	14	15	14	15	
Frequency	**per day**	2					
Set point pH value in rack	**-**	2					
Soaking time	**min**	15					
Filtrate Injection during CEB							
Flux	**l/(m²·h)**	120					
Duration Drain (Bottom/Top)	**s**	90 (70/20)					
Rinsing							
Flux	**l/(m²·h)**	230					
Duration	**s**	60					

APPENDIX D - Development of the fouling indices using a resistance-in-series approach

The derivation of fouling indices from A.H Nguyen [48] is shown:

In general, the pressure driven water flux through a low pressure membrane is described as,

$$J_v = \frac{\Delta P}{\mu R} = \frac{TMP}{\mu R}$$

Where ΔP or TMP is the trans-membrane pressure. R is the resistance to flow through the membrane and μ is the water viscosity.

According to the resistance-in-series model, R is the sum of resistance from a clean membrane, cake formation, hydraulic irreversible fouling and chemical irreversible fouling denoted as R_{mem}, R_{cake}, R_{HIFI} and R_{CIFI}.

$$R = R_{mem} + R_{cake} + R_{HIFI} + R_{CIFI}$$

If the resistance due to fouling increases linearly with the volume of filtrate produced, then

$$R_i = k_i S_{vol}$$

Where k_i is the rate constant for the increase in resistance and S_{vol} is the specific volume. Thus the total resistance can be rewritten as

$$R = R_{mem} + (k_{HR} + k_{HI} + k_{CI})\, S_{vol}$$

$$R = R_{mem} + (k_{total}\, S_{vol})$$

Where

k_{HR} is the rate constant for increase due to hydraulic reversible fouling
k_{HI} is the rate constant for increase due to hydraulic irreversible fouling
k_{CI} is the rate constant for increase due to chemical irreversible fouling

Combining J_v and R,

$$Perm = \frac{J_V}{\Delta P} = \frac{1}{\mu(R_{mem} + k_{total} S_{vol})}$$

For new membranes, S_{vol} is zero and so $Perm_0 = \frac{1}{\mu R_{mem}}$

Membrane performance can be normalized by dividing Perm at any specific volume by initial conditions as follows

$$Perm' = \frac{Perm}{Perm_o} = \frac{1}{1 + \frac{k_{total}}{k_{mem}} S_{vol}}$$

or $\frac{1}{Perm'} = 1 + (\frac{k_{total}}{k_{mem}})\, S_{vol}$

Membrane performance data for different operational cycles and cleaning procedures can be used to observe and possibly quantify various fouling indices: the Total Fouling Index (TFI), Hydraulic Irreversible Fouling Index (HIFI) and chemical irreversible fouling index (CIFI). The indices have units of inverse length and can be described as follows,

For any single cycle between hydraulic backwashes, referred to as one hydraulic backwash cycle, TFI can be related to the normalized specific flux (or permeability) and the specific volume as

$$\frac{1}{\mathrm{Perm}'} = 1 + (\mathrm{TFI})S_{vol}$$

For multiple hydraulic backwash cycles without any chemical cleaning (referred to as one chemical cleaning cycle), HIFI can be similarly be related to average values if L'_p during individual filtration cycles and S_{vol} as

$$\frac{1}{\mathrm{Perm}'} = 1 + (\mathrm{HIFI})S_{vol}$$

Average values for all data for a series of chemical cleaning cycles can be used to determine the CIFI based on data from one complete multiple chemical cleaning cycle experiment as

$$\frac{1}{\mathrm{Perm}'} = 1 + (\mathrm{CIFI})S_{vol}$$

APPENDIX E - Energy requirement calculations for compressor

Volume of pressurized tank = 3.65 Nm^3

This amount of air was calculated based on the assumption that three Capillary Drains were to be conducted within an hour as a safety factor.

Total time for three Capillary Drain is 45 seconds. The flow in Nm^3/h is

$$= \left(\frac{3.65\ Nm^3}{45\ s}\right)\left(\frac{3600s}{1\ h}\right)$$

= 292 Nm^3/h or 17 acfm (actual cubic feet per min) [59]

The pressure of 11bar,a is equal to 147 psig.

With reference to technical specification of Kaeser Compressors in Figure 48, a model SX 5T is suitable for the application [60]. The motor power of 5hp will be applied to calculate the energy consumption.

Technical Specifications

Model	Operating Pressure (psig)	Capacity at Operating Pressure (cfm) (1)	Motor (hp)	Dimensions W x D x H (in.)	Weight (lb.)(2)	Sound Level (dB(A)) (3)
SX 3*	125	12	3	23 1/4 x 24 7/8 x 38 1/8	309	61
SK 3T*				23 1/4 x 36 x 38 1/8	408	
SX 3 AIRCENTER*	160*	9		23 1/4 x 42 7/8 x 61 3/8	628	
SX 4	125	16	4	23 1/4 x 24 7/8 x 38 1/8	309	62
SX 4T	160	13		23 1/4 x 36 x 38 1/8	408	
SX 4 AIRCENTER	217	9		23 1/4 x 42 7/8 x 61 3/8	628	
SX 5	125	21	5	23 1/4 x 24 7/8 x 38 1/8	320	63
SX 5T	160	17		23 1/4 x 36 x 38 1/8	419	

Figure 47: Technical specification of Kaeser compressors [60].

The following equation [61] can be applied to determine the energy consumption of compressor:

$$\text{Energy consumption} = \text{horsepower(hp)} \times \frac{0.746\text{kW}}{\text{hp}} \times \frac{operating\ time}{motor\ efficiency}$$

Motor Efficiency can vary from 75% to 95%. In this case, a motor efficiency of 90% is assumed.

For operating time, three Capillary Drain within an hour is considered (compressed air for pneumatic instruments and other purposes are not included).

Energy consumption

$$= 5\ \text{hp} \times \frac{0.746\text{kW}}{\text{hp}} \times \frac{45}{3600} \times \frac{1}{0.9}$$

= 0.052 kWh (for three Capillary Drain within an hour)